UNIVERSITY OF OKLAHOMA

GRADUATE COLLEGE

THE IMPACT OF LONG-TERM ELEVATED ATMOSPHERIC CARBON DIOXIDE ON BELOWGROUND MICROBIAL COMMUNITY AT CONTRAST NITROGEN CONDITIONS

A DISSERTATION

SUBMITTED TO THE GRADUATE FACULTY

in partial fulfillment of the requirements for the

Degree of

DOCTOR OF PHILOSOPHY

By

FEIFEI LIU
Norman, Oklahoma
2017

THE IMPACT OF LONG-TERM ELEVATED ATMOSPHERIC CARBON DIOXIDE ON BELOWGROUND MICROBIAL COMMUNITY AT CONTRAST NITROGEN CONDITIONS

A DISSERTATION APPROVED FOR THE
DEPARTMENT OF MICROBIOLOGY AND PLANT BIOLOGY

BY

_____
Dr. Jizhong Zhou, Chair

_____
Dr. Elizabeth Karr

_____
Dr. Bradley Stevenson

_____
Dr. Yiqi Luo

_____
Dr. Michael Patten

Acknowledgements

This is a dissertation studying microbial community and it is really a work of a community. Many people contributed to this study and I would like to express my gratitude to all of them who encouraged me and helped me out through the past years. First, my advisor, Jizhong Zhou, was generous to take me on as a student and introduced me to the field of environmental microbiology. Dr. Zhou is an excellent, incredibly hard-working scientist. He has provided much guidance, encouragement, and patience over the years. This project would not be possible without his support.

Dr. Zhili He and Dr. Kai Xue also contributed much to this project for instructing me to gather, analyze, and interpret of the large datasets. Dr. Liyou Wu spent lots of efforts to develop the high-throughput sequencing pipelines. Without their help, I could be still struggling working on generating data and making sense of it. I truly learned a lot from them in organizing massed results into logical scientific work.

I also owe great thanks to my committee members—Dr. Elizabeth Karr, Dr. Yiqi Luo, Dr. Bradley Steven, and Dr. Michael Patten for serving as my committee members for this long time. As a graduate student trying to develop his own background in a multidisciplinary area, I deeply appreciated their guidance by providing valuable suggestions and assistance for every stages throughout this degree period. The different perspectives they look at questions greatly benefitted me to address problems comprehensively.

Members of IEG have been very helpful, particularly Dr. Joy Van Nostrand, Dr. Daliang Ning, Dr. Renmao Tian, Dr. Arthur Escalas, Dr, Anyi Hu, Dr. Jialiang Kuang, Dr. Ye Deng, and Yujia Qin. The data analysis methods and scientific writing skills I

learned from them would also benefit me for life. Dr. Peter Reich and Dr. Sarah Hobbie from the University of Minnesota also kindly offered perspective on potential research ideas, helped me collect samples, and generously shared data.

Grants from several agencies have supported my research including the US Department of Energy and the China Scholarship Council. Thank you for the investment and the trust placed in me.

My final sincerest gratitude belongs to my family, my parents, and my fiancée, for their continuous encouragements and support in my whole life. It is them who helped me to survive all the stress for years and not letting me give up. Nothing could compensate the great efforts and sacrifice they have made for my achievements.

Table of Contents

List of Tables

List of Figures

Abstract

Global terrestrial ecosystems are subjected to various climate change factors, including the concurrent elevated CO_2 (eCO_2) and nitrogen deposition (eN). Despite the increasing appreciation that eCO_2 and eN can interactively affect aboveground plants, how they will affect soil microbial communities and associated ecoprocesses remain understudied. This dissertation addresses this gap by examining the response of soil microbial communities associated with two plant functional groups (C3 grass and legumes) to eCO_2 and eN in a long-term (12-year) field experiment (BioCON).

In the beginning of this study, we investigated soil bacterial and archaeal communities subjected to CO_2 (ambient, 368 μmol mol^{-1}, versus elevated, 560 μmol mol^{-1}) and N (ambient, 0 g m^{-2} yr^{-1}, versus elevated, 4 g m^{-2} yr^{-1}) treatments using Illumina MiSeq sequencing of 16S rRNA gene amplicons. Over 2.3 million passing sequences were obtained from a total 24 samples, corresponding to 38 known phyla, 96 classes, and 565 genera. Elevated CO_2 significantly altered the diversity and structure of microbial communities, but these changes vary greatly depending on soil N conditions and plant functional groups. In C3 grass plots, community diversity increased with eCO_2. A positive eN effect on community richness was also observed. These shifts in community structure and composition may be driven by differential responses of microbial taxonomic groups to eCO_2 and/or eN. For example, *Actinobacteria* abundance decreased with the main effect of eCO_2, accounting for about 20.3% of the total population in the C3 grass. *Chlamydiae* increased with eCO_2 but only under eN condition. The abundance of *Woesearchaeota* increased with eN, but no effect of eCO_2 on its abundance was observed. Whereas in legume plots, community richness increased with

eCO_2. The abundance of *Actinobacteria*, *Chloroflexi*, *Armatimonadetes*, *Saccharibactiera*, and *Euryarchaeota*, accounting for about 21.2% of the total population in legume plots, decreased with eCO_2, eN or both. Only *Nitrospirae* and *Latescibacteria* increased with eCO_2 in their abundance. Changes in community diversity and composition were significantly related to plant and soil properties including plant biomass, biomass N content and C/N ratio, soil ammonium and nitrate, pH, moisture, temperature, and soil C and N contents by Mantel analysis. In addition, our results suggested that copiotrophic-like bacteria appear to be more abundant in the legume than in the C3 grass plots, whereas oligotrophic-like bacteria appear to be more abundant in the C3 grass than in the legume plots. Collectively, these results revealed different impacts of eCO_2 and eN on soil microbial community diversity and composition with few common trends observed across plant functional groups, providing new information for our understanding of the feedback response of soil microbial communities to global change factors.

In the following, we used high-throughput microbial functional gene microarray (GeoChip), stable isotope-based microbial C-sequestration and N-fixation measurements to detect and identify the impacts of eCO_2 and eN on soil microbial functional communities. We found that long-term changes in CO_2 and N availability dramatically altered the diversity and structure of C3 grass-associated soil microbial functional genes via several mechanisms, such as altering plant fine root production, exudation and soil moisture. There was an antagonistic relationship between eCO_2 and eN that affected a large number of microbial functional genes, with eCO_2 generally increasing the abundance of these genes at aN, but either decreasing or increasing abundance to a

minimal degree at eN. These results imply that eCO_2 may accelerate C and nutrient cycling in the C3 grass system, but the magnitude of effect is strongly dependent on the relative availability of N. Particularly, microbial activities associated with chemically recalcitrant soil organic matter (SOM) turnover significantly increased with eCO_2 in low fertility condition (unfertilized C3 grass plots of this study). These changes in C degradation genes suggested enhancement of microbial N mining under long-term eCO_2, an effect may limit soil C storage and stability. Meanwhile, eCO_2 and eN had surprisingly minor effects in the legume-associated soil microbial functional community with generally lower gene abundances at eCaN condition and higher gene abundances at eCeN condition, suggesting that the impacts of eCO_2 and eN are plant-functional-group-specific. This study provides new insights into our understanding of microbial functional processes in response to multiple global change factors.

The potential impact of global change factors (e.g., eCO_2, eN) on microbial activities, such as decomposition of various organic compounds, remains largely inferred from metagenomic analysis targeting the 16S, 28S rRNA, ITS or functional genes. However, the actual activity of microorganism can't be directly measured by such DNA-based technologies. Thus, the following study focused on assessing the influence of long-term eCO_2 on belowground microbial metabolic potential on different C sources provided on Biolog EcoPlate and determining whether the effect of eCO_2 was regulated by soil N conditions in the two plant functional groups (C3 grass and legumes). By cultivating soil samples on Biolog EcoPlate containing 31 low molecular weight C substrates, we constructed sole C source utilization profiles of microbial communities in soil samples mentioned above. We found that community composition of soil microbes based on

metabolic potential (utilization rates of 31 C sources) in the C3 grass plot soils was significantly different from those in the legume plot soils by both DCA and nonparametric dissimilarity tests. Microbial communities in legume plots had significantly higher metabolic potential than in C3 grass plots for decomposing organic substrates. Specifically, compared to the C3 grass plots, microbes in legume plots can use a larger number of C sources provided on EcoPlate and with greater decomposition rates during the measured time. Elevated CO_2 and eN didn't significantly alter metabolic potential of microorganisms in the C3 grass plots. In contrast, overall microbial metabolic activities significantly increased with eCO_2 by 20.6% in the fertilized legume plots, while there was no evidence for a CO_2 effect in the non-fertilized legume soils. Total soil N content, root ingrowth biomass, aboveground biomass, and root biomass N content as environmental attributes were closely correlated with microbial C utilization patterns as suggested by the Mantel test. In addition, PLFA analysis showed both total microbial and bacterial biomass were significantly lower in legume than in C3 grass plots, showing an opposite trend to the microbial metabolic potential in these plots. Collectively, these results demonstrated that eCO_2 effects on active microbial metabolic activities are contingent on N conditions, and such effect differs between plant functional groups. Differences in microbial metabolic potential among treatments and between plant functional groups were not attributed to population size (biomass) but likely attributed to changes in community structure and/or enzymatic activities of belowground microbes.

We further analyzed the impacts of long-term eCO_2 and eN on AOA communities by using 454 pyrosequencing of archaeal-*amoA* gene amplicons. A total of 87 *amoA* OTUs (95% identity cutoff) were generated from 26,211 qualified reads. The diversity of

AOA communities measured by OTU richness (Chao1), Pielou evenness, Shannon and phylogenetic hill number were significantly reduced by eCO_2 but the CO_2 effects were confined within ambient N condition. PCoA, βMNTD and non-parametric dissimilarity tests revealed significant CO_2 effects on the community structure of AOA regardless of N deposition, but no effect of N was observed. We also detected significant changes of several AOA taxa in their relative abundance, which were significantly correlated with plant root biomass, proportional soil moisture, and pH. In addition, significant positive correlations between AOA taxa and soil nitrification rate were observed, indicating AOA may be actively involved in the nitrification process in grassland soil. Interestingly, eCO_2 and eN alone and combined did not significantly alter the abundance of AOA. These results are important in furthering the understanding of the global change impacts on AOA community in the long term.

All studies included in this work provided novel insights into the long-term eCO_2 effects on belowground microbial communities. Our results demonstrated that eCO_2 effects are contingent on soil N conditions and plant functional groups, underscoring the difficulty toward predictive modeling of soil ecosystem under future climate scenarios and necessitating more detailed studies.

Keywords: **Climate change; Elevated CO_2; N fertilization; Soil microbial community; 16S rRNA; microbial functional genes; microbial metabolic potential; *amoA*; ammonia oxidizing archaea; AOA; Illumina sequencing; 454 pyrosequencing; GeoChip; Biolog EcoPlate; progressive nitrogen limitation; priming effect; BioCON**

Chapter 1: Introduction

1.1 Atmospheric CO_2: the background

Global atmospheric carbon dioxide (CO_2) concentration is rising at a record pace. The annual mean global atmospheric CO_2 concentration has increased by more than 40% since the start of the Industrial Revolution, reaching 409 ppm in mid-2017 (Stocker 2013). This is an unprecedented level in the human history and likely the highest over the past 2.6 to 5.3 million years. Anthropogenic activities, primarily fossil-fuel combustion, released an enormous amount of ancient carbon (6-8 PgC/year) that locked within the Earth and directly related to the CO_2 builds up in the atmosphere (Stocker 2013). Land use change (mainly deforestation and agricultural) also strongly contributed to the CO_2 emission. According to the Intergovernmental Panel on Climate Change (IPCC) report, the concentration of atmospheric CO_2 is expected to further increase, reaching approximately 985 ppm by the end of this century if fossil fuels maintain their dominant position in the global energy production (Stocker 2013). As one of the most important atmospheric components that interact with Earth's biosphere, such a rapid increase in CO_2 concentration would bring dramatic impacts on the Earth's ecosystem. Primary impacts of increasing atmospheric CO_2 on ecosystem include the magnitude and rate of climate changes (e.g. global warming, ocean acidification, extreme weather). Secondarily, increasing atmospheric CO_2 is expected to change global C and nutrient cycling by altering phenology, physiology, community composition and interaction, and functional activities of macro- and microorganisms (Walther et al. 2002, Drigo et al. 2008, Stocker 2013).

1.2 Consequences of elevated atmospheric CO_2 for macroecosystems

Elevated CO_2 atmospheric concentrations can cause an immediate stimulation of plant photosynthesis and net primary production (NPP), referred to as the CO_2 fertilization effect (Amthor 1995). In particular, C3 plants respond markedly to elevated CO_2, and in the coming century, a 30-50% increase of C3 plant photosynthetic activity is expected (Kuzyakov and Domanski 2000, Long et al. 2004). The CO_2 fertilization effect could increase terrestrial C uptake and is expected to provide negative feedback to CO_2 accumulation (IPCC 2007), although it is uncertain how sustainable this effect is and to what extent it will promote C allocation to soil (Oren et al. 2001, Schneider et al. 2004, Reich et al. 2006, Inauen et al. 2012). One major aspect of this uncertainty is that the increase in plant N uptake and immobilization of N at eCO_2 could lead to progressive N limitation (PNL), a decrease of soil N availability over time. PNL theory suggests that soil N availability should be gradually reduced over time by elevated CO_2 and that the CO_2 fertilization effect should occur only in short time in N limited ecosystems (Johnson 2006). However, over the past three decades, empirical evidence across studies in pots, growth chambers, open-top chambers and FACE (Free Air Carbon Dioxide Enrichment) experiments showed inconsistent and controversial results that CO_2 fertilization effect either down-regulated over long-term CO_2 enrichment (Ainsworth and Long 2005, Norby et al. 2010, Reich and Hobbie 2013), or increased and accompanied by an increase in plant N uptake (Finzi et al. 2007, McCarthy et al. 2010). The mechanism by which plants retain long-term growth response to eCO_2 in these studies remains unclear. Soil N levels were extremely limited in some of these studied ecosystems (e.g. BioCON FACE experiment), thus it is unlikely that PNL was simply

delayed. It has been proposed that the priming effect, an opposing mechanism, may play a role simultaneously in these ecosystems in offsetting the PNL effects (Reich and Hobbie 2013). In addition, a stimulation of microbial N fixation by additional plant organic input was documented in some CO_2 enrichment studies, which may help in alleviating or preventing the PNL effects (Lee et al. 2003, van Groenigen et al. 2006, He et al. 2010).

Under nutrient limited conditions (particularly low N availability), even if there is no significant CO_2 stimulation of total or aboveground plant biomass production (Korner and Arnone 1992, Zak et al. 2000, Oren et al. 2001, Shaw et al. 2002, Hungate et al. 2003, Luo et al. 2004), plants exposed to elevated CO_2 can allocate a greater amount of photosynthate to enhance root development and exudation to 'mine' nutrients from soil (Johnson 2006). Such enhancement of belowground C allocation by elevated CO_2 was documented in several CO_2 enrichment experiments (Korner and Arnone 1992, Diaz et al. 1993, Hungate et al. 1997, Jones et al. 1998, Schlesinger and Lichter 2001, Lukac et al. 2003, Norby et al. 2004, Heath et al. 2005, Korner et al. 2005, Carney et al. 2007, Finzi et al. 2007, Pollierer et al. 2007, Pritchard et al. 2008, Phillips et al. 2009), and to a greater amount with low than high soil N availability (Phillips et al. 2011). Concomitant changes in the chemical composition (e.g. C/N ratio) of litter and exudates were also widely reported in these studies.

1.3 Consequences of elevated atmospheric CO_2 for microbial communities belowground

The concentration of CO_2 in soil pore space is much higher (10 to 15 times) than in the atmosphere, thus the direct influence of rising CO_2 atmospheric concentration on soil

microbial community should be negligible compared to the indirect effects, such as stimulating plant organic matter inputs, altering plant physiological characteristics and soil chemistry (Kandeler et al. 1998, Janus et al. 2005).

As soil microorganisms are generally C-limited, the increase in plant-derived carbon (C) inputs could enhance the biomass and activity of belowground microbes. Increased microbial activities, such as decomposition, will enhance organic matter turnover, offsetting the effect of plant C fixation from the air. Meanwhile, the rates of nutrient cycling (e.g. N, S and P) are expected to increase as dynamics of these nutrients are strongly coupled with C turnover. Particularly, under nutrient limited conditions, stimulated microbial population by elevated CO_2 can synthesize more extracellular enzymes for depolymerization of N from old soil organic matter (SOM) to meet their increasing nutrient demand (priming effect) (Cheng 2005). This N will eventually be released for plant uptake during microbial biomass turnover, which could support plant growth response under long-term elevated CO_2 (Dijkstra et al. 2009). There is a consensus that C cycling mediated by microbes is essential in influencing C storage and soil N availability, thus understanding the response of microbial biomass, activity and the potential shifts in microbial community structure is central to predicting changes in soil C and N cycling under elevated CO_2 conditions.

Although common responses of plants (e.g. higher NPP and C allocation to soil, altered nutritional quality) to elevated atmospheric CO_2 were documented, a corresponding picture of common patterns in belowground microbial community responses to elevated CO_2 have not yet emerged (Jossi et al. 2006, Carney et al. 2007, Jin and Evans 2007, Lesaulnier et al. 2008, Austin et al. 2009, Dunbar et al. 2012, Xu et al.

2013, Berthrong et al. 2014, Yu et al. 2016). Studies examining effects of elevated CO_2 concentrations on microbial community biomass and activity are highly variable and ecosystem-specific. Previous studies reported mainly positive effects of elevated CO_2 concentration on soil microbial growth and activities (e.g. decomposition and nutrient cycling) as a result of alterations in C inputs (Zak et al. 1993, Cotrufo and Gorissen 1997, Sadowsky and Schortemeyer 1997, van Ginkel et al. 2000, Zak et al. 2000, He et al. 2010, Tu et al. 2015). However, contrasting observations were also found with a decrease (Diaz et al. 1993, Ebersberger et al. 2004) or no change in the growth and/or activities of belowground microbial communities by elevated CO_2 (Jones et al. 1998, Kandeler et al. 1998, Hu et al. 1999). Since soil N conditions can drastically regulate plant physiological responses to elevated CO_2 and vary among sites and over time, it may cascade to alter the responses of belowground microbial community to elevated CO_2 and largely contribute to the mixed results in these studies (Hu et al. 2001).

Community diversity and composition of microorganisms are major factors responsible for ecosystem multifunctioning and stability (McCann 2000, Hector and Hooper 2002, Tilman et al. 2006, Hector and Bagchi 2007, Zavaleta et al. 2010, Wagg et al. 2014). A number of previous studies across FACE experiments detected either no or minor significant changes in microbial community composition by elevated CO_2 (Zak et al. 2000, Chung et al. 2006, Austin et al. 2009). In contrast, significant compositional and structural shifts of microbial communities and decreased microbial richness under elevated CO_2 were observed as a result of CO_2-induced plant and soil properties changes, such as plant biomass, soil moisture, and soil C and N contents (Deng et al. 2012, He et al. 2012). In addition, increased bacterial diversity and/or decreased archaeal diversity as

a result of elevated CO_2 were also reported (Janus et al. 2005, Lesaulnier et al. 2008). Disparity of microbial responses to elevated CO_2 in these studies could be due to the following major aspects: (1) the extreme diversity of soil microbial communities; (2) ecosystem differences (e.g. ecosystem-specific environmental attributes); (3) differences among the methodologies used, such as restriction fragment length polymorphism (RFLP), denaturing gradient gel electrophoresis(DGGE), enzyme activities, phospholipid fatty acid (PLFA), and 16S rRNA gene-based sequencing, which may resolve differences in the soil community caused by elevated CO_2 to differing degrees.

Soil microbial community tends to shift in consistent ways in the taxonomic and functional traits along higher nutrient availability (e.g. N, P), with the faster-growing copiotrophic bacterial taxa being increased in relative abundances and slower-growing oligotrophic bacterial taxa being decreased in relative abundances (Leff et al. 2015). Such changes in microbial community may relate to shifts in general life history strategies with bacterial taxa that are faster growing and more copiotrophic being favored under conditions of elevated nutrient availability (Leff et al. 2015, Roller and Schmidt 2015, Roller et al. 2016).

Methodologically, the fast developing high-throughput technologies (e.g. 454, Illumina sequencing), targeting the 16S rRNA or other functional gene markers (e.g. *amoA*), offer quick screening of community-wide spatial and temporal information on microbial composition and functional potential. More importantly, deep sequencing by these approaches provides more thorough characterization of microbial communities and allows capture of the response of less abundant taxa (Austin et al. 2009, Dunbar et al. 2012). Therefore, advanced sequencing methods may help to detect changes in microbial

community composition at finer, previously unexamined taxonomical levels by relatively coarse methods (e.g. PCR-DGGE, RFLP). However, sequencing-based approaches suffer from high sensitivity to random sampling errors, contaminated non-target DNA and dominant populations (Zhou et al. 2008). Currently, the use of advanced sequencing technologies in characterizing the belowground microbial community is still challenging, especially for the genetic and functional diversity. On the other hand, microarray-based metagenomics technologies (e.g. GeoChip, PhyloChip) do no suffer from these limitations, and provide community-wide information on microbial functional structure and potential activity (Zhou et al. 2008). An integration of high-throughput metagenomic approaches such as 454 and Illumina sequencing and microbial gene microarray such as GeoChip would be ideal to work in a complementary way in characterizing microbial community.

1.4 Foci of this study

Despite the wide range of key ecological processes and the mediation of ecosystem responses to global changes that belowground microbial communities support (Chapin et al. 2000, Francis et al. 2007), the response of these communities to elevated atmospheric CO_2, particularly possible interactive effects of elevated CO_2 concentration with dynamic soil N availability, remains largely unclear (van Groenigen et al. 2006, Craine et al. 2007). Meanwhile, in contrast to the numerous studies on small scale, short-term CO_2 enrichment experiments, results of long-term elevated CO_2 effects on belowground microbial community biomass, composition, and activities are still rare due partly to the low number of long-term experiments manipulating CO_2 concentrations (e.g. FACE

experiments). Short duration of CO_2 enrichment experiments often ignored the co-limitation by N supply on CO_2 fertilization effect, which can generate inconsistent results and make the extrapolation of these results to long-term ecosystem feedbacks to elevated CO_2 problematic (He et al. 2010, Xiong et al. 2015). By integrating traditional microbiological methods (e.g. PLFA, Biolog), high-throughput metagenomic approaches (e.g. 454 and Illumina sequencing, functional gene array), and stable isotope-based microbial C-sequestration and N_2-fixation measurements, this study aimed to reveal whether and how soil N conditions affect the ecological effects of long-term elevated CO_2 on microbial community and soil ecoprocess in a comprehensive manner. Major results are presented in chapter 2 to chapter 5.

This study was conducted at the BioCON (the Biodiversity, CO_2, and Nitrogen Experiment) experiment site, one of the longest CO_2 manipulation experiments (established since 1998) in the world by using the free-air CO_2 enrichment (FACE) technology (Reich et al. 2001, Reich et al. 2004). The BioCON experiment is located at the Cedar Creek Natural History Area, in central Minnesota, USA with CO_2, N deposition and plant diversity treatments arranged in 296 2 × 2 m plots. All the plots were merged into six rings with nearly 20 m diameter each. Half of the rings receive air with increased concentration of CO_2 (560 μmol mol^{-1}) during the growing seasons (April to October), the other half of the rings receive ambient CO_2 (368 μmol mol^{-1}). N enrichment was conducted by applying N fertilizer (4 g m^{-2} yr^{-1} of NH_4NO_3) to half of these plots three times per growing season (mid-May, mid-June, and mid-July). Plant species numbers were directly manipulated (1, 4, 9, or 16 perennial grassland species randomly chosen from a pool of 16 species, planted as seed in 1997). The BioCON experiment allows us

to examine the effects of elevated CO_2 concentration in natural field conditions (e.g., natural amounts of rain, wind, light). With N manipulation, it allows the study of elevated CO_2 concentration impacts on plant growth and soil microbial changes as affected by soil N availability.

Chapter 2 describes the plant-mediated impact of elevated CO_2 on belowground microbial communities of two plant functional groups, C3 grass and N-fixing legume. Analyses focused on characterizing the profile of bacterial and archaeal community diversity and structure. The microbial communities were profiled by high-throughput Illumina sequencing, targeting the 16S rRNA gene amplicons. Greater sequencing depth of such technology provides more thorough characterization of microbial communities and allows capture of the responses of previously undetected less abundant taxa. In **chapter 3**, I examined effects of elevated CO_2 on microbial functional structure and activities, using respectively microbial functional gene array (GeoChip 3.0), soil respiration measurement and stable isotope-based microbial C-sequestration and N-fixation measurements. Subsequently, multivariate statistical analyses were used to link those community responses with plant and properties, and compare the relative impact of elevated CO_2, N addition treatments versus plant and soil effects on these communities. **Chapter 4** aims to assess if soil N status influences the response of microbial metabolic potential to elevated CO_2. To gain insight into the actual activity of active microbial populations that can't be directly measured by such DNA-based technologies, community-level physiological profile (CLPP), based on the utilization pattern of various carbon sources was measured using Biolog EcoPlate. **Chapter 5** focuses on a subset of soil microbes: ammonia oxidizing archaea (AOA), a group of phylogenetically distinct

microorganisms that possess the same functional trait — the gene *amoA* encoding ammonia monooxygenase and functioning as nitrification. Using a PCR-based 454-pyrosequencing approach, this chapter examines how AOA community are influenced by CO_2 treatment and N addition. The results of the different studies are summarized, discussed and evaluated in **chapter 6**. Overall, this work provided novel insights into the microbial community diversity, composition, functional structure and potential activity changes in response to long-term elevated CO_2 under contrast soil N conditions, and be of merit for a mechanistic understanding of the ecosystem responses to elevated atmospheric CO_2.

Chapter 2: Responses of soil microbial communities to elevated carbon dioxide and nitrogen deposition differ by C3 and legume plants

2.1 Abstract

Understanding soil microbial responses to global change factors, such as elevated CO_2 (eCO_2) and N deposition (eN), is crucial for estimating ecosystem feedbacks and predicting future climate change. This study investigated soil bacterial and archaeal communities subjected to CO_2 (ambient, 368 µmol mol^{-1}, versus elevated, 560 µmol mol^{-1}) and N (ambient, 0 g m^{-2} yr^{-1}, versus elevated, 4 g m^{-2} yr^{-1}) treatments for over 12-years in a grassland (BioCON) using Illumina MiSeq sequencing of 16S rRNA gene amplicons. Over 2.3 million passing sequences were obtained from a total 24 samples, corresponding to 38 known phyla, 96 classes, and 565 genera. Elevated CO_2 significantly altered the diversity and composition of microbial communities, but these changes varied greatly depending on soil N conditions and plant functional groups. In C3 grass plots, community diversity and richness increased with eCO_2 and eN, respectively. *Actinobacteria* abundance decreased with eCO_2, accounting for about 20.3% of the total population in the C3 grass. *Chlamydiae* increased with eCO_2 and eCO_2+eN, and *Woesearchaeota* increased with eN. In legume plots, community richness measured by Chao1 estimator increased significantly with eCO_2 at both N conditions. The abundance of *Actinobacteria*, *Chloroflexi*, *Armatimonadetes*, *Saccharibactiera*, and *Euryarchaeota*, accounting for about 21.2% of the total population in legume plots, decreased with eCO_2, eN or both. Only *Nitrospirae* and *Latescibacteria* significantly increased with eCO_2 in their relative abundances. Changes in community diversity and composition were significantly correlated to plant and soil properties including plant biomass, biomass N

content and C/N ratio, soil ammonium and nitrate, pH, moisture, temperature, and soil C and N contents by Mantel analysis. Collectively, our results revealed different impacts of eCO_2 and eN on soil microbial community diversity and composition with few common trends observed across plant functional groups. This study provides new information of the feedback response of soil microbial communities to global change factors.

Keywords: 16S rRNA; Illumina sequencing; Climate change; Elevated CO_2; N fertilization; Soil microbial community; BioCON

2.2 Introduction

Elevated CO_2 (eCO_2) fertilization effect is commonly found to stimulate plant growth and enhance carbon (C) allocation toward soils, which may lead to negative feedback to climate change (Zak et al. 2000, Reich et al. 2001, Ainsworth and Long 2005, Drigo et al. 2008, Souza et al. 2010). However, an increase in the soil organic C pool is not always observed (Lichter et al. 2008) under eCO_2, despite greater plant primary productivity and root exudation. For example, Jastrow et al (2005) reported a 5.6% increase in soil C over 2-9 years of eCO_2 at a median rate of 19 g C m^{-2} yr^{-1} (Jastrow et al. 2005). While other studies revealed barely any change (van Groenigen et al. 2014) through meta-analysis or a slight decrease of soil C pool as a result of enhanced decomposition via long-term (3 years) field experiments (Peralta and Wander 2008). The discrepancy between modeling and empirical evidence suggests our understanding of ecosystem feedback mechanisms to eCO_2 is incomplete.

Elevated CO_2-enhanced plant primary production doesn't always lead to greater C accumulation in the soil because rates of microbial growth and metabolism can also increase in response to the extra organic matter input (Blagodatskaya et al. 2010) (Field et al. 1995, Reed et al. 2011). These phenomena could be more pronounced under N-limited conditions, releasing larger amount of C than fixed due to enhanced microbial decomposition of both fresh substrates and native soil organic matter, known as 'priming effect' (Kuzyakov et al. 2000, Hoosbeek et al. 2004). N fertilization (eN), another major environmental change factor, could decrease the priming effect by suppressing the oligotrophic microbial taxa (e.g., *Actinobacteria, Verrucomicrobia*) and their N-mining activities on SOM (Fierer and Schimel 2003, van Groenigen et al. 2006, Ramirez et al.

2010, Ramirez et al. 2012, Chen et al. 2014). However, it is also suggested that N fertilization may induce greater decomposition from higher availability of labile litter with high C/N ratio possibly by favoring copiotrophic microbial taxa (e.g., *Firmicutes*) (Wild et al. 2014). Therefore, the consequences of increased plant C allocation toward soil on ecosystem C storage depend on the responses of soil microbial communities of different composition and C decomposition capabilities (Phillips et al. 2011). However, few common responses of microbial community composition and structure, biomass and activity to these environmental change factors were found across sites (Jossi et al. 2006, Carney et al. 2007, Jin and Evans 2007, Lesaulnier et al. 2008, Austin et al. 2009, Dunbar et al. 2012, Xu et al. 2013, Berthrong et al. 2014, Yu et al. 2016), making it hard to predict the changes in soil C storage under eCO_2. In addition, although impacts of eCO_2 and eN on soil microorganisms have been thoroughly studied individually, their interactive effects on soil microbial community remain notoriously understudied which further hampers our ability to accurately predict soil C dynamics under global climate change.

Our study was conducted at the BioCON experiment site, one of the longest CO_2 manipulation experiments in the world by using the free-air CO_2 enrichment (FACE) technology (Reich et al. 2001, Reich et al. 2004). It allows us to examine the effects of eCO_2 in natural field conditions (i.e. natural amounts of rain, wind, light). Ammonium nitrate was applied to the experimental plots, allowing the study of eCO_2 impacts on plant growth and soil microbial changes as affected by soil N availability. A number of previous studies on BioCON and other FACE experiment soils detected either no or minor changes in microbial community composition by eCO_2 (Zak et al. 2000, Chung et al. 2006, Austin et al. 2009). However, significant changes in functional gene abundances

and enzymatic activities were noted under conditions of eCO_2 (Chung et al. 2006, He et al. 2010), indicating changes in microbial community composition at finer, previously unexamined taxonomical levels due largely to the relatively coarse methods (i.e. PCR-DGGE, clone libraries), or altered metabolic strength. To address this knowledge gap, we conducted in-depth analysis to characterize more complete profile of microbial diversity, compositional and structural responses to eCO_2 and eN, and how it is affected by different plant functional groups (C3 grass and legume). We also aimed to link those community responses with plant properties and soil geochemistry. The microbial communities were profiled by high-throughput Illumina sequencing, targeting the 16S rRNA gene amplicons. Greater sequencing depth of such technology would provide more thorough characterization of microbial communities and allows capture of the responses of previously undetected less abundant taxa (Austin et al. 2009, Dunbar et al. 2012). Given that eCO_2 and eN commonly change C inputs to soil through greater litter fall and root activity (Lukac et al. 2009, Phillips et al. 2011), and alter nutritional quality of plant litter or root exudates (Parsons et al. 2008, Phillips et al. 2009) and soil chemistry (Field et al. 1995, Saarsalmi et al. 2006), we predicted that increased C input into soil as a result of stimulated plant biomass production under eCO_2 would reduce microbial competitions and increase overall microbial diversity, and significantly change the community structure and composition. The response of certain microbial populations to eCO_2 may be altered by soil N status. For example, low limiting resource (N) availability should select for efficient growth and have greater oligotrophic membership in response to eCO_2, whereas the relative abundance of copiotrophs may promote in response to eCO_2-induced additional organic matter input in N enrich soil (Koch 2001, Roller and Schmidt 2015).

We also predicted that microbial communities in the C3 grass and legume plots will respond differently to eCO_2 and eN due to varied plant mediated soil C, N inputs and soil chemistry (Lee et al. 2001, Craine et al. 2003, Craine et al. 2003, Lee et al. 2003).

2.3 Materials and Methods

2.3.1 Site description and experimental design:

The BioCON experiment at Cedar Creek Natural History Area, in central Minnesota (45°24′13.5″N, 93°11′08″W), was established on a glacial outwash comprised of loamy sand soils with poor nitrogen availability (Reich et al. 2001). A total of 296 2 × 2 m plots were merged into six rings with nearly 20 m diameter each. Half of the rings receive air with increased concentration of CO_2 (560 μmol mol^{-1}) during the growing seasons (April to October), the other half of the rings receive ambient CO_2 (368 μmol mol^{-1}). The CO_2 manipulation was achieved through Free-Air Carbon dioxide Enrichment (FACE) technology. N enrichment was conducted by applying N fertilizer (4 g m^{-2} yr^{-1} of NH_4NO_3) to half of these plots 3 times per growing season (mid-May, mid-June, and mid-July). For a more detailed site description refer to Reich, et al. (2001) (Reich et al. 2001).

Soil samples without plant root from a subset of plots of the FACE experiment were collected for analyses, specifically, the 24 4-plant species plots (12 with C3 grass, and 12 with legume) receiving CO_2 and/or N treatments, with 3 biological replicates each. C3 grass and N-fixing legume were used to assess soil microbial community responses to the treatment factors (eCO_2 and eN) as affected by distinct plant functional groups. Plots were manually weeded on a regular basis to remove unwanted species. Bulk soil samples were taken in June 2009, during the growing season, and each sample was

composited from five randomly collected soil cores at a depth of 0-15 cm. All samples were immediately transported to the laboratory and stored at 4^{o}C and -80^{o}C for following analyses.

2.3.2 Plant and soil property measurements

Plant biomass. The aboveground and belowground (0–20 cm) biomass were measured as previously described (Reich et al. 2001, Reich et al. 2006). Briefly, a 10 x 100 cm strip was clipped at just above the soil surface, and all plant material was collected, sorted to live material and senesced litter, dried and weighed. Roots were sampled at 0–20 cm depth using three 5-cm diameter cores in the area used for the aboveground biomass clipping. Roots were washed, sorted into fine (< 1 mm diameter) coarse and crowns classes, dried and weighed.

Soil physical properties. Soil pH and volumetric soil moisture were measured at depths of 0-17, 42-59, and 83-100 cm in a KCl slurry and with permanently placed TRIME Time Domain Reflectometry (TDR) probes (Mesa Systems Co., Medfield MA), respectively (Fig. S2.1). Other soil properties including temperature, total soil C and N concentrations, soil NO_3^+-N and NH_4^--N were measured on site and described previously (Reich et al. 2006).

Soil processes. Net N mineralization rates were measured concurrently in each plot for one-month in situ incubations with a semi-open core at 0-20 cm depth during mid-summer of each year (Reich et al. 2001, Reich et al. 2006). Net N mineralization rates were determined by the difference between the final and initial NH_4^+-N + NO_3^--N pool sizes determined with 1 M KCl extractions. Net ammonification was determined by

the difference between the final and initial NH_4^+-N pool sizes. Net nitrification was determined by the difference between the final and initial NO_3^--N pool sizes.

2.3.3 DNA isolation, PCR amplification of the 16S rRNA gene and Illumina sequencing

Microbial community DNA was extracted from 5 g of soil from each sample using a freeze-grinding method and purified through agarose gel electrophoresis (Zhou et al. 1996). DNA quality was assessed by the ratios of 260/280 nm and 260/230 nm using a NanoDrop ND-1000 Spectrophotometer (NanoDrop Technologies Inc., Wilmington, DE), and DNA concentration was measured by PicoGreen using a FLUOstar OPTIMA fluorescence plate reader (BMG LABTECH, Jena, Germany). The V4 region of the 16S rRNA genes was amplified using a two-step PCR amplification method with the primer pair 515F (5'-GTGCCAGCMGCCGCGGTAA-3') and 806R (5'-GGACTACHVGGGTWTCTAAT-3') combined with Illumina adapter sequences, a pad and a linker of two bases, as well as barcodes on the reverse primers (Wu et al. 2015). Sample libraries were generated from purified PCR products. The Miseq 300 cycles kit was used for 2 × 150 bp paired-ends sequencing on Miseq machine.

2.3.4 Sequence data preprocessing and statistical analysis

Illumina sequencing of the 16S gene was performed on a Miseq (Illumina, San Diego, CA, USA), producing 250 bp reads per end, according to manufacturer's instructions. Raw sequences were processed through Galaxy pipeline developed by Yujia Qin. Briefly, raw sequences with 100% matches to barcodes were split to sample libraries and were trimmed using BTRIM (Kong 2011) with threshold of QC higher than 20 over 5 bp window size and the minimum length of 100 bp. Forward and reverse reads with at least 10 bp overlap and lower than 5% mismatches were joined using FLASH (Magoc and

Salzberg 2011). After trimming of ambiguous bases (i.e. N), joined sequences with lengths between 240 and 260 bp were subjected to chimera removal by U-Chime (Edgar et al. 2011). Operational taxonomic unit (OTU) clustering was performed through UCLUST (Edgar 2010) at 97% similarity level, and taxonomic assignment was through SILVA public 16S rRNA database (Quast et al. 2013). Singletons were removed from each treatment for downstream analyses. Samples were rarefied at 50,000 sequences per sample. Subsequent analyses were performed in R , version 2.9.1 (R Foundation for Statistical Computing, Vienna, Austria). Dissimilarity tests were based on Jaccard and Bray-Curtis dissimilarity indices using Adonis under the package of VEGAN (Dixon 2003). To make a principal coordinate analysis (PCoA) of UniFrac distances, OTU representative sequences were aligned against GreenGenes 16S rRNA database using PYNAST, followed by tree computation with FASTTREE. The PCoA analysis was based on weighted and unweighted UniFrac distance matrix using the classical multidimensional scaling method. Differences in abundance across treatments were determined by ANOVA analysis followed by Least Significance Difference (LSD) test.

2.4 Results

2.4.1 Structure of soil bacterial and archaeal communities

Over 2.3 million qualified sequences were obtained from the total 24 samples. After OTU clustering at 97% sequence identity, removal of singletons and rarefaction at 50,000 sequences per sample, 62,248 OTUs remained (with 42,446 in C3 grass plots and 39,841 in legume plots), out of which 25,653 OTUs were affiliated to 38 known phyla, 96 classes, and 565 genera. Archaea accounted for 0.44% (113 OTUs) of the total population, of which 91% were *Thaumarchaeota* and 8% were *Euryarchaeota*. Within the bacterial

domain, *Proteobacteria* were the most abundant phylum in both C3 grass (29.8% in relative abundance) and legume plots (34.7%), followed by *Actinobacteria* (20.3% in C3 grass and 16.1% in legume), *Acidobacteria* (18% in C3 grass and 16% in legume) and *Verrucomicrobia* (14.6% in C3 grass and 10.4% in legume) (Fig. 2.1). Meanwhile, 0.23% OTUs in the C3 grass and 0.25% OTUs in legume plots were not assigned to any known phylum (Fig. 2.1).

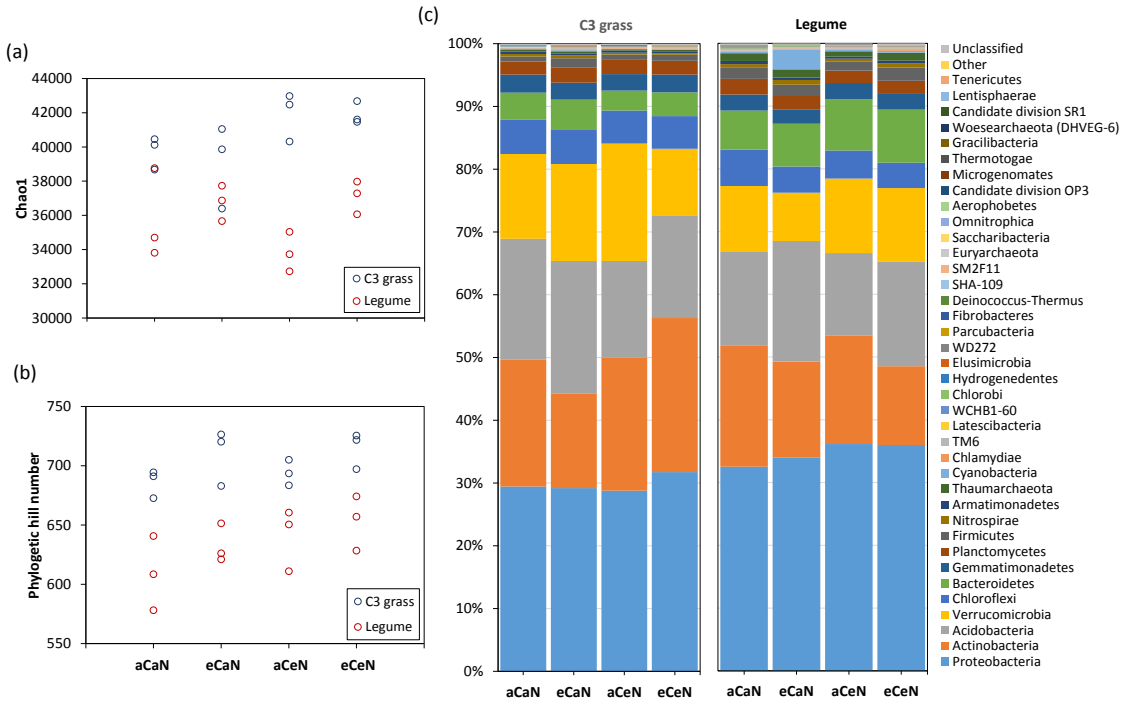

Fig. 2.1 Effects of eCO_2 and eN on microbial richness measured as Chao1 estimator (a) and diversity measured as phylogenetic hill number (b). Community composition of C3 grass and legume plots under different CO_2 and N regimes at the phylum level (c).

At the genus level, OTUs belonging to the *Chthoniobacterales* DA101 soil group of *Verrucomicrobia* was the most dominant group in both C3 grass (13.0%) and legume plots (8.8%), along with Subgroup 4 of *Acidobacteria* (7.9%), *Afipia* (7%), Subgroup 6 of *Acidobacteria* (3.8%), *Sphingomonas* (3.1%), *Massilia* (2.7%), *Gaiellales* of *Actinobacteria* (2.1%), *Gemmatimonadales* of *Gemmatimonadetes* (2.0%),

Solirubrobacter (1.2%), *Chitinophagaceae*, *Acidobacteriaceae* (Subgroup 1) (1.2%), *Pseudonocardiaceae* (1.1%), *Micrococcaceae* (1.1%), *Nitrosomonadaceae* (1.0%), and *Mycobacteriaceae* (1.0%), accounting for 50.5% of total abundance in C3 grass; and along with Subgroup 4 of *Acidobacteria* (6.9%), *Sphingomonas* (4.2%), Subgroup 6 of *Acidobacteria* (3.0%), *Sphingobacteriales* of *Bacteroidetes* (2.4%), *Afipia* (2.3%), *Variibacter* (2.0%), *Massilia* (2.0%), *Gemmatimonadales* of *Gemmatimonadetes* (1.8%), *Acidobacteriales* of *Acidobacteria* (1.7%), *Gaiellales* of *Actinobacteria* (1.7%), *Arthrobacter* (1.4%), and *Nitrosomonadales* of *Proteobacteria* (1.1%), accounting for 39.5% of total abundance in legume plots.

2.4.2 Effect of eCO_2 and eN on microbial community diversity and structure

Elevated CO_2 and eN differentially altered the α-diversity of microbial communities of C3 grass and legume plots. Phylogenetic diversity as measured by phylogenic hill number (q=0, a species richness estimator) (Chao et al. 2010) in C3 grass plots and OTU richness as measured by Chao1 diversity estimator (Chao 1984, Colwell and Coddington 1994) in legume plots increased with eCO_2 ($P < 0.05$) (Fig. 2.1). OTU richness also increased in C3 grass plots with eN ($P < 0.05$) (Fig. 2.1).

The principle coordinates analysis (PCoA) based on both weighted and unweighted UniFrac distances showed a combined effect of eCO_2, eN and soil physio-chemical properties on the β-diversity of the bacterial communities in C3 grass and legume plots (Fig. S2.2). Based on the weighted PCoA models, the first three dimensions together explained 69.94% and 65.32% of the observed variations in C3 grass and legume plots, respectively. Community compositions under four CO_2 and N levels were

significantly different from each other based on Jaccard distance method regardless of plant functional groups (Table 2.1), which was also reflected on the ordination plot.

Table 2.1 Effects of eCO_2 and eN on additional plant and soil attributes.

	Groups	adonis.F (Jaccard)	adonis.p (Jaccard)	adonis.F (Bray-Curtis)	adonis.p (Bray-Curtis)
C3 grass	aCaN vs eCaN	1.374	**0.001**	0.866	0.600
	aCaN vs aCeN	1.373	**0.001**	1.036	0.506
	aCaN vs eCeN	1.345	**0.017**	0.984	0.609
Legume	aCaN vs eCaN	1.399	**0.001**	1.049	0.379
	aCaN vs aCeN	1.355	**0.001**	0.772	0.756
	aCaN vs eCeN	1.374	**0.001**	0.976	0.670

2.4.3 Changes in community composition along eCO_2 and eN

Treatment effects of eCO_2 and eN, individually or together, were inconsistent on the abundance of microbial groups at the phylum level between C3 grass and legume plots. Within C3 grass plots, the abundances of three phyla were significantly altered by treatments as compared to the control receiving no additional CO_2 and N, including *Actinobacteria*, *Chlamydiae* and *Woesearchaeota*, accounting 20.4% of the total population (Fig. 2.2, $P < 0.05$). Among these phyla, the abundance of *Actinobacteria* (20.3% in relative abundance) decreased with eCO_2 but only in unfertilized soil (aN). *Chlamydiae* increased with eCO_2 in both fertilized and unfertilized soil. Within legume plots, abundances of seven phyla were altered by treatments, accounting 21.8% of the total population within legume plots (Fig. 2.2, $P < 0.05$). Most of these phyla decreased with eCO_2 in the unfertilized soil, including *Chloroflexi*, *Armatimonadetes*, *Saccharibactiera*, and *Euryarchaeota* (5.1% in relative abundance). *Actinobacteria*, accounting 16.1% of the total population in legume plots, decreased with eCO_2 regardless

of N fertilization. Whereas, *Nitrospirae* and *Latescibacteria* increased with eCO_2 in unfertilized and fertilized soil, respectively.

	a	ab	b	bc	c

	Phylum	aCaN mean	eCaN mean	aCeN mean	eCeN mean	Abundance (%)	Treatment effects vs. aCaN
C3	*Actinobacteria*	10116	7538	10573	12259	20.262%	Decreased with eCaN
	Chlamydiae	41	77	46.7	60	0.116%	Increased with eCaN & eCeN
	Woesearchaeota	0	0	4	0	0.001%	Increased with aCeN
	Saccharibacteria	2.3	0.3	0.7	4	0.004%	None
Le	*Chloroflexi*	2902.3	2079	2226.3	1966.7	4.624%	Decreased with eCaN
	Armatimonadetes	253.7	188.7	169.7	225.7	0.422%	
	Saccharibacteria	7	3	5	3.7	0.009%	
	Euryarchaeota	7	0	3.3	0.7	0.006%	
	Actinobacteria	9661	7618	8597.7	6102.7	16.099%	Decreased with eCaN & eCeN
	Latescibacteria	10	30	13.3	21.3	0.038%	Increased with eCaN
	Nitrospirae	251.7	378.7	219.3	303.3	0.582%	Increased with eCaN & eCeN
	Chlamydiae	73.3	93.7	52.3	115.7	0.170%	None
	Acidobacteria	7423	9603	6578.3	8116.3	15.996%	None

Fig. 2.2 Phyla with different abundance levels among treatments. The color panel under 'aCaN', 'eCaN', 'aCeN' and 'eCeN' reflects both the absolute abundance (mean of sequence count) of the corresponding phylum and the relative abundance level at each treatment by LSD test. Red toned cells, (a); Blush toned cells, (ab); White toned cells, (b); Sapphire toned cells, (bc); and Blue toned cells, (c).

Further examination revealed significant changes occurred in several microbial populations at finer taxonomic levels, many of which were associated with those unchanged phyla under treatments at the phylum level. At the class level, the abundance of 13 and 22 classes were significantly altered in response to treatments in the C3 grass and legume plots, respectively (Fig. S2.3, $P < 0.05$). Of these groups, four classes decreased in response to eCO_2 within C3 grass plots (20.0% in relative abundance), with *Actinobacteria* and *Thermoleophilia* in the unfertilized soil, and *Acidimicrobiia* and *Planctomycetes* BD7-11 in fertilized soil. On the contrary, abundance of four classes (1.8% in relative abundance), including *Gammaproteobacteria*, *Chlamydiae*, *Verrucomicrobia* UA11, and *Bellilinea*, increased with eCO_2 in unfertilized soil. Within legume plots, nine classes decreased in abundance in response to eCO_2 (9.5% in relative abundance), of which three decreased in unfertilized soil (*Deltaproteobacteria*,

Phycisphaerae, and *Chloroflexi* JG30-KF-CM66), three decreased in fertilized soil (*Chloroflexi* TK10, *Chloroflexi* Gitt-GS-136, and *Actinobacteria* TakashiAC-B11), and another three decreased regardless of soil N levels (*Chloroflexi* JG37-AG-4, *Thermoleophilia*, *and Thermoplasmata*). Contrarily, five classes were increased in response to eCO_2 (2.6% in relative abundance), among which *Acidobacteria* Subgroup 22 and 26 increased in the unfertilized soil, *Gammaproteobacteria* and *Bacteroidetes* VC2.1 Bac22 increased in fertilized soil, and *Latescibacteria* increased in both soil N levels. At the genus level, the abundance of 20 genera in C3 grass plots were decreased with eCO_2, either in unfertilized soil (*Patulibacter* and *Virgisporangium* associated with *Actinobacteria*), or in fertilized soil (10 genera, i.e. *Acidobacteria* Subgroup 5 and Subgroup 17, *Frankiales*), or in both (eight genera, i.e. *Sphingobacteriales*, *Acidimicrobiales*, *Herpetosiphon*) (Fig. S2.4, $P < 0.05$). Whereas abundance increased with eCO_2 in another 84 genera, of which 46 increased in unfertilized soil (i.e. *Acidobacteria* Subgroup 4, *Hyphomicrobium*, *Paenibacillus*), 30 increased in fertilized soil (i.e. *Mycobacterium*, *Solirubrobacterales*, *Micromonosporaceae*), and eight increased in both soil N levels (i.e. *Kribbella*, *Gammaproteobacteria* NKB5, *Legionella*). In legume plots, 34 genera decreased in abundance, with 11 decreased in unfertilized soil (i.e. *Solirubrobacterales*, *Haliangium*, *Sorangium*), nine decreased in fertilized soil (i.e. *Acidimicrobiales*, *Singulisphaera*, *Actinobacteria* TakashiAC-B11) and 14 decreased in both N levels (i.e. *Chloroflexi*, *Phycisphaerae* WD2101 soil group, *Jatrophihabitans*) (Fig. S2.5, $P < 0.05$). There were 54 genera increased with eCO_2 in legume plots. Of these groups, 25 increased in unfertilized soil (i.e. *Rhodoplanes*, *Betaproteobacteria*, *Adhaeribacter*), 19 increased in fertilized soil (i.e.

Bradyrhizobiaceae, *Thaumarchaeota* Soil Crenarchaeotic Group, *Myxococcales*) and 10 increased in both N levels (i.e. *Acidobacteria* Subgroup 4, *Holophagae*, *Phyllobacteriaceae*).

Collectively, the results show that significant changes in microbial community diversity, richness, and community composition under eCO_2 were plant functional group-specific (C3 grass and legume), and such changes were largely affected by soil N status.

2.4.4 Distribution of copiotrophic-, oligotrophic-like microorganisms along treatments in C3 grass and legume plots

Previous studies demonstrated that oligotrophic bacteria tend to encode fewer ribosomal RNA operons (*rrn*) copies in their genomes than copiotrophs (Lauro et al. 2009, Eichorst et al. 2011), thus *rrn* copy numbers can be used to infer bacteria of different life strategies: copiotrophic or oligotrophic. Here, we further examined the distribution of copiotrophic- and oligotrophic-like microorganisms among the 24 soil samples in this study by examining the number of *rrn* in detected bacteria genomes. The *rrn* copy numbers of detected bacteria using 16S rRNA sequencing were determined using the Gene Copy Number Adjustment function of RDP Classifier (https://rdp.cme.msu.edu/classifier/class_help.jsp#copynumber). Copy numbers of *rrn* of 168 genera were identified across the 24 samples, ranging from 1 to 15 copies per genome. Cluster analysis showed that samples in C3 grass plots were clustered together and well separated from samples in legume plots (Fig. 2.3). Bacteria encoding a larger number of *rrn* copies were more abundant in legume plots (e.g., Group 2), whereas smaller copy number of *rrn* encoding bacteria were more abundant in C3 grass plots (e.g.,

Group 5). However, there was no clear clustering pattern for samples under treatments of eCO_2 and eN within each plant functional groups. These results suggest that N richer legume plots may harbor more copiotrophic-like, but less oligotrophic-like microorganisms compare to the C3 grass plots. And long-term of eCO_2 and eN didn't alter the distribution of copiotrophic- and oligotrophic-like microorganism within neither C3 grass nor legume plot soils based on this test.

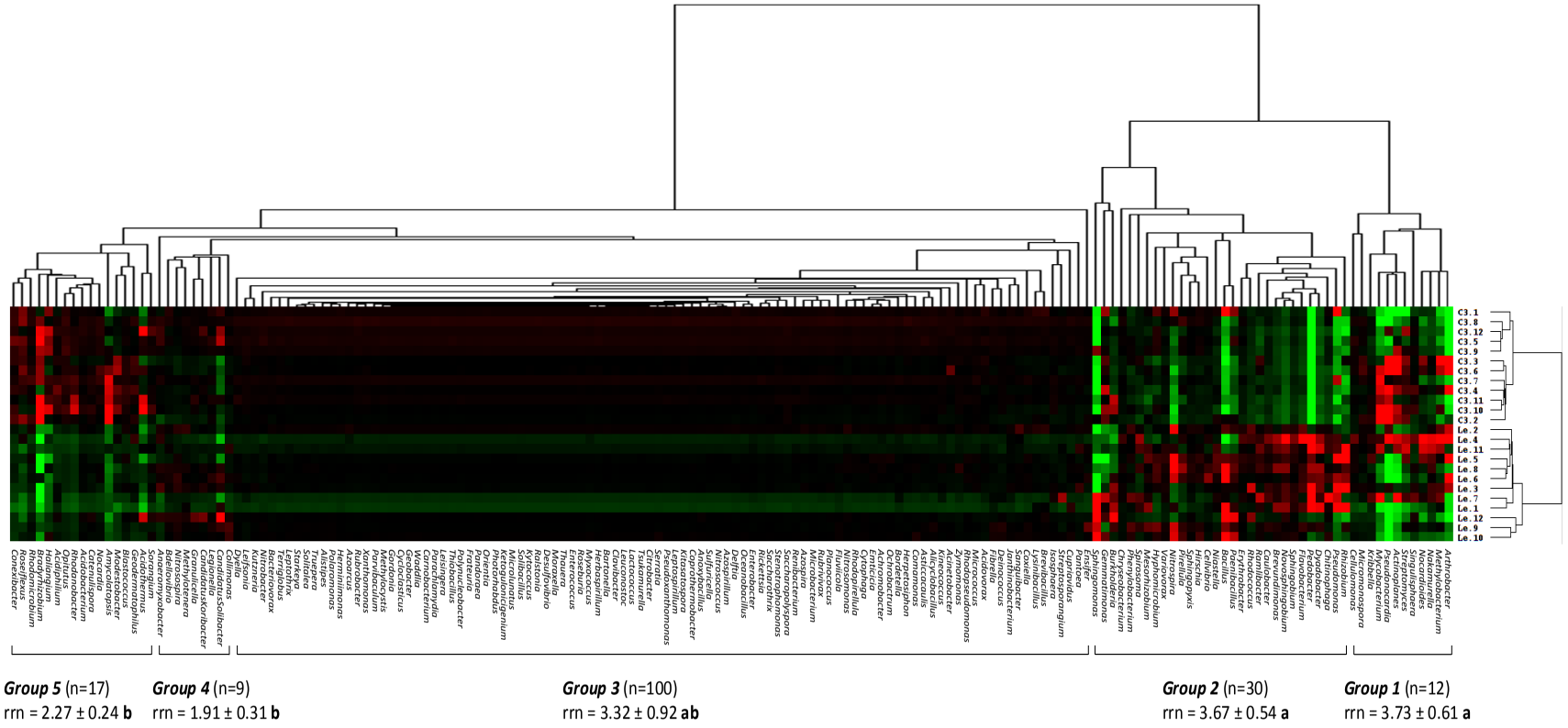

Fig. 2.3 Hierarchical cluster analysis of relative abundances of 168 genera among the 24 samples from C3 grass and legume plots. *rrn*: 16S rRNA copy number. Data are presented with mean ± se. Values labeled with different letters are significantly different ($P < 0.05$) according to ANOVA with pairwise comparison. Results were generated in CLUSTER and visualized using TREEVIEW. Green indicates signal intensities below background, whereas red indicates signal intensities above background. Brighter red color indicates higher signal intensities. Sample in C3 grass plots clustered together and were well separated from samples in legume plots. No clear clustering pattern for samples under treatments of CO_2 and N within each plant functional groups.

2.4.5 Linkages between microbial composition and selected environmental properties

We performed partial Mantel tests to link the observed taxonomic structure of microbial communities with selected plant properties (Clarke and Ainsworth 1993), including aboveground biomass, root biomass (0-20 cm, fine roots), aboveground biomass N and C/N, root biomass N and C/N, root ingrowth biomass (RIB), and soil geochemistry, including pH, moisture, temperature (Tm), total C (TC) and N (TN) content, nitrate, and ammonium. The results showed that microbial community was significantly correlated with selected plant properties on the whole ($r = 0.457$, $P = 0.001$), but not with soil properties ($r = 0.157$, $P = 0.058$).

Variation partition analysis (VPA) (Ramette and Tiedje 2007) was performed to further assess the contributions of CO_2, N, plant and soil properties to the taxonomic structure of microbial communities (Fig. S2.8). Individual variables CO_2 and N were found to contribute similarly to the observed variations in microbial taxonomic structure (4.8% and 4.5%). Seven plant properties and seven soil properties could independently explain 28.6% and 17.6% of the variation, respectively. The interactive effects between plant and soil, plant and CO_2, plant and N, Soil and N, and CO_2 and N were 6.8%, 4.8%, 3.4%, 3.2%, and 1.2%. Furthermore, the interactions among plant, soil, CO_2, and N was 5.2%, and other interactive effects were less than 1.0%. 27.5% of the variation in microbial community composition remains unexplained by the environmental variables measured. Plant properties play the most important role in shaping microbial communities in this study.

Individual taxa at different taxonomic categories (phylum, class, and genus) were further screened for potentially significant correlations with measured

environmental properties using Spearman's rank correlation coefficient. Changes in taxa were found to be significantly related to several of the selected environment properties, with more significant correlations found with plant properties ($P < 0.05$, Fig. 2.4, S2.6, and S2.7). At the phylum level, 10 phyla were significantly correlated with the plant and/or soil properties (Fig. 2.4, $P < 0.05$). Of these phyla, similar patterns were observed for *Acidobacteria, Bacteroidetes, Chlamydiae, Nitrospirae,* and *Verrucomicrobia* which generally positively correlated with aboveground biomass, aboveground and root biomass N content, and negatively correlated with root biomass, aboveground and root biomass C/N ratio, and root ingrowth biomass (Fig. 2.4). Contrarily, *Chloroflexi* and *Cyanobacteria* were negatively correlated with aboveground biomass, aboveground and root biomass N content, and soil NO_3^+, and positively correlated with aboveground and root biomass C/N ratio. Positive correlations were observed for *Actinobacteria* with soil temperature, NH_4^-, root biomass and ingrowth root biomass. In addition, negative correlations were observed for *Thaumarchaeota* with soil temperature, NH_4^-, root biomass, aboveground and root biomass C/N ration, and ingrowth root biomass. Similarly, significant correlations between microbial taxa and the selected plant and/or soil properties were detected in 21 classes and 90 genera (Fig. S2.6 and S2.7, $P < 0.05$). In addition, many unclassified phylotypes were significantly correlated with the selected plant and/or soil properties, suggesting that plant and soil factors may also greatly shape taxonomically uncharacterized microorganisms ($P < 0.05$).

	pH	Moisture	Tm (°C)	TC (%)	TN (%)	NO_3^+ (mg kg^{-1})	NH_4^- (mg kg^{-1})	AB (g m^{-2})	RB (g m^{-2})	AB-N (%)	AB-C/N	RB-N (%)	RB-C/N	RIB (g m^{-2})
Acidobacteria			-0.52**			0.42*	-0.51*	0.67***	-0.75***	0.62**	-0.65***	0.66***	-0.68***	-0.75***
Actinobacteria			0.59**				0.52**		0.55**					0.50*
Armatimonadetes														
Bacteroidetes			-0.44*						-0.54**	0.41*	-0.47*	0.46*	-0.48*	-0.51*
Chlamydiae						0.52*		0.49*		0.48*	-0.51*	0.46*	-0.45*	
Chloroflexi			0.54**			-0.54**	0.41*	-0.70***	0.75***	-0.68***	0.71***	-0.82***	0.82***	0.77***
Cyanobacteria		0.50*				-0.60**		-0.69***		-0.59**	0.58**	-0.58**	0.55**	
Firmicutes			-0.43*		0.44*		-0.47*		-0.49*					-0.47*
Gemmatimonadetes														
Nitrospirae			-0.55**				-0.55**	0.51*	-0.65***	0.49*	-0.52*	0.44*	-0.48*	-0.66***
Planctomycetes														
Proteobacteria														
Thaumarchaeota			-0.57**				-0.48*		-0.52**		-0.42*		-0.43*	-0.55**
Verrucomicrobia				0.43*	0.43*	0.59**		0.51*	-0.45*	0.45*	-0.50*	0.46*	-0.48*	

Fig. 2.4 Spearman's rank correlation coefficient rho of selected phyla (with different abundance levels among treatments) with environmental attributes. Coral toned cells represent significant positive correlations; Cyan toned cells represent significant negative correlations. Only phyla with different abundance levels among treatments were subjected to this test. P values have been adjusted for multiple comparisons by FDR. The first seven columns correspond to correlations of each phylum with soil attributes including pH, moisture, temperature (Tm), total C (TC) and N (TN) content, nitrate, and ammonium. The next seven columns correspond to correlations of each phylum with plant attributes including aboveground biomass (AB), root biomass (RB) (0-20 cm, fine roots), aboveground biomass N (AB-N) and C/N (AB-C/N), root biomass N (RB-N) and C/N (RB-C/N), and root ingrowth biomass (RIB).

2.5 Discussion

Predicting long-term climate change impacts to ecosystem carbon and nitrogen dynamics require detailed knowledge of biodiversity response patterns and the linkages between such responses to environmental factors. By using 16S rRNA Illumina deep sequencing to characterize the profile of soil microbial communities, we showed that the microbial community diversity and structure was significantly altered under eCO_2 conditions. Particularly, the responses of several microbial populations to eCO_2 differ at contrasting N levels. With eCO_2, several environment properties significantly correlated with the changes in microbial populations at varied soil N levels, with plant properties, such as biomass production and C/N ratio, playing a more important role in shaping microbial taxonomic structure.

Current efforts to predict whether terrestrial ecosystems will serve as a carbon sink or source under future climate scenarios are hampered by the difficulty of characterizing processes beneath the earth's surface (e.g. soil C dynamics). A major approach to understanding the soil processes under climate changes is to survey the responses of soil microbial communities, which mediate important biogeochemical cycles, such as C, N, P and S. However, existing observations on microbial communities regarding the responses of their biomass, community composition and structure, and activities to climate change factors are highly variable and site-specific (Zak et al. 2000, Lipson et al. 2005, Jossi et al. 2006, Carney et al. 2007, Drissner et al. 2007, Drigo et al. 2009, Deng et al. 2012, Dunbar et al. 2012). Site-specific microbial behavior under climate change yields conflicting observations on soil C and nutrient dynamics, which further limit robust ecological modeling. Our results showed variability in community composition and the response to eCO_2 between C3 grass and legume plots, providing limited predictive value to the response of microbial communities across a wide range of ecosystems.

The experimental plots in this study have been exposed to contrasting CO_2 and N levels for over 12 years. Thus, the observed changes in microbial community composition and structure are expected to represent permanent, rather than transient responses of microbial communities to eCO_2 and/or eN. We detected only three and seven significantly changed phyla in response to treatments in the C3 grass and legume plots, respectively, among a total of 38 phyla detected, suggesting that microbial communities were generally resilient to eCO_2 at coarse taxonomic levels. Similar results were also reported in previous studies (Chung et al. 2006). For example, a study

on soil samples at the Rhinelander WI FACE experiment using PLFA and PCR-DGGE methods showed that microbial community composition did not significantly change between each of the triplicate FACE plots for either ambient or elevated CO_2 (Chung et al. 2006). At the same site, a follow-up experiment by Lesaulnier et al. (2008) examined detailed and deeper branching profile of population responses to eCO_2 by analyzing the 16S and 18S rRNA clone libraries and qPCR quantification, which revealed no changes in trembling aspen associated bacterial community structure at the phylum level (Lesaulnier et al. 2008).

Furthermore, it was proposed that numerically dominant microbial taxa may be less responsive to eCO_2 effects compared with less abundant taxa (Dunbar et al. 2012). A study assessing soil microbial community responses across six filed FACE experiments showed that only a small fraction (about 2%) of identified bacterial taxa were potentially responsive to eCO_2 (Dunbar et al. 2012). Our 16S Illumina deep sequencing results were generally in agreement with these results. We evaluated overall changes in soil microbial communities using both the quantitative dissimilarity index (Bray-Curtis), which gives abundant OTUs the most weight, and a non-quantitative index (Jaccard), which is based on presence or absence and OTUs with lower abundance exert a larger effect. Both C3 grass and legume ecosystems showed significant treatment effects on Jaccard index but not on Bray-Curtis index, indicating that overall community shifts were largely due to changes in abundances of those less dominant or rare microbial taxa. Such changes may have implications for ecosystem function, especially via effects on the cycling of essential elements.

In both C3 grass and legume soils of this study, the soil microbial communities were primarily dominated by members of the phylum *Proteobacteria*, followed by the *Actinobacteria*, *Acidobacteria*, and *Verrucomicrobia*, as is typical for soils (Janssen 2006). This result agrees well with our former synthesis of soil microbial community composition studies at BioCON in the 16-plant species plots during 2007 that showed *Proteobacteria* (23.2%), *Actinobacteria* (17.0%), *Bacteroidetes* (12.8%), and *Acidobacteria* (10.5%) dominated microbial community regarding their abundance (Deng et al. 2012). Similar dominant groups were also detected in soils of other FACE study (e.g., Oak Ridge National Laboratory FACE site) (Austin et al. 2009). Together, these results indicate a general consistency of dominant groups of microbial communities across BioCON plots of different plant functional groups and richness.

Actinobacteria are microorganisms that tend to prefer oligotrophic habitats (Fierer et al. 2003), and most of them seem to be out competed in soils of eCO_2 plots in this study likely as a result of increased flux of C. It is noteworthy that the not all *Actinobacteria* subgroups showed consistent trend to decrease in relative abundance at eCO_2. For example, several genera of *Actinobacteria* (e.g., *Microbispora, Smaragdicoccus, Streptacidiphilus, Hamadaea, Streptomonospora, Tsukamurella, Microlunatus, and Sinosporangium*) were selectively increased in response to eCO_2 in unfertilized soil. *Actinobacteria* play important role in organic matter turnover (e.g., cellulose and chitin decomposition) (He et al. 2010), and abundance changes in these microorganisms under eCO_2 may alter soil C cycling in this grassland ecosystem. *Chloroflexi*, another abundant phylum detected in this study, decreased in abundance at eCO_2 in the legume plots. Such change was also observed previously at this site (He et

al. 2012), supporting assumptions of adaptation of *Chloroflexi* to nutrient-limited habitats. However, a closer look at populations at the genus level showed there was a pretty diverse response to eCO_2 for taxa that closely affiliated with *Chloroflexi*. For example, the abundance of *Herpetosiphon*, *Ktedonobacteria*, and an unclassified *Chloroflexi*-affiliated genera significantly decreased at eCO_2 in the unfertilized soil, whereas *Ktedonobacterales, Bellilinea,* and *Litorilinea* significantly increased at eCO_2. These results reflect the various metabolic feature of *Chloroflexi* that capable of utilizing recalcitrant organic compounds and other more labile sources (Cho and Azam 1988, Jorgensen and Boetius 2007). It could also be related to soil heterogeneity or to the persistence of micro-niches of nutrient poor environments.

Although a phylum level significant change was lacking, a large number of *Proteobacteria* at lower taxonomic levels across α-, β-, γ-, and δ-subgroups were predominantly stimulated by eCO_2, either in unfertilized or in N enriched soils (e.g. *Hirschia, Holosporaceae, Desulfuromonas, Nitrosococcus, Rudaea, Coxiella*), which are generally consistent with our previous observation at BioCON and from other FACE sites (Feng et al. 2009, He et al. 2012). Enhanced plant growth under eCO_2 require higher rates of inorganic nitrogen uptake and assimilation (Reich et al. 2006, Reich and Hobbie 2013), microbial populations which are able to produce NH_4^+ from various sources were proposed to be favored under such conditions (Zehr et al. 2003, Craine et al. 2007), thus we would expect the trend towards an increase in these populations. Indeed, populations such as *Rhodobacter, Azospirillum, Rhizobium, Mesorhizobium,* and *Rhizobiales* that capable of fixing N_2 were generally promoted at eCO_2 in this study. Also, a recent study at the same site showed that the abundance of key genes involved in

microbial N fixation was significantly increased at eCO_2. These changes may modify soil N availability and cycling at this site.

Other than the indirect effects mediated by plants, eCO_2 may have direct impacts on the soil microbial community and their processes. A former study at this site measuring microbial functional genes showed that microbial genes involved in C fixation were significantly increased at eCO_2 (He et al. 2010). Similarly, using C table isotope analysis, our following experiment showed that eCO_2 significantly increased the C sequestration potential as measured by the changes in ^{13}C in soils. These changes in soil microbial functional potential are evidence for the direct impacts of eCO_2 on soil microorganisms. However, given that the concentration of CO_2 in soil pore space is 10 to 15 times higher than in the atmosphere, it is expected that such direct effects of eCO_2 on soil microbial community should be negligible compared to the indirect effects, such as altering plant organic matter inputs and soil chemistry (Kandeler et al. 1998, Janus et al. 2005). The results in the current study support this hypothesis and showed that direct effects of eCO_2 contribute to nearly 5% of the observed community variations, which is much smaller than measured plant properties (28.6%) and soil variables (17.6%) in shaping microbial community structure.

Previous studies demonstrated that *rrn* copy number is a reliable and generalizable proxy for determining bacteria of different life strategies and their adaptation to resource availability (Koch 2001, Lauro et al. 2009, Eichorst et al. 2011, Roller and Schmidt 2015). Consistent with the observations by Roller and colleagues showing that higher nutrients (e.g., N, P) availability tend to favor copiotrophs and reduce the abundance of oligotrophs (Koch 2001, Roller and Schmidt 2015), our results showed that copiotrophic bacteria

appear to be more abundant in the legume than the C3 grass plots. This was likely due to the significantly higher N content in legume plots. Furthermore, copiotrophs are expected to be more capable of decomposing labile C substrates with low C use efficiency (CUE), while oligotrophs are specialized in degrading recalcitrant SOM for N (Koch 2001). The differential distribution of copiotrophic- and oligotrophic-like bacteria in C3 grass and legume plots may lead to selective decomposition of organic substrates in these plot soils.

In conclusion, this study examined the profile of soil microbial communities in response to 12 years of eCO_2 at the BioCON site and demonstrated dramatic changes in community diversity, composition and structures and their relationship to the direct effects of CO_2 and indirect effects through plant and soil properties. We also demonstrated that the responses of several microbial populations to eCO_2 significantly depend on soil N levels. The long-term experiment enabled us to avoid transient responses, as such providing prolonged responses to assess the influence of climate change factors on the community dynamics of soil microorganisms. These findings provide fundamental, predictive understanding of ecosystem responses to global climate change and their feedbacks.

Chapter 3: Contingency in belowground microbial functional responses to rising atmospheric CO_2 at contrast nitrogen conditions

3.1 Abstract

Soil N availability alters plant photosynthate partitioning under elevated CO_2 (eCO_2), with effects that cascade to belowground microbial communities and associated ecological processes. Plants exposed to rising CO_2 increase root development and exudation, and such effect by eCO_2 is commonly greater at low than high nutrient conditions. These interactive effects between CO_2 and N can also change plant tissue chemistry. For example, previous meta-analysis of litter exposed to elevated CO_2 found a 7.1% decline in N concentration and a 6.5% increase in lignin concentration across species. The C/N ratio of both leaf and root has also been shown to change with CO_2 enrichment. These chemistry changes in plant tissue under eCO_2, however, were generally weaker when additional N is applied. Plant organic matter input through litter, root biomass turnover and root-exudation dramatically affects belowground microbial community composition and functional activities.How quantitative and qualitative changes in plant organic matter input in response to the interactive effects of CO_2 and N will affect soil microbial communities and associated ecoprocesses remain understudied.

Here, we used high-throughput microbial functional gene microarray (GeoChip), stable isotope-based microbial C-sequestration and N-fixation measurements to detect and identify the impacts of eCO_2 and eN on soil microbial functional communities. We found that long-term changes in CO_2 and N availability dramatically altered the diversity and structure of C3 grass-associated soil microbial functional genes via several mechanisms, such as altering plant fine root production, exudation and soil moisture.

There was an antagonistic relationship between eCO_2 and eN that affected a large number of microbial functional genes, with eCO_2 generally increasing the abundance of these genes at aN, but either decreasing or increasing abundance to a minimal degree at eN. These results imply that eCO_2 may accelerate nutrient cycling in the C3 grass system, but the magnitude of effect is strongly dependent on the relative availability of N. Elevated CO_2 and eN exerted surprisingly minor effects in the legume-associated soil microbial functional community, with eCO_2 generally decreasing gene abundance at aN, but increasing it at eN, suggesting that the impacts of eCO_2 and eN are ecosystem-specific. This study provides new insights into our understanding of microbial functional processes in response to multiple global change factors.

Keywords: elevated CO_2; nitrogen fertilization; microbial community; GeoChip; functional genes; progressive nitrogen limitation; priming effect

3.2 Introduction

Current efforts to accurately predict ecosystem feedbacks to the rising atmospheric CO_2 are hampered by uncertainties of the microbial responses beneath the Earth's surface which mediate key biogeochemical cycles (Luo et al. 2006, Reich et al. 2006, van Groenigen et al. 2006, Carney et al. 2007, He et al. 2010). Numerous studies have reported that rising atmospheric CO_2 stimulates belowground microbial growth and activities (He et al. 2010, Xu et al. 2013, Xiong et al. 2015, Butterly et al. 2016), and alters microbial community composition and structure (Austin et al. 2009, Berthrong et al. 2014) through increasing primary production in plants and C inputs into soil (Rich et al. Norby et al. 2005; Finzi et al. 2007). However, the commonly found nutrient limitations, particularly nitrogen (N) limitations in terrestrial ecosystems, restrict the magnitude of CO_2-induced plant growth enhancement (Zak et al. 2000, Oren et al. 2001, Shaw et al. 2002, Hungate et al. 2003, Luo et al. 2004) and alters plant physiological activities in response to rising CO_2 (e.g. photosynthate partitioning) (Gleeson and Tilman 1992, Reich and Hobbie 2013) thus, potentially altering belowground microbial processes accordingly.

Conceptual models of nutrient limitation suggest that plants exposed to rising CO_2 should allocate a greater amount of photosynthate to enhance root development to 'mine' nutrients from soil (Johnson 2006), and such belowground C allocation by elevated CO_2 should be greater at low than high N conditions (Reich and Hobbie 2013). In support of this, empirical evidence showed increased belowground C allocation and fine root production in low N availability soils in several CO_2 enrichment experiments (Lukac et al. 2003, Norby et al. 2004, Pritchard et al. 2008). It is also widely observed

that root exudation, low molecular weight organic substrates (e.g. sugars, amino acids and low molecular weight organic acids), increases in response to eCO_2 (Korner and Arnone 1992, Diaz et al. 1993, Hungate et al. 1997, Jones et al. 1998, Schlesinger and Lichter 2001, Heath et al. 2005, Korner et al. 2005, Carney et al. 2007, Finzi et al. 2007, Pollierer et al. 2007, Phillips et al. 2009), and to a greater amount with low than high soil N availability (Phillips et al. 2011). These changes in plant organic matter input in response to the interactive effects of CO_2 and N may further affect soil microbial communities and associated ecoprocesses but yet remain less studied.Fine root turnover, root cell sloughing, and root exudation deliver chemically labile organic substrates directly to soil (Meier et al. 2008). Compare to other plant-derived C input (e.g. leaf litter), they are preferred and readily consumed by soil microbes, providing essential C and energy sources (Drigo et al. 2008). Enhanced root growth and exudation under eCO_2 may therefore greatly impact ecosystem C and nutrient dynamics by altering belowground microbial community and activities (Korner and Arnone 1992, Diaz et al. 1993, Hungate et al. 1997, Jones et al. 1998, Schlesinger and Lichter 2001, Heath et al. 2005, Korner et al. 2005, Carney et al. 2007, Finzi et al. 2007, Pollierer et al. 2007)**.** For example, in responses to this extra C input under eCO_2, stimulated microbial population may synthesize more extracellular enzymes for depolymerization of N from soil organic matter (SOM) to meet their increasing nutrient demand, an effect known as 'priming effect' (Cheng 2005). Consequently, greater microbial immobilization of N will eventually be released for plant uptake during microbial biomass turnover, which may help sustaining plant N requirements under long-term eCO_2 (Dijkstra et al. 2009). Previous study showed that the strength of priming effect largely depends on the amount

of soil available N as it is more energetically efficient for microbes to assimilate mineral N from soil than mining it from SOM (Cheng 2005).

Meanwhile, a number of studies have suggested that eCO_2-induced increase in leaf litter production can stimulate SOM decomposition through priming effects and drive soil C loss (Carney et al. 2007, Talhelm et al. 2009). Similarly, recent work also showed that enhanced root growth and exudation in response to eCO_2, particularly in low fertility soils, stimulated SOM decomposition which may prevent soil C accumulation in forest ecosystems (Phillips et al. 2011). However, no studies have yet comprehensively measured how N availability affects the responses of belowground microbial functional processes under eCO_2. Moreover, most CO_2 enrichment experiments have been relatively short in duration (3 years or less), thereby reducing their utility for understanding long-term interactive effects between eCO_2 and N availability on belowground microbial processes.

In this study, we examined belowground microbial communities associated with C3 grass and legume plant functional groups in a 12-year grassland free-air CO_2 enrichment (FACE) experiment. We predicted that the abundance of microbial functional genes related to C and N cycling, and associated activities under eCO_2 will be higher than under ambient CO_2 (aCO_2) as a result of the greater primary production of plants. We predicted that the strength of these CO_2 effects would be reduced for plots fertilized with inorganic N, particularly for microbial functional groups related to chemically recalcitrant C decomposition and N-fixation, due to a lesser amount of root production and exudation.

3.3 Materials and Methods

3.3.1 Site description and sampling

The BioCON experiment is located at Cedar Creek Natural History Area, in central Minnesota, USA (Inouye and Tilman 1988, Reich et al. 2001) with CO_2, N deposition and plant diversity treatments arranged into 296 2 × 2 m plots. A free-air-CO_2 enrichment (FACE) technology was employed to maintain elevated CO_2 concentration at 560 ppm versus the ambient CO_2 concentration at 368 ppm in 6 rings (20 m diameter). Half of the plots receive an N addition of 4 $g \cdot m^{-2} \cdot y^{-1}$ (NH_4NO_3) in three applications (mid-May, mid-June, and mid-July), which doubles the rate of N deposition at the site. There are 4 levels of plant diversity with 1, 4, 9 and 16 species, respectively. A detailed description of the site can be found in Reich *et al*. (2001).

In this study, soil samples were collected in July (the growing season) 2009, 12 years after establishment of the BioCON experiment, from all 24 plots with 4 plant species associated with two functional groups: C3 grass (*Agropyron Repens, Bromus Inermis, Koeleria Cristata, Poa Pratensis*) and N-fixing legume (*Amorpha Canescens, Lespedeza Capitata, Lupinus Perennis, Petalostemum Villosum*). All plant species in this study were native or naturalized to the Cedar Creek Ecosystem Science Reserve. Within each plant group, there were two treatments: CO_2 and N with 3 biological replicates.

Five soil cores were collected at a depth of 0-20 cm from each plot and mixed as one composite sample and sealed in a plastic sampling bag, then placed on ice until transported to the laboratory. All samples were then passed through a 2 mm sieve to remove roots. A subsample was kept at 4^{o}C for soil characterization, C sequestration and N deposition measurements and the remainder was stored at -80^{o}C for DNA extraction.

Plant and soil properties were measured routinely on site (described elsewhere, (Reich et al. 2001, Reich et al. 2006)).

3.3.2 Soil DNA extraction, amplification, and labeling

Microbial community DNA was extracted from 5 g of soil from each sample using a freeze-grinding method (Zhou et al. 1996) and purified by agarose gel electrophoresis. DNA quality was assessed by the ratios of 260⁄280 nm and 260⁄230 nm using a NanoDrop ND-1000 Spectrophotometer (NanoDrop Technologies Inc., Wilmington, DE), and final DNA concentrations were quantified with PicoGreen (Ahn et al. 1996) using a FLUOstar Optima (BMG Labtech, Jena, Germany). DNA (100 ng) was then amplified through a rolling circle amplification using the Templiphi Kit (GE Healthcare, Piscataway, NJ, USA). Single-strand binding protein (200 ng ul^{-1}) and spermidine (0.04 mM) were applied to the reaction buffer to facilitate amplification (Wu et al. 2006). The reactions were incubated at 30ºC for 3 h. All the amplified DNA were then labeled with cyanine-5 dye, purified and dried at 45ºC for 45 min (SpeedVac, ThermoSavant, Waltham, MA, USA) (Wu et al. 2006).

3.3.3 Microarray hybridization

Hybridizations were performed using GeoChip 3.0 on a Maui Hybridization Station (BioMicro, Salt Lake City, UT, USA). Before hybridization, dried samples were resuspended in 50 ul hybridization solution (45% formamide, 5 × SSC, 0.1% SDS and 0.1 mg/ml Salmon sperm DNA) and 2 ul of universal standard DNA labeled with cyanine-3 dye (Liang et al. 2010), incubated at 98ºC for 3 min and then kept at 65ºC until hybridization.

GeoChip slides were placed in a prehybridization buffer (74% DI water, 5 × SSC, 0.1% SDS and 1 mg/ml BSA) at 42°C for 45 min. The slides were then washed twice using wash buffer III (0.1 × SSC) for 5 min each and dried using the Maui Wash Station (BioMicro, Salt Lake City, UT, USA). Maui Mixer AO (BioMicro) was adhered to the dried slides to form hybridization chambers. Hybridization solution with dissolved DNA (50 ul) was then injected into the chamber and hybridization was performed at 42°C for 12 h on a Maui Hybridization station (BioMicro). After hybridization, the Mixer was removed, and the slide was washed and dried using Maui Wash Station at 42°C with 40 s agitation using buffer I (1 × SSC, 0.1% SDS), 30 s agitation at RT using buffer II (0.1 × SSC, 0.1% SDS), 50 s agitation at RT using buffer III and for 3 min drying.

3.3.4 Microarray scanning and data pre-processing

Microarrays were scanned using a ScanArray® 5000 (PerkinElmer, Boston, MA, USA), and digitally analyzed using ImaGene™ v6.0 to quantify the pixel density (intensity). A signal-to-noise ratio [SNR, (signal mean-background mean)/background standard deviation] of ≥ 2 was considered as a positive signal (He and Zhou 2008). Then, the signal intensity was normalized using a two-step normalization method as described previously (Xue et al. 2013). Sample intensity was first normalized by using the intensity of universal standards within each sub-grid. The normalized sample intensity was then further normalized by the mean universal standard intensity across all slides. For data reliability, a gene was considered positive only if it was detected at least twice among the three replicates (He et al. 2010, Xiong et al. 2010). Then, relative abundance of each sample was calculated by dividing the individual signal intensity of each probe by the total signal intensity for all detected probes in that sample. The relative abundance was then multiplied

by the mean value for the sum of signal intensity of all samples. A natural logarithm transformation was performed afterward for the amplified relative abundance plus 1.

3.3.5 Ecosystem C flux measurement

Soil heterotrophic respiration measurement: soil samples (50 g, dry weight equivalent) were put into Duran bottles and incubated for 24 days. The concentration of CO_2 was measured with a Micro-Oxymax Respirometer (Columbus Instrument, Columbus, OH) every 12 hours. Soil C flux was measured routinely on site (described elsewhere, (Reich et al. 2006)).

3.3.6 Stable isotope analysis of soil C sequestration and N fixation

Microbial incorporation of $^{13}CO_2$ into soil in relation to controls were measured through lab incubation. Soil samples (50 g, dry weight equivalent) were incubated in containers at 25ºC, 40% water holding capacity, with air supplemented with either 368 or 568 ppm of 99% atom $^{13}CO_2$ (same as the BioCON site). A halogen lamp (400 – 700 nm, visible spectrum) with an infrared filter was used to provide incident irradiance from 8 am to 6 pm during the experiment, and samples were incubated in the dark for the rest of time. Gas was sampled every 5 days to measure $^{13}CO_2$ concentration and then renewed. After 30 days, 75 mg subsamples of the soil were collected and the ^{13}C content was measured by a PDZ Europa ANCA-GSL elemental analyzer interfaced to a PDZ Europa 20-20 isotope ratio mass spectrometer (Sercon Ltd., Cheshire, UK) in the Stable Isotope Facility at the University of California, Davis (Davis, CA).

Microbial incorporation of $^{15}N_2$ into soil in relation to controls were measured through lab incubation. Since $^{15}NH_4{}^{15}NO_3$ was used as N fertilizer in all N-enriched plots at the BioCON experiment, the lab incubation for measuring $^{15}N_2$ fixation was carried out

only using samples from the aN plots. Soil samples (50 g, dry weight equivalent) were placed into 25 ml Balch tubes (Bellco Glass, Vineland, NJ, USA). The headspace of the tubes was evacuated and replaced with synthetic air (20% O_2 and 80% $^{15}N_2$; 98 atom % ^{15}N, Isotec, Miamisburg, OH, USA). Controls were set up using unlabeled N_2. Tubes were incubated horizontally at 25ºC in the dark for 30 days. After incubation, 75 mg subsamples were weighted out and sent to the Stable Isotope Facility at the University of California, Davis (Davis, CA) to determine the ^{15}N content by a PDZ Europa ANCA-GSL elemental analyzer interfaced to a PDZ Europa 20-20 isotope ratio mass spectrometer (Sercon Ltd., Cheshire, UK). The net potential N-fixation rate was then calculated.

3.3.7 Statistical analysis

Diversity indices were calculated as described previously (He et al. 2010). Detrended correspondence analysis (DCA) was performed to determine the distances between microbial functional composition and structure among treatments. Permutational multivariate analysis of variance (Adonis) was applied to test the significant differences in overall functional structure among treatments. Multivariate regression tree (MRT) analysis was used to partition the relative effects of plants, CO_2 and N amendment on soil microbial functional composition and structure. Canonical correlation analysis (CCA) was used to evaluate possible linkages between overall microbial functional structure and environmental attributes. A forward selection procedure and variance inflation factors values (999 Monte Carlo permutations) were used to identify common sets of plant and soil attributes important in shaping the microbial community and these attributes were used in the CCA model. Mantel tests were used to elucidate correlations between soil

processes (e.g., soil C flux, heterotrophic respiration, C sequestration potential, N fixation potential, ammonification rate, nitrification rate) and detected key functional gene categories. The significant differences were defined as $P < 0.05$, or with listed P values. All analyses were performed by using R, v.2.9.1 (R foundation for Statistical Computing, Vienna, Austria). Effects of CO_2 and N on plant, soil and microbial functional genes were tested by a two-way analysis of variance (ANOVA), using the agricolae-package in R. In all ANOVA models, CO_2 and N were considered fixed effects and the block effect was random. The *post hoc* Fisher's least-significant-difference (LSD) test with Holm-Bonferroni adjustment was used to establish the significance of the differences among means.

3.4 Results

3.4.1 Effects of eCO_2 and eN on plant and soil attributes

Elevated CO_2 and eN had greater influence on C3 grass than legume in terms of total biomass, aboveground biomass, different types of roots and C/N ratio. For example, total C_3 grass biomass significantly increased with eCO_2 compared to aCO_2 ($P = 0.006$) and to a greater extent at eN (+60.9%) than aN condition (+6.1%) ($CO_2 \times N$ interaction $P = 0.012$). Aboveground biomass and coarse root of C3 grass significantly increased with eCO_2 at eN condition only (+28.1% and +492.5%, respectively. Fig 3.1a). In contrast, fine root of C3 grass significantly increased by 355.7% with eCO_2 at aN, but was unaffected by eCO_2 at eN condition (Fig 3.1a). No changes were observed for legume growth, except a significant decrease in aboveground biomass by 44.4% with eCO2 at aN condition (Fig 3.1a).

Neither eCO_2 nor eN had a strong influence on measured soil attributes including pH, temperature, and total soil C and N. However, the moisture of C3 grass plot soils significantly increased (+70.4%) with eCO2 at aN, while there was no CO_2 effect at eN (Table S3.1).

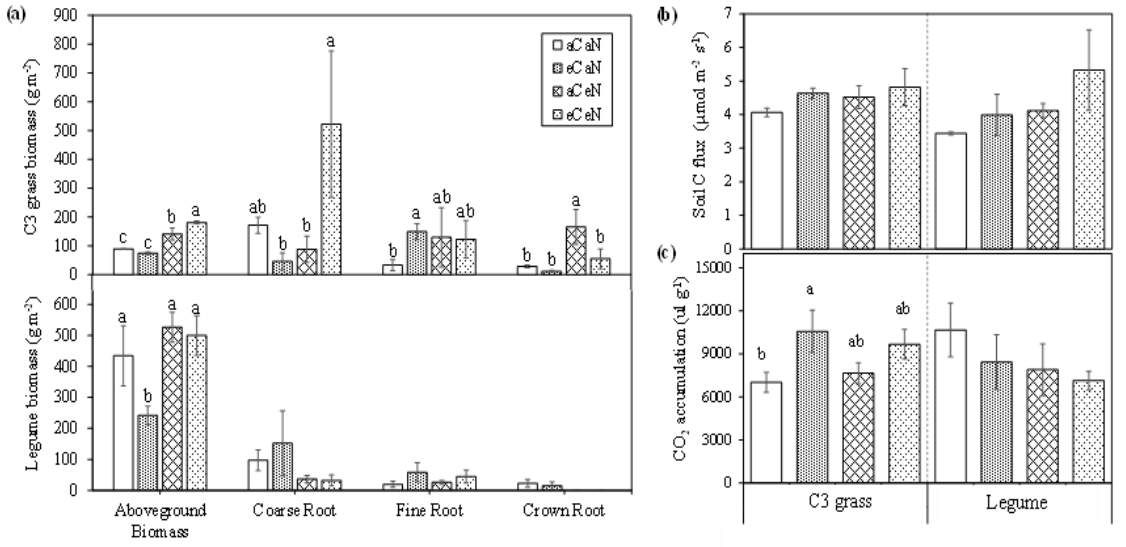

Fig. 3.1 Effects of eCO_2 and eN on plant biomass and ecosystem C fluxes. a. Aboveground and root biomass (0-20 cm, coarse, fine, and crown root) of C3 grass and legume in June 2009, the sampling year. b. Soil C flux, calculated as the average of all five measurements from June to August during the sampling year to minimize variation caused by time the reading was taken during the day. c. Heterotrophic respiration rate. All data are presented with mean ± SE (error bars). Values labeled with different letters are significantly different ($P < 0.05$) according to ANOVA, followed by Fisher's least significant difference (LSD) test with Holm-Bonferroni adjustment. Abbreviations: aCaN: ambient CO_2 and no fertilization; eCaN: elevated CO_2 and no fertilization; aCeN: ambient CO_2 and fertilized; eCeN: elevated CO_2 and fertilized.

3.4.2 Overall responses of soil microbial functional genes to eCO_2 and eN

Nearly 1.7 times as many probes/genes (13956 *vs.* 8433) were detected by GeoChip in C3 grass than in legume plots ($P < 0.05$), indicating higher microbial functional potential in C3 plots. Within each plant group, only around half of the detected functional genes at eCO_2 and eN alone or together overlapped with those receiving no treatments (Tables

S3.2). In C3 plots, eCO_2 plots under aN harbored the largest number of unique genes (25.19%), coinciding with a significantly ($P < 0.05$) higher overall microbial functional richness and diversity (Tables S3.3). Ambient CO_2 plots under eN harbored the least number of unique genes (8.97%). In legume plots, eCO_2 plots under aN had the least number of unique genes (9.26%) (Tables S3.2). No significant treatment effects were observed on overall microbial functional richness and diversity (Tables S3.3).

Overall microbial community structures of both plant groups were significantly altered by eCO_2 and eN as indicated by three non-parametric multivariate statistical tests (ANOISM, Adonis, and MRPP) (Table 3.1).

Table 3.1 Significance tests of the effects of eCO_2 and eN on the overall microbial functional gene structure

			CO_2	N	$CO_2 \times N$
C3 grass	ANOSIM[1]	*R*	0.250	0.5222	NA
		P	**0.035**	**0.005**	NA
	Adonis[2]	*F*	0.1982	0.2696	0.1903
		P	**0.025**	**0.002**	**0.001**
	MRPP[3]	δ	404.4	404.4	NA
		P	**0.009**	**0.003**	NA
Legume	ANOSIM	*R*	0.4037	0.237	NA
		P	**0.003**	**0.025**	NA
	Adonis	*F*	0.2155	0.2044	0.214
		P	**0.001**	**0.007**	**0.001**
	MRPP	δ	330.5	330.5	NA
		P	**0.003**	**0.009**	NA

Based on 999 permutations.
1. Analysis of similarities.
2. Non-parametric multivariate analysis of variance (MANOVA) with the Adonis function.
3. A Nonparametric approach depends on the internal variability of the data.

DCA-based ordination of overall detected microbial functional genes revealed a clear separation of samples between the two plant groups, and with more distinct treatment effects on assembling the C3 associated samples (Fig. 3.2). Moreover, multiple

regression tree was first split by plant groups. Of the C3 grass branch, it was further split by "N" and then "CO_2". Whereas, within the legume branch, it has first split by "CO_2" and then "N" (Fig. S3.1).

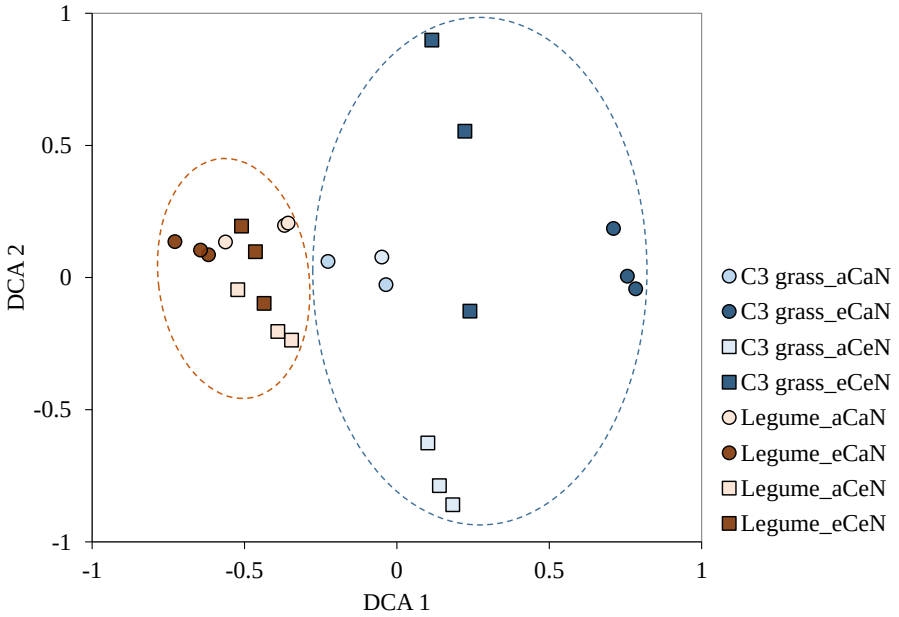

Fig. 3.2 Detrended correspondence analysis (DCA) showing that eCO_2 and eN had substantial influences on microbial functional gene composition and structure

3.4.3 Effects of eCO_2 and eN on key functional genes

Key function genes involved in important biogeochemical processes such as C, N, P and S cycling were further examined.

(i) C decomposition genes. A total of 26 gene families involved in C degradation were detected by GeoChip. These ranged from genes involved in the degradation of simple sugars (e.g., starch, hemicellulose, cellulose) to recalcitrant polycyclic C structures (e.g., chitin, aromatics and lignin). Among these genes, eCO_2 and eN significantly altered the abundance of several of them ($P < 0.05$), but to a greater extent in the C3 grass (Fig. 3.3) than in legume plots (Fig. 3.4).

In C3 grass plots, there were significant CO_2 × N interactions on 12 C degradation gene families ($P < 0.05$, Fig. 3.3). Compared to aCO_2, eCO_2 consistently increased the abundance of these genes (+24% to +151%) at aN, but either increased to a lesser extent (+0.1% to +5%) or decreased them (-3% to -41%) at eN. Notably, the interactive effects were predominantly affected genes involved in recalcitrant C decomposition (e.g., acetylglucosaminidase, endochitinase, isocitrate lyase, malate synthase, vanillate monooxygenase, vanillin dehydrogenase, manganese peroxidase, phenol_oxidase). As a main effect, eCO_2 significantly altered the abundance of 13 C degradation genes (12 increase and 1 decrease) across N levels ($P < 0.05$, Fig. 3.3). N also had a highly significant effect for 19 C degradation genes ($P < 0.05$, Fig. 3.3). Relative to aN, eN significantly ($P < 0.05$) decreased the abundance of all these genes.

In legume plots, CO_2 × N interactions significantly affected eight C degradation genes, wherein eCO_2 predominantly decreased the abundance of these genes (-4% to -56%) at aN, but increased them (+0.3% to +95%) at eN ($P < 0.05$, Fig. 3.4). Very few significant changes by the main effects of eCO_2 were observed for C degradation genes in legume plots (Fig. 3.4). Interestingly, the main effects of eN significantly increased the abundance of five genes involved in degrading labile C substrates (e.g. alpha, amylase, pullulanase, xylanase, and endoglucanase) ($P < 0.05$, Fig. 3.4).

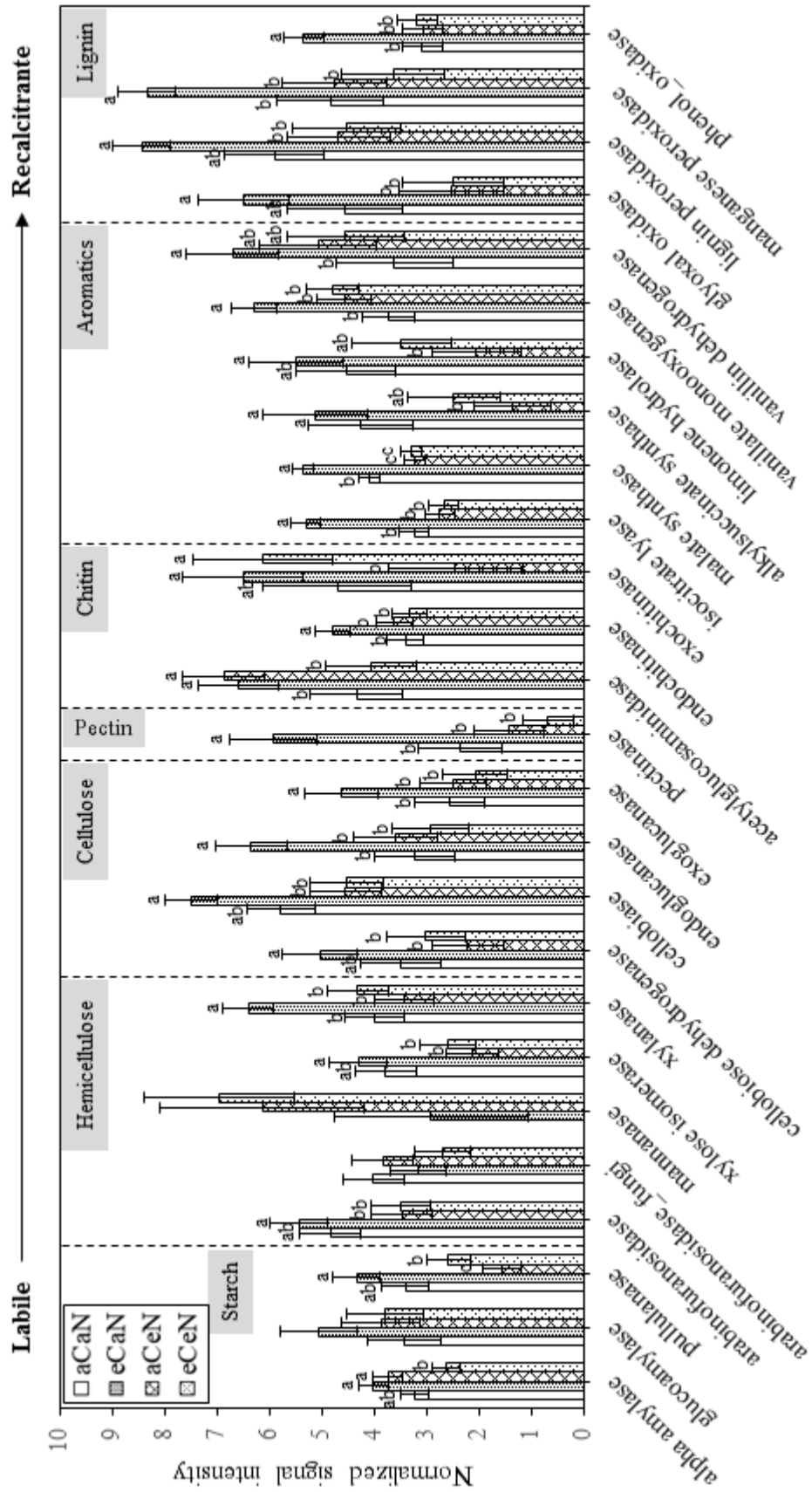

Fig. 3.3 Effects of eCO_2 and eN on C degradation genes detected in C3 grass plots. Bars labeled with different letters are significantly different ($P < 0.05$) according to ANOVA, followed by Fisher's least significant difference (LSD) test with Holm-Bonferroni adjustment

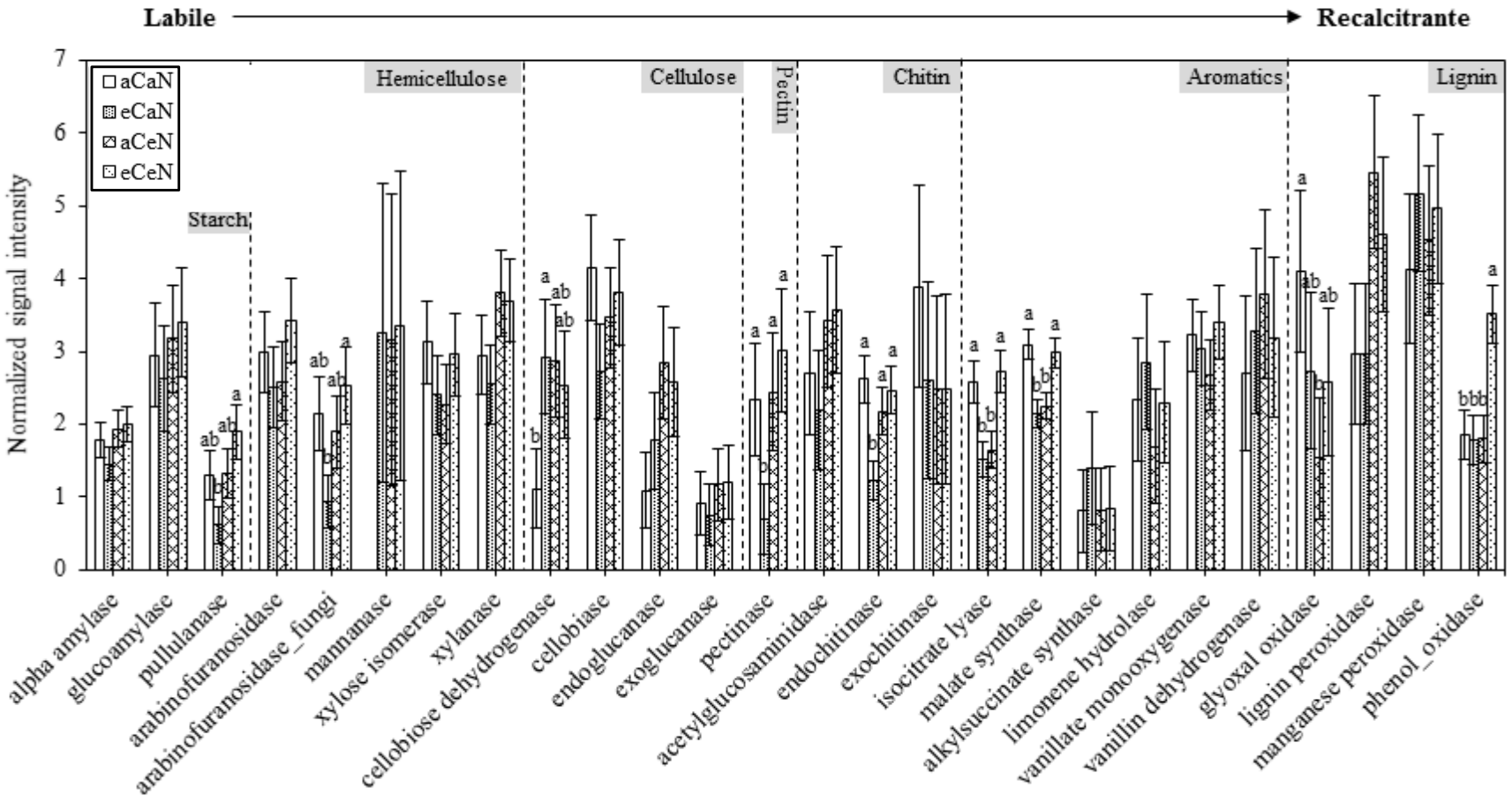

Fig. 3.4 Effects of eCO_2 and eN on C degradation genes detected in legume plots. Bars labeled with different letters are significantly different ($P < 0.05$) according to ANOVA, followed by Fisher's least significant difference (LSD) test with Holm-Bonferroni adjustment

(ii) C fixation genes. CO_2 and N exhibited significant main and interactive effects on all the detected genes involved in microbial C fixation ($P < 0.05$), including *pcc* encoding propionyl-CoA carboxylase, ribulose-1, 5-bisphosphate carboxylase/oxygenase (RuBisco) genes, and C monoxide dehydrogenase (CODH) genes, but with different patterns between C3 grass and legume plots. In C3 grass plots, relative to aCO_2, eCO_2 stimulated the abundance of C fixation genes to a greater extent at aN (+52% to +101%) than at eN (+8% to +9%) (Fig. S3.2). Across two N levels, eCO_2 significantly increased the abundance of all the three C fixation genes ($P < 0.05$) (Fig. S3.2). Whereas, across two CO_2 conditions, eN significantly reduced the abundance of these genes ($P < 0.05$) (Fig. S3.2). In legume plots, CO_2 × N interactions significantly altered the abundance of two C fixation genes (CODH and Rubisco), wherein eCO_2 decreased the abundance of these genes at aN but increased them at eN ($P < 0.05$, Fig. S3.2).

(iii) N cycling genes. A total of 15 genes related to N fixation, ammonification, nitrification, denitrification, dissimilatory N reduction, assimilatory N reduction and anammox were detected. Among these genes, six were significantly affected by the CO_2 and N interactive effects in C3 grass plots including *nifH* for N fixation, *ureC* for ammonification, *nirK* and *nirS* for denitrification, *nasA* for assimilatory N reduction, and *hzo* for anammox ($P < 0.05$, Fig. S3.2). Relative to aCO_2, eCO_2 increased the abundance of these genes (+36% to +192%) at aN, but increased to a smaller extent (*nirK* and *nasA*, +28% to +35%) or even decreased them (*nifH*, *ureC*, *nirS*, and *hzo*, -2% to -67%) at eN. As a main effect, eCO_2 consistently increased the abundance of *nifH*, *ureC*, *narG*, *nirK*, *nirS*, *nosZ*, *nasA*, and *nirA*; whereas eN significantly reduced the abundances of these genes except for *nirA* ($P < 0.05$, Fig. S3.2). In legume plots, CO_2 × N interactions had

significant impacts on *nifH*, *ureC*, *narG*, *nirS* and *hzo* ($P < 0.05$, Fig. S3.3). Relative to aCO_2, eCO_2 reduced the abundance of those genes under aN but increased them under eN. Furthermore, only a few genes were significantly affected by the main effects of CO_2 and N. Significant positive correlation was detected between soil ammonification rate and the abundance of *ureC* gene (Mantel test $P < 0.05$, Fig. S3.4d). Significant positive correlation was also found between soil nitrification rate and the abundance of bacterial-amoA but not archaeal-amoA gene abundances (Mantel test $P < 0.05$, Fig. S3.4d), indicating that ammonia oxidizing bacteria (AOB) were more important than ammonia oxidizing archaea (AOA) in mediating soil N cycling at this site.

(iv) P/S cycling genes. In C3 grass plots, interactive effects between CO_2 and N significantly affected all the three detected genes involved in P cycling, including *ppk* for polyphosphate biosynthesis, phytase for organic phytate hydrolysis, and *ppx* for inorganic polyphosphate hydrolysis ($P < 0.05$, Fig. S3.2). Relative to aCO_2, eCO_2 increased the abundances of *ppk* by 31% and *ppx* by 27% at aN, but decreased *ppk* by 21% and increased *ppx* by only 2% at eN. And phytase was only detected in eCO_2 plots. In legume plots, only *ppk* was significantly reduced by eCO_2 at aN ($P < 0.05$, Fig. S3.2). Meanwhile, four genes involved in S cycling were detected including *aprA* encoding adenylylsulfate reductase, *dsrA* and *dsrB* encoding sulfite reductase, and *sox* for sulfur oxidation. In C3 grass plots, half of these genes were significantly altered by $CO_2 \times N$ interactions ($P < 0.05$, Fig. S3.2). Specifically, the abundance of *dsrA* and *sox* were increased by eCO_2 at aN but decreased at eN, as compared to those from aCO_2. CO_2 main effect significantly increased the abundance of these genes except for *dsrB* ($P < 0.05$, Fig. S3.2). Whereas, all the four genes were significantly reduced by eN across two CO_2 levels. By contrast,

in legume plots, three genes (*aprA*, *dsrA*, and *sox*) were reduced by eCO_2 at aN but increased by eCO_2 at eN compare to those from aCO_2 ($P < 0.05$, Fig. S3.3). Only main effect of N was observed that significantly stimulated the relative abundance of *dsrA* and *dsrB* ($P < 0.05$, Fig. S3.3).

3.4.4 Soil and microbial heterotrophic respiration

In C3 grass plots, a significant CO_2 main effect on belowground microbial heterotrophic respiration (HR) was detected, which was increased by 38% at eCO_2 than aCO_2 ($P < 0.05$, Fig. 1c). However, no treatment effects were detected on the ecosystem respiration (SCF, represented by the soil C flux measured on site, Fig. 1b). Furthermore, strong positive correlations were observed between both SCF and HR, and the functional gene groups involved in degrading various C compounds targeted by GeoChip, including starch, cellulose, pectinase, chitin, aromatics and lignin (Fig. S3.4a). Thus, changes in abundance of these genes appeared to contribute to the alteration of SCF and HR in C3 grass plots. By contrast, no significant changes in HR or SCF were observed in response to treatments in legume group (Fig. 1b and 1c).

3.4.5 Stable isotope analysis of soil C sequestration and N fixation

In C3 grass plots, eCO_2 significantly increased the C sequestration potential across two N levels as measured by the changes in ^{13}C in soils ($P < 0.05$, Fig. 3.5). Mantel tests showed that the changes in C sequestration potential were significantly correlated with the C fixation genes as a whole ($P < 0.05$, Fig. S3.4c). For individual genes involved in C fixation, significant (CODH, $P < 0.05$) or marginally significant (*pcc* and Rubisco, $P < 0.1$) correlations with the C sequestration potential were also detected, indicating that CODH had a greater contribution to the microbial assimilation of CO_2 in C3 grass plots

of this study. In addition, there were no significant treatment effects on C sequestration potential in legume plots were detected (Fig. 3.5).

No significant changes in N fixation potential were detected either in the C3 grass or in legume plots in response to eCO_2, possibly due to a lack of statistical power (Fig. 3.5). However, a marginally significant correlation between soil N_2-fixation potential and *nifH* gene was detected ($P < 0.1$, Fig. S3.4c).

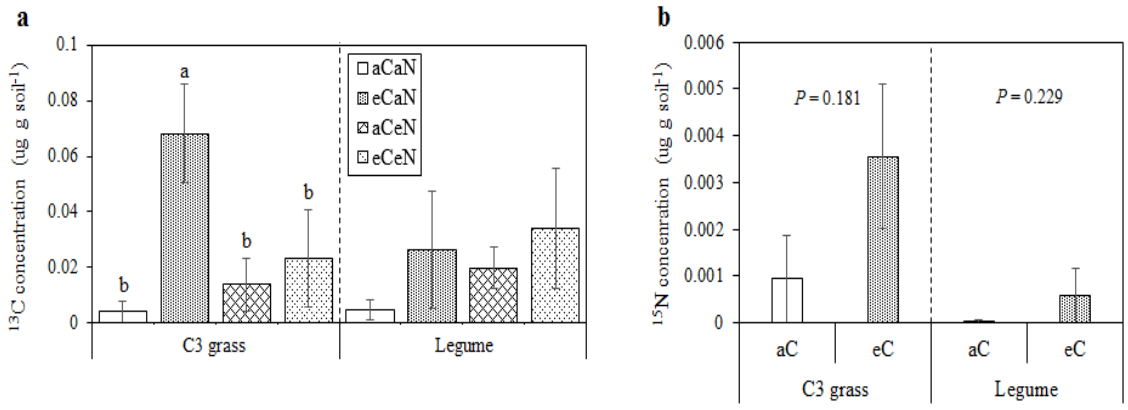

Fig. 3.5 Quantitative ^{13}C and ^{15}N enrichment in soils from C3 grass and legume plots at CO_2 and N treatments. ^{13}C (a) and ^{15}N (**b**) concentrations (mean, error bars indicate SEs, n=3) were calculated from the ^{13}C and ^{15}N excess values (obtained by IRMS) in the soils over the incubation time. *P*-values shown in (a) are based on two-way ANOVA and *P*-values in (b) are based on student's t-test.

3.4.6 Linkages between microbial functional structure and selected environmental attributes

We performed canonical correspondence analysis (CCA) to link microbial functional structure and attributes of plant and soil. A forward selection procedure and VIF (variance inflation factors with 999 Monte Carlo permutations) assessment were used to identify common sets of plant and soil attributes important in shaping the microbial community. CCA revealed that community functional structure within the C3 grass plots was significantly shaped by plant (e.g. aboveground biomass and C/N ratio; root biomass

including coarse, crown and fine roots, and root C/N ratio) and soil attributes (e.g. moisture) (Fig. 3.6a, P = 0.005). Samples under different treatments were clustered closely with the first two CCA constrained axes explaining 51.9% of the total variance. As indicated by the projections of environmental attributes, fine root biomass, root C/N ratio and soil moisture seem to play important roles in shaping community structure under eCO_2 at aN condition; while aboveground and coarse root biomass, and crown root biomass seem to predominantly influence the structure of communities under aCO_2 and eCO_2, respectively, at eN condition. In contrast, only three plant attributes were selected (e.g. aboveground and crown root biomass, and root C/N ratio) for CCA model of the legume plots which could explain 29.5% of the total variance for the first two CCA constrained axis (Fig. 3.6b, P = 0.06). CCA axis 1 and 2 appear to reflect the effects of eN and eCO2, respectively. Noticeably, aboveground biomass had a negative relationship to communities under eCO2 at aN condition, whereas crown root biomass may positively affect communities at the aN condition.

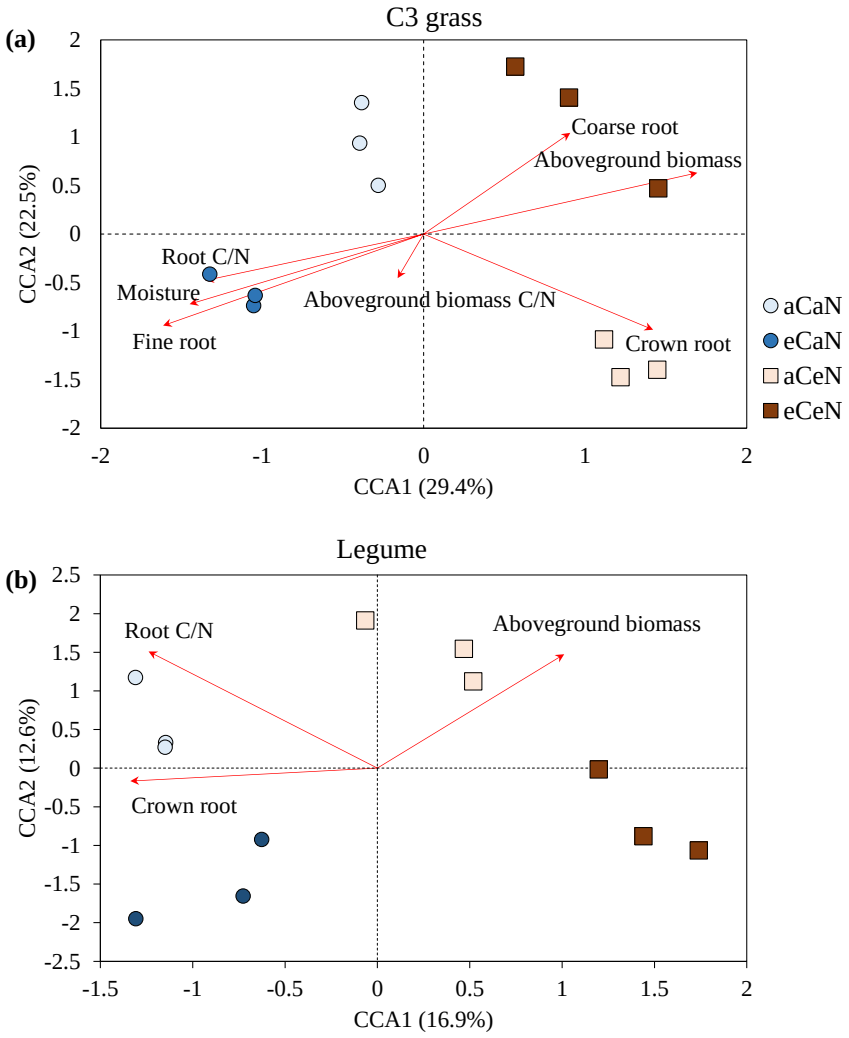

Fig. 3.6 Canonical correspondence analysis (CCA) of microbial community composition based on detected functional genes with selected environmental variables. a. C3 grass plots. b. Legume plots

Variation partition analysis (VPA) (Ramette and Tiedje 2007) was performed to further assess the contributions of plant and soil attributes to the functional structure of microbial communities (Fig. 3.7). Selected belowground and aboveground plant properties, and soil property could explain 36.3%, 15.3%, and 9.3% of the total variation of community structure in C_3 grass plots, respectively. Interactions of belowground × aboveground C3 grass properties, belowground C3 grass properties × soil moisture, and

all three groups could explain 6.0%, 1.0% and 5.9% of the total variation, respectively. In legume plots, belowground and aboveground legume properties, and their interactions could explain 22.3%, 10.9% and 3.1% of the total variation, respectively.

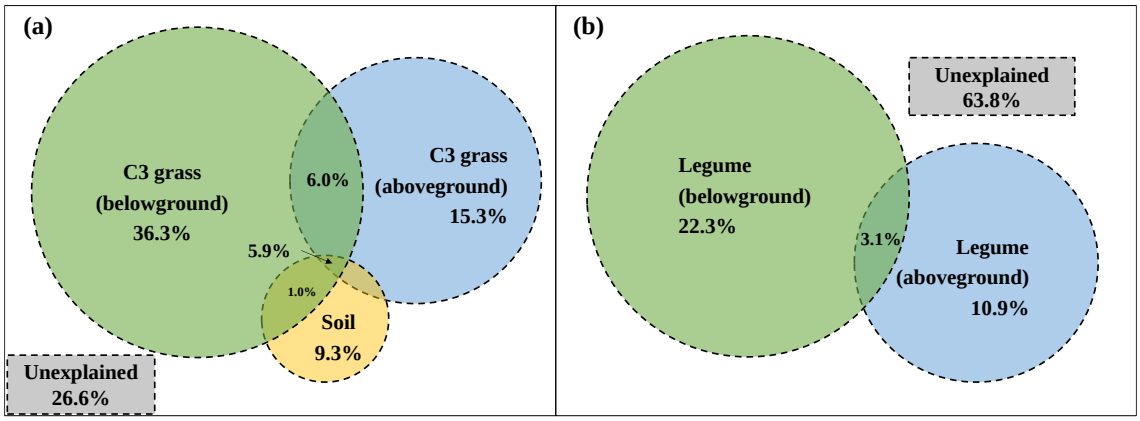

Fig. 3.7 Variation partitioning analysis (VPA) of microbial functional gene structures explained by plant and soil variables in C3 grass plots (a) and legume plots (b). Each circle shows the percentage of variation explained by a single factor alone. The overlapped area represents the percentage of variation explained by interactions between two or three of the factors. Same plant and soil variables screened for the CCA model were used. Only contribution of variation larger than 1% was shown.

3.5 Discussion

Grassland ecosystems cover about one fourth of Earth's surface and provide various ecosystem services (e.g. C storage, provision of food and water, biodiversity preservation) (IPCC 2007, Joyce et al. 2016). Understanding the mechanisms by which belowground microbial communities mediate C and nutrient cycling under elevated CO_2 is critical for predicting grassland ecosystem feedbacks to climate change. Here, we show that 12-year elevated CO_2 increased belowground microbial functional potential and activities, but the magnitude of such effect depends on soil fertility.

Although previous studies have widely reported elevated CO_2-induced stimulation of soil microbial growth and activities, these studies were largely conducted in short-term CO_2 enrichment experiments and ignored the co-limitation by N supply

on CO_2 fertilization effect (He et al. 2010, Xiong et al. 2015), making the extrapolation of these results to long-term ecosystem feedbacks to elevated CO_2 problematic. Our results indicate that belowground microbial functional composition and structure are strongly influenced by elevated CO_2, and microbial functional potential related to C, N, S and P cycling in low fertility soils were stimulated more by elevated CO_2 than fertilized ones. At the BioCON site, ambient N supply was reported to limit potential biomass accumulation in response to elevated CO_2 (Reich and Hobbie 2013), an effect that was observed in the C3 grass response to elevated CO_2 of this study. However, fine root production of C3 grass significantly increased in response to elevated CO_2 in non-fertilized soils only (Fig. 3.1a). Similar results were observed in the Duke Forest FACE site that CO_2 enrichment increases C allocation to fine root production (Pritchard et al. 2008), with greater total C allocation to soil occurring in low fertility soils (Palmroth et al. 2006). Another study at the Duck FACE site also documented higher exudation rates with 13 years of CO_2 enrichment during the primary growing season only when N was not added (Phillips et al. 2011). Thus, much of the additional plant growth under elevated CO_2 in low nutrient soils is allocated to soil in the form of labile organic matter which can be readily consumed by microorganisms, and likely contributed to the greater microbial functional responses to elevated CO_2 in N-poor than N-rich soils of this study.

Progressive N limitation (PNL) theory suggests that soil N availability should be gradually reduced over time by elevated CO_2, and that the CO_2 fertilization effect should occur only in short time in N limited ecosystems (Johnson 2006). However, empirical evidence across FACE experiment sites showed inconsistent and controversial results that CO_2 fertilization effect either down-regulated over long-term

CO_2 enrichment (Norby et al. 2010, Reich and Hobbie 2013), or increased and accompanied by an increase in plant N uptake (Finzi et al. 2007, McCarthy et al. 2010). Previous studies at BioCON showed, although ambient N constrained the potential CO_2 fertilization effect on plant biomass production, it did not preclude stimulation of plant productivity by decade-long elevated CO_2 (the stimulation at ambient N was around half of that under enriched N). The mechanism by which plants retain long-term growth response to elevated CO_2 at such N-poor grassland ecosystem remains unclear. It is been suggested that the opposing mechanism, Priming, may play a role simultaneously at BioCON in offsetting the PNL effects (Reich and Hobbie 2013).

In this study, microbial genes related to chemically recalcitrant C degradation (e.g. phenol_oxidase, manganese peroxidase, vanillin dehydrogenase, vanillate monooxygenase, malate synthase, isocitrate lyase, endochitinase, acetylglucosaminidase) were selectively increased with elevated CO_2 in non-fertilized C3 grass plot soils only, indicating that microbial N-mining through decomposition of soil organic substrates may increase with elevated CO_2 in low nutrient conditions at BioCON. This process may be intensified by increased soil moisture in these plots which could stimulate soil microbial biomass and decomposition rate (He et al. 2010). Meanwhile, a positive effect of elevated CO_2 on net N mineralization in non-fertilized C3 grass plots, whereas a negative effect in fertilized plots was observed (Fig. S3.5). In support of this, *ureC* abundance, associated with ammonification, was increased with elevated CO_2 in non-fertilized C3 grass plot soils only, and a significant correlation between *ureC* and measured rates of ammonification in these plots were found. Collectively, our results suggest that Priming occurs simultaneously with PNL and

being stronger in low than the high nutrient condition of this grassland ecosystems. Such effect may contribute to the long-term stimulation of plant productivity, but persistent turnover of chemically recalcitrant C by microbes also accelerates soil C loss under elevated CO_2 particularly when N is limited, offering a partial explanation for the lack of C accumulation in the C3 grass plot soils at this site despite 12 years of CO_2-induced increases in NPP (Reich and Hobbie 2013).

Other mechanisms may also contribute to an increase in N cycling under elevated CO_2 in non-fertilized C3 grass plots. For example, elevated CO_2 can influence N dynamics by stimulating N fixation, an effect commonly observed in several CO_2 enrichment experiments including BioCON (Lee et al. 2003, Luo et al. 2006, van Groenigen et al. 2006, He et al. 2010). In this study, the abundance of *nifH* genes increased by 35.5% with elevated CO_2 in non-fertilized C3 grass plots, suggesting more N could have been fixed in these plots. Consistently, such change in *nifH* was mirrored by measured N-fixation rate in these plots which showed similar response patterns under elevated CO_2 and significantly correlated with the relative abundance of *nifH* genes. Therefore, enhanced N fixation by belowground microbes at elevated CO_2 positively affect the soil N budget in this grassland ecosystem, but such effect was confined to low fertility soils. Likely, N-fixing microbes which carry *nifH* genes and respond strongly to elevated CO_2 in C3 grass plots were actively using energy derived from decaying fine roots and exudates to fix N_2.

Nitrogen addition can decreases SOM decomposition rates, by reducing N mining of microbial decomposers (Craine et al. 2007). Such decline in microbial decomposition of complex C compounds appears to be common in studies with increases

in N (Sinsabaugh et al. 2005, Waldrop and Zak 2006, Ramirez et al. 2012). We found a significant negative effect of N fertilization on genes involved in recalcitrant C decomposition (e.g. endochitinase, isocitrate lyase, malate synthase, alkylsuccinate synthase, limonene epoxide hydrolase, glyoxal oxidase, lignin peroxidase or ligninase, manganese peroxidase, and phenol_oxidase) in the C3 grass plots, suggesting a decrease in SOM decomposition in these plots. However, several labile C decomposition genes (e.g. alpha amylase, pullulanase, arabinofuranosidase, mannanase, xylanase) were also decreased in relative abundance in response to N fertilization. Together, these effects may contribute to C accumulation but reduce N-gain through microbial N-mining in fertilized C3 grass plot soils in the long-term. Furthermore, N fertilization can reduce the competitive advantages of other NH_4^+-producing microorganisms (e.g. N-fixers) over non-NH_4^+-producing microorganisms, because N uptake from soil is less costly than driving from N_2-fixation or mineralization (Lee et al. 2003, Reich et al. 2006). Accordingly, a significantly lower abundance of *nifH* genes was observed in fertilized than non-fertilized C3 grass plots, suggesting fertilization may suppress the N gain via decreased N_2-fixation and ammonification in these plots.

3.6 Conclusions

Our results demonstrated the contingency in belowground microbial functional responses to long-term elevated atmospheric CO_2 at contrast N conditions, and highlight the importance of understanding the role of soil N availability in mediating plant and belowground microbial community responses to elevated atmospheric CO_2. Elevated CO_2 induces major shifts in overall microbial functional composition and structure; and,

to a greater extent, stimulates microbial functional genes that associated with C, N, S and P cycling in low fertility than fertilized conditions. These responses of belowground microbial community were closely related to the enhancement of fine root production and C flux from roots to soil under elevated CO_2. Particularly, microbial activities associated with chemically recalcitrant SOM turnover increases with elevated CO_2 in low fertility condition which may limit soil C storage and stability. To what extent, these changes in microbial functional potential will alter total C and N budgets in this grassland ecosystem requires further study.

Chapter 4: Impact of Elevated CO_2 and N Addition on Metabolic Diversity of C3 grass- and Legume-associated Microbial Communities

4.1 Abstract

The impact of elevated atmospheric CO_2 on qualitative and quantitative changes in plant-derived C inputs belowground will have important consequences of C storage and nutrient cycling in soil. The aim of this work was to assess whether and how soil N conditions affect the influence of long-term eCO_2 on belowground microbial metabolic potential and diversity; and whether such effect varies between microbial communities associated with distinct plant functional groups (C3 grass and legumes). We investigated soil microbial communities in a grassland ecosystem exposed to two levels of atmospheric CO_2: ambient (aCO_2, 368 ppm) vs. elevated (eCO_2, 560 ppm); and two levels of N deposition: ambient (aN, 0 $g \cdot m^{-2} \cdot yr^{-1}$) vs. enriched (eN, 4 $g \cdot m^{-2} \cdot yr^{-1}$) for 12 years, growing either C3 grass or N-fixing legume forb. Biolog EcoPlate containing 31 low molecular weight C substrates, was used to construct sole C source utilization profiles of these communities. We found that community composition of soil microbes based on metabolic potential (C utilization rate) in the C3 grass plot soils was significantly different from those in the legume plot soils by both DCA and nonparametric dissimilarity tests. Microbial communities in legume plots had significantly higher metabolic potential than in C3 grass plots for decomposing organic substrates. Specifically, compared to the C3 grass plots, microbes in legume plots can use a larger number of C sources provided on EcoPlate and with greater decomposition rates within the measured time. We also found that eCO_2 and eN didn't significantly alter metabolic potential of microorganisms in the C3 grass plots. But overall microbial metabolic activities significantly increased with

eCO_2 by 20.6% in the fertilized legume plots, while there was no evidence for a CO_2 effect in the non-fertilized legume soils. Mantel test unveiled total soil N content, root ingrowth biomass, aboveground biomass, and root biomass N content as environmental attributes were closely correlated with microbial C utilization patterns. In addition, PLFA analysis showed both total microbial and bacterial biomass were significantly lower in legume than in C3 grass plots, showing an opposite trend to the microbial metabolic potential in these plots. Collectively, these results demonstrated that eCO_2 effects on active microbial metabolic activities are contingent on N conditions, and such effect differs between plant functional groups. Differences in microbial metabolic potential among treatments and between plant functional groups were not due to population size (biomass) but likely attributed to changes in community structure and/or enzymatic activities of belowground microbes.

Keywords: Biolog EcoPlate; microbial metabolic potential; elevated CO_2; N fertilization

4.2 Introduction

Grasslands cover about 40% of the global land surface and store approximately 34% of the global terrestrial stock of organic C pool, mostly in grassland soil (Scurlock and Hall 1998, Lal 2004). Microbial communities in grassland soil play a pivotal role in organic matter decomposition and thus essential to the global ecosystem C and nutrient cycling. The composition and activities of soil microbial communities could be significantly altered under global change factors such as elevated CO_2 (eCO_2) and N deposition (eN) (Field et al. 1995, Fierer and Schimel 2003, van Groenigen et al. 2006, Blagodatskaya et al. 2010, He et al. 2010, Ramirez et al. 2010, Adair et al. 2011, Reed et al. 2011, Deng et al. 2012, He et al. 2012, Ramirez et al. 2012, Chen et al. 2014), thus potentially affect the ecosystem function of grasslands of being sink or source for atmospheric CO_2 under future climate scenarios. Yet, the capability of decomposing various organic compounds by soil microbiota as affected by eCO_2 and/or eN remain largely inferred from metagenomic analysis targeting the 16S, 28S rRNA, ITS or functional genes (He et al. 2010, Langille et al. 2013, Tu et al. 2015). However, the actual activity of microorganims can't be directly measured by such DNA-based technologies (McGrath et al. 2010, Simon and Daniel 2011).

Community-level physiological profiling (CLPP), based on the utilization pattern of various carbon sources, has been widely employed with the aim to characterize and classify the metabolic versatility of heterotrophic microbial communities in many different environments such as soils, wetlands, marine, and air environments (Grayston et al. 1998, Collins et al. 2004, Lyons et al. 2010, Wu et al. 2013, Mastrogianni et al. 2014). Biolog EcoPlate (BIOLOG Inc, Hayward, CA, USA) represents one of the most

widely used tools for evaluating CLPP of communities as well as microbial isolates. Biolog EcoPlates contain replicated wells, each with a single low molecular weight C source, a nutrient medium, and a tetrazolium dye that becomes blue in proportion to the amount of C used and can be used to identify patterns in heterotrophic microbial metabolic capabilities (Garland and Mills 1991). A total of 31 different C sources along with a blank well used as a negative control are merged on EcoPlate (Table 4.1). EcoPlate has been shown to be useful as an assay to detect and measure environmental change effects on microbial communities (Preston-Mafham et al. 2002, Gryta et al. 2014, Xiong et al. 2015). Particularly, EcoPlate has been proved to be effective in revealing fast growing, copiotrophic bacteria present in environments such as soil and lake (Kenarova et al. 2013, Lima-Bittencourt et al. 2014, Llado et al. 2016).

In this context, this work aims to assess global change factors including eCO_2 and eN on the C utilization capabilities of soil microbial communities by using the Biolog EcoPlate approach. Our study was conducted at the BioCON experiment site, one of the longest CO_2 manipulation experiments in the world by using the free-air CO_2 enrichment (FACE) technology (Reich et al. 2001, Reich et al. 2004).

4.3 Materials and Methods

4.3.1 Site description and sample collection

The same samples collected from the BioCON experimental site were used. Please refer to Chapter 2 for more details.

4.3.2 Sample preparation

For microbial community recovery, 5 g of soil samples representing each treatment was diluted using 50 mL of sterile deionized water in a 50 ml conical centrifuge tube and agitated for 45 min at 200 rpm. Followed by 30 min settlement at 4°C. Then, the bacterial fraction in the supernatant was serially diluted (10^{-1}, 10^{-2}, and 10^{-3}) using deionized water, and the 10^{-3} dilution was used to inoculate the Biolog EcoPlate.

4.3.3 EcoPlate assays

A volume of 100 uL of each 10^{-3} soil dilution was loaded into each well of the EcoPlate. The plates were then incubated in a Biolog Omni Log PM System at 25°C for 156 h. The color development of each well was scanned at a wavelength of 595 nm every 15 min by a moving camera located on top of the incubation chamber. Average well color development of each plate ($AWCD_{all}$) and individual C sources on each plate ($AWCD_{sub}$) were calculated by averaging the mean difference between the optical density of all the C-source-containing wells and the control wells.

$$\mathrm{AWCD}_{all/sub} = \frac{\sum(O.D.well - O.D.neg)}{n}, \text{ where}$$

(*O.D. well – O.D. neg*) is the O.D. of C-source-containing well minus the O.D. of the negative control well, and n is the number of C sources (n = 93 in $AWCD_{all}$ and n = 3 in $AWCD_{sub}$). The area under the curves (AUC) based on AWCD values were calculated to better estimate the microbial C utilization among samples (Guckert et al. 1996). Richness (the number of oxidized C substrates), Shannon's diversity (*H'*) and Pielou's evenness (*J'*) indices were calculated using an O.D. of 0.25 as the threshold for a positive response (Garland 1996). Shannon's diversity index was calculated as: $H' = -\sum pi(\ln pi)$ where p_i is the ratio of the activity on each substrate ($O.D._i$) to the sum of activities on all

substrates $\sum(O.D._i)$. Pielou's evenness was calculated as: $J' = H' / H'_{max}$ where H' is the number derived from the Shannon diversity index and H'_{max} is the maximum possible value of H'.

4.3.4 Microbial biomass analysis by Phospholipid Fatty Acid Analysis (PLFA)

The same soil samples used in the metabolic profiling were used to estimate microbial biomass by PLFA (Chung et al. 2007). Briefly, microbial lipids were extracted from 2g of vacuum-dried soil with a solvent system that included methanol, chloroform, and a phosphate buffer. Extracts were purified on a SPE 96-well plate containing 50 mg of silica per well (Phenomenex, Torrance, CA, USA) and dried in clean vials (60 ^{o}C for 45 min). Each sample was dissolved with transesterification reagent (0.2 ml) and incubated at 37 ◦C for 15 min. Acetic acid (0.075 M) and chloroform (0.4 ml each) were then added. After shaking for 10 s the phases were allowed to separate. The bottom layer was removed into a clean vial, tried (60 ^{o}C for 20 min) and dissolved in 100 µl hexane. Fatty acid methyl esters (FAMEs) were identified by an Agilent (Agilent Technologies, Wilmington, DE, USA) 6890 gas chromatograph (GC) based on their retention times and in combination with the Sherlock™ Fatty Acid ID System (MIDI, Inc., Las Vegas, USA).

4.3.5 Statistical analysis

Significance of differences in microbial oxidation rates among treatments was examined by two-way analysis of variance (ANOVA), with a probability defined at $P < 0.05$ or with list P values. And the procedure of LSD test with a false discovery rate (fdr) adjustment was used as a post-hoc test. The structure of microbial metabolic potential was ordinated using detrended correspondence analysis (DCA). Three nonparametric tests (multiple-response permutation procedure [MRPP], permutational multivariate analysis of variance

[Adonis], and analysis of similarity [ANOSIM]) were used to evaluate dissimilarities between treatments and control samples. Mantel tests were used to examine the correlation between the microbial community structure and environmental factors (plant and soil properties). All of the above analyses were performed with R, version 2.9.1 (R Foundation for Statistical Computing, Vienna, Austria).

Table 4.1 Biolog EcoPlate C source guild groupings by chemical structures (Weber and Legge 2009). Each of the carbon sources is replicated 3 times on the 96 well EcoPlate.

Well number	Carbon source	Compound group
A1	Water	–
B1	Pyruvic acid methyl ester	Carbohydrates
C1	Tween 40	Polymers
D1	Tween 80	Polymers
E1	α-Cyclodextrin	Polymers
F1	Glycogen	Polymers
G1	D-Cellobiose	Carbohydrates
H1	α-D-Lactose	Carbohydrates
A2	β-Methyl-D-glucoside	Carbohydrates
B2	D-Xylose	Carbohydrates
C2	i-Erythritol	Carbohydrates
D2	D-Mannitol	Carbohydrates
E2	*N*-Acetyl-D-glucosamine	Carbohydrates
F2	D-Glucosaminic acid	Carboxylic and ketonic acids
G2	Glucose-1-phosphate	Carbohydrates
H2	D,L-α-Glycerol phosphate	Carbohydrates
A3	D-Galactonic acid-γ-lactone	Carboxylic and ketonic acids
B3	D-Galacturonic acid	Carboxylic and ketonic acids
C3	2-Hydroxybenzoic acid	Carboxylic and ketonic acids
D3	4-Hydroxybenzoic acid	Carboxylic and ketonic acids
E3	γ-Hydroxybutyric acid	Carboxylic and ketonic acids
F3	Itaconic acid	Carboxylic and ketonic acids
G3	α-Ketobutyric acid	Carboxylic and ketonic acids
H3	D-Malic acid	Carboxylic and ketonic acids
A4	L-Arginine	Amino acids
B4	L-Asparagine	Amino acids
C4	L-Phenylalanine	Amino acids
D4	L-Serine	Amino acids
E4	L-Threonine	Amino acids
F4	Glycyl-L-glutamic acid	Amino acids
G4	Phenylethylamine	Amines/amides
H4	Putrescine	Amines/amides

4.4 Results

4.4.1 Plant and soil properties

Hierarchical cluster analysis based on the biogeochemical properties showed that the analyzed samples were well separated into two groups owing to the distinct environmental conditions (Fig. 4.1). Specifically, Group 1 were associated with C3 grass plots and containing significantly lower total soil C (TC) and N (TN) content, aboveground biomass (AB), N content of aboveground biomass (AB-N) and root (RB-N); but higher soil temperature (Tm), plant root ingrowth biomass (RIB), root biomass (RB), C/N of aboveground biomass (AB-C/N) and root biomass (RB-C/N) comparing with Group 2 which were associated with legume plots (*t*-test, $P < 0.05$).

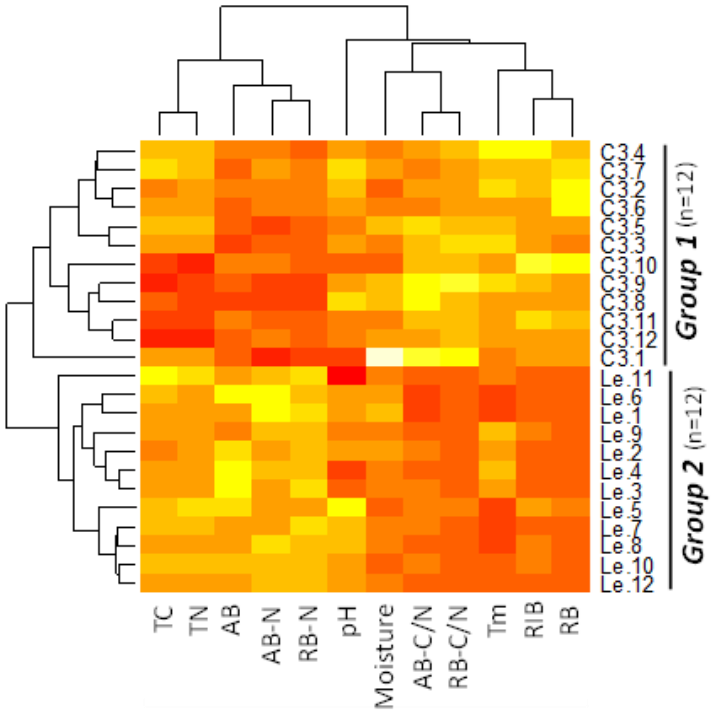

Fig. 4.1 Hierarchical cluster analysis of environmental properties of 24 samples in both C3 grass and legume plots. The first seven columns correspond to correlations of each phylum with soil attributes including pH, moisture, temperature (Tm), total C (TC) and N (TN) content, nitrate, and ammonium. The next seven columns correspond to correlations of each phylum with plant attributes including aboveground biomass (AB), root biomass (RB) (0-20 cm, fine roots), aboveground biomass N (AB-N) and C/N (AB-C/N), root biomass N (RB-N) and C/N (RB-C/N), and root ingrowth biomass (RIB).

4.4.2 Community C Substrate Utilization Profile

In this study, AWCD and AUC were used to determine the utilization of C substrates by microbes, and to estimate the activity and physiological function of microbial communities (Guckert et al. 1996, Zhang et al. 2017). Oxidation of all 31 C substrates on EcoPlates after 156 h of incubation was first measured based on $AWCD_{all}$ which showed that microbial communities in legume plots had significantly higher $AWCD_{all}$ values than in C3 grass plots (Fig. 4.2A, ANOVA, $P < 0.05$). Consistently, greater AUC was observed for samples in legume than in C3 grass plots across the entire incubation period (Fig. 4.2B, ANOVA, $P = 0.017$). Similarly, for individual C substrates, significantly higher oxidation of 11 C substrates were observed by communities in legume plots compare to those in C3 grass plots, including Pyruvic acid methyl ester (Methyl pyruvate), i-Erythritol, L-Asparagine, a-Cyclodextrin, L-Threonine, Glycogen, Itaconic acid, Glycyl-L-glutamic acid, N-Acetyl-D-glucosamine, D-Cellobiose, and a-D-Lactose (ANOVA, $P < 0.001$). Together, these results indicate a greater microbial metabolic capability in the legume than C3 grass plot soils on low-molecular-weight organic substrates provided on EcoPlate.

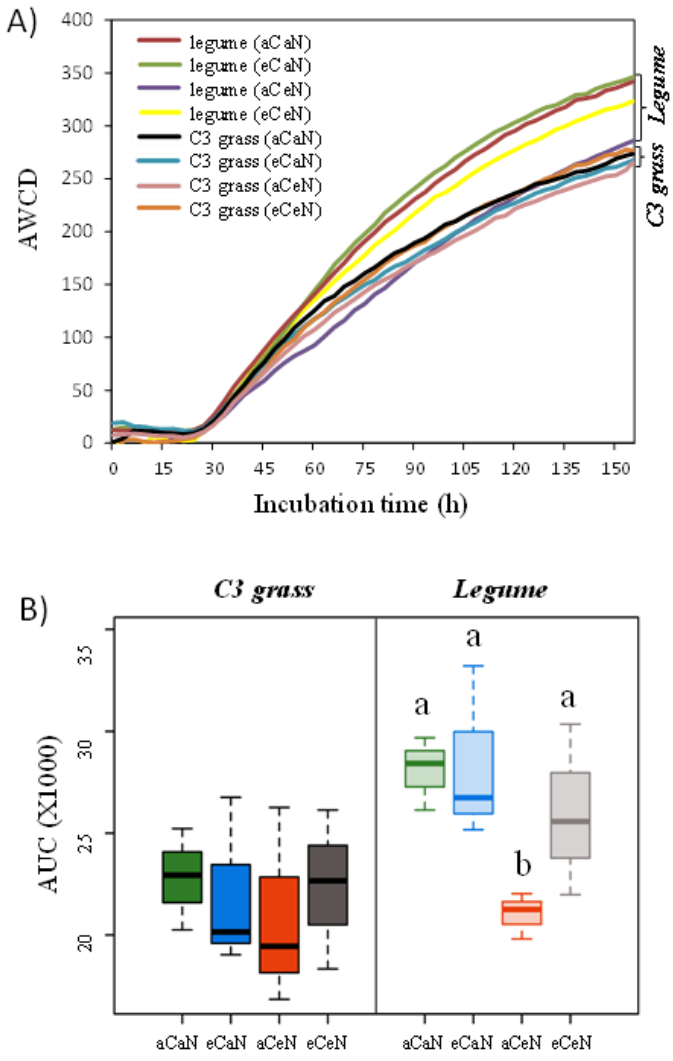

Fig. 4.2 Microbial C substrate utilization patterns based on 156 h incubation. AWCD (A) and AUC (B) of metabolized substrates of all 31 C substrates in Biolog EcoPlates. Boxes labeled with different letters are significantly different ($P < 0.05$) according to ANOVA, followed by Fisher's least significant difference (LSD) test with Holm-Bonferroni adjustment. Abbreviations: aCaN: ambient CO_2 and no fertilization; eCaN: elevated CO_2 and no fertilization; aCeN: ambient CO_2 and fertilized; eCeN: elevated CO_2 and fertilized.

Overall microbial metabolic activities on 31 C substrates responded to experimental treatments (eCO_2 and eN) in the legume but not in the C3 grass plot soils. Within the legume plots, overall microbial metabolic activities significantly increased by 20.6% with eCO_2 in the fertilized soils, while there was no evidence for a CO_2 effect in

non-fertilized soils (Fig. 4.2B). In contrast, none of these effects were significant within the C3 grass plots (Fig. 4.2B). Similar to the pattern of overall C decomposition, CO_2 effects on individual C substrate decomposition activities occurred primarily within the legume plots, with significantly increased metabolic activities in fertilized soils but unchanged activities in unfertilized soils (e.g. L. Arginine, L. Asparagine, L. Phenylalanine, and Tween 80) (Fig. 4.3).

A)

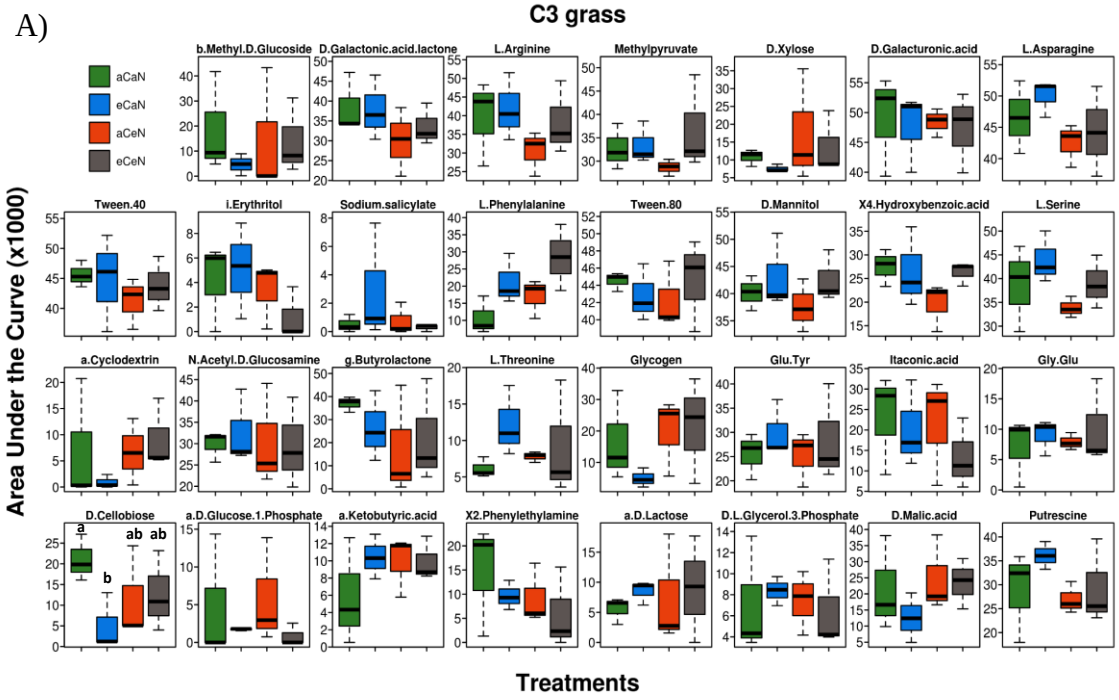

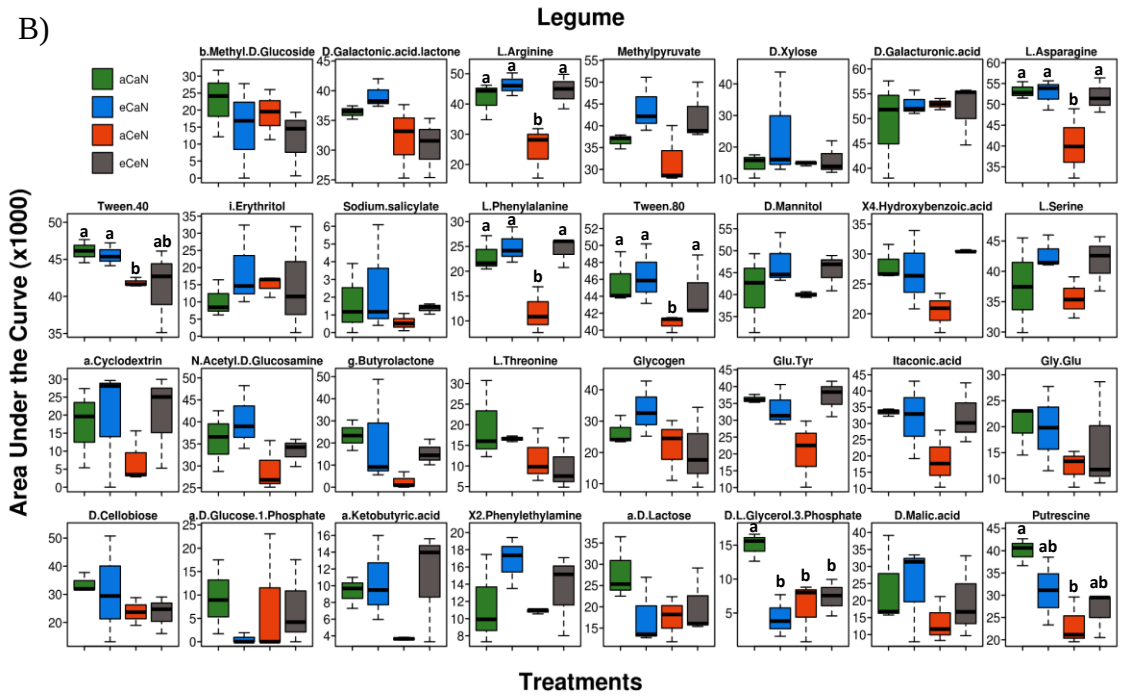

Fig. 4.3 Oxidation of individual C substrates in the EcoPlate measured by AUC. (A) C3 grass plots. (B) Legume plots. Boxes labeled with different letters are significantly different ($P < 0.05$) according to ANOVA, followed by Fisher's least significant difference (LSD) test with Holm-Bonferroni adjustment. Abbreviations: aCaN: ambient CO_2 and no fertilization; eCaN: elevated CO_2 and no fertilization; aCeN: ambient CO_2 and fertilized; eCeN: elevated CO_2 and fertilized.

4.4.3 Microbial catabolic diversity

Shannon, richness and evenness indices were used to reflect the functional diversity of microbial metabolisms (Zhang et al. 2017). A significantly higher number of substrates on EcoPlate (Richness) were able to be used by communities in legume than in C3 grass plots (27 vs. 23 on average), showing a metabolic diversification in the C source oxidation between communities in two plant functional groups. Furthermore, the number of usable C substrates under eCO_2 was significantly lower than under aCO_2 (22 vs. 24 on average) in non-fertilized C3 grass plots, but no significant CO_2 effects were detected in fertilized C3 grass or all legume plot samples (Fig. S4.1). In addition, Shannon and Evenness indices significantly increased with eCO_2 in non-fertilized legume plots (Fig. S4.1).

4.4.4 Shifts in microbial communities functional structure under treatments

Three nonparametric tests (MRPP, Adonis, and ANOSIM) were performed by utilizing the $AWCD_{all}$ value after 156h incubation and consistently showed that the communities in C3 grass were significantly different from those in legume plot soils, while communities within each plant functional groups generally did not differ among different levels of eCO_2 and eN (Table 4.2). Consistently, the DCA profile illustrated that C3 grass samples were separated clearly from those of legume along DCA1, while samples of different CO_2 or N regimes were less distinctly separated along DCA2 (Fig. S4.2).

Table 4.2 Significance tests of the effects of eCO_2 and eN on microbial metabolic diversity using three different statistical approaches*

		MRPP[1]		anosim[2]		adonis[3]	
		Delta	*P*	*R*	*P*	R^2	*P*
C3 grass *vs.* Legume		0.209	< **0.001**	0.437	**0.002**	0.167	**0.001**
C3 grass	aCaN *vs.* eCaN	0.215	0.47	0.037	0.517	0.207	0.307
	aCaN *vs.* aCeN	0.227	0.594	0.185	0.816	0.185	0.552
	aCaN *vs.* eCeN	0.228	0.802	0.111	0.892	0.183	0.607
Legume	aCaN *vs.* eCaN	0.201	0.282	0.222	0.406	0.259	0.097
	aCaN *vs.* aCeN	0.195	0.0989	0.852	0.091	0.348	**0.001**
	aCaN *vs.* eCeN	0.196	0.196	0.333	0.201	0.294	0.055

* Distance method: Bray-Curtis.
1. A Nonparametric approach depends on the internal variability of the data.
2. Analysis of similarities.
3. Non-parametric multivariate analysis of variance (MANOVA) with the Adonis function.

4.4.5 Linkage between microbial metabolic potential and environmental properties

Mantel tests were performed based on Bray–Curtis and Euclidean indices to determine if the microbial metabolic potential was associated with measured plant and soil properties (Table 4.3). In this analysis, five soil attributes including moisture, pH, total C and N content, and temperature; and seven plant attributes including root ingrowth biomass, aboveground biomass, root biomass (0-20 cm, fine roots), aboveground biomass N

content and C/N ratio, and root biomass N content and C/N ratio were included. Mantel test of microbial metabolic potential patterns and each plant and soil property suggested that soil total N content, aboveground and root biomass, and root biomass N content to be the major factors responsible for differences in microbial metabolic potential (Table 4.3).

Table 4.3 The relationships of microbial metabolic potential to plant and soil properties by Mantel test

		Statistic r	*P-value*
Soil	Moisture	-0.07472	0.708
	pH	0.0344	0.308
	Total C (%)	0.1188	0.134
	Total N (%)	0.1768	**0.045**
	Temperature (^{o}C)	-0.05238	0.727
Plant	Root ingrowth biomass (g m^{-2})	0.1987	**0.046**
	Aboveground biomass (g m^{-2})	0.172	**0.027**
	Root biomass (g m^{-2})	0.07145	0.18
	Root ingrowth biomass N content (%)	-0.00191	0.486
	Aboveground biomass C/N	0.03266	0.318
	Root biomass N content (%)	0.1082	**0.049**
	Root biomass C/N	0.07007	0.199

4.4.6 Microbial biomass

Both total microbial and bacterial biomass were significantly higher in C3 grass plots than in legume plots, whereas fungal biomass showed no difference between plant functional groups (Fig. 4.4 A). Within C3 grass plots, eN significantly increased total microbial biomass and bacterial biomass by 20.4% and 21.3%, respectively (Fig. 4.4 B). Meanwhile, total microbial and bacterial biomass under eCO_2 were 7.8% and 9.3% higher than under aCO_2, respectively, although these difference were not statistically significant (P = 0.07). Within legume plots, no significant difference was observed for microbial biomass under different treatment conditions (Fig. 4.4 C). It appears that microbial

biomass was not connected to the differences in microbial metabolic potential. Instead, possible changes in community structure and/or enzymatic activities of belowground microbes may be responsible for the difference in microbial metabolic potential between plant functional groups and among treatments.

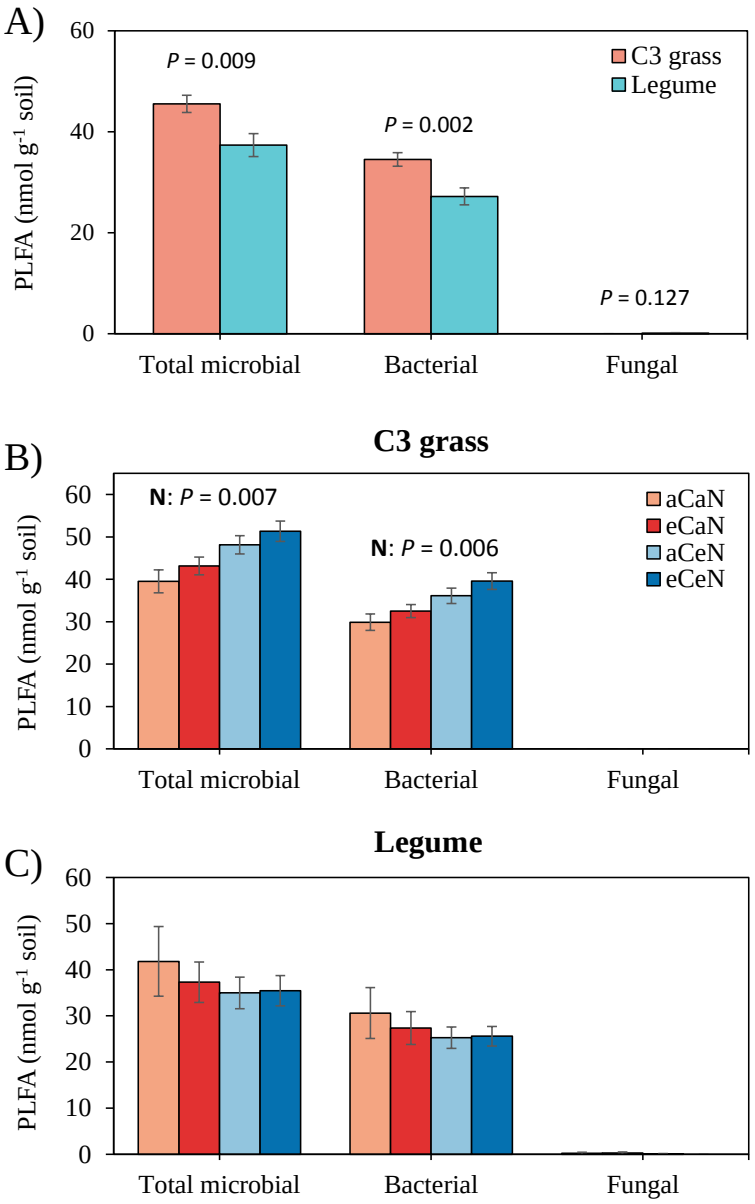

Fig. 4.4 Microbial biomass in the C3 grass and legume plot soils (A), and the effects of eCO_2 and eN on microbial biomass in the C3 grass (B) and legume plots (C).Total microbial, bacterial or fungal biomass was the sum of the signature phospholipid fatty acid (PLFA). All data are presented with mean ± SE (error bars), and the significance of eCO_2 or eN on microbial biomass is shown by *P* values.

4.5 Discussion

Understanding the mechanism of environmental changes on the soil microorganisms mediated C cycling is essential for estimating the alteration of soil C pools. Analyzing the differences in microbial C utilization abilities were useful to understand functional shifts in soil microbial community (Zhang et al. 2017). In this study, AWCD and AUC of Biolog data were used to represent the utilization of different C substrates by microbes, and to estimate the activity and physiological function of microbial communities (Guckert et al. 1996), while Shannon, Richness and Evenness indices could reflect the functional diversity of microbial metabolisms (Zhang et al. 2017). Our studies indicated that between plant functional groups, microbial communities in legume plots had greater metabolic potential than in C3 grass plots for decomposing organic substrates. Specifically, compared to the C3 grass plots, microbes in legume plots can use a larger number of C sources provided on EcoPlate and with greater decomposition rates within the measured time. We also found that, within each plant functional group, eCO_2 and eN had moderate effects on microbial metabolic potential with a significant increase in metabolic potential with eCO_2 in fertilized legume plots.

Our results indicate that the community composition of soil microbes based on metabolic potential measured by EcoPlate in the C3 grass plot soils was significantly different from those in the legume plot soils by both DCA and nonparametric dissimilarity tests. The impacts of different plant functional group, plant species on soil microbial community have been widely observed (Bremer et al. 2007, Mendes et al. 2014, Ridl et al. 2016). Physiological traits differ among plant species which affect plant C uptake, release (exudation) and repartition, therefore the structure and functional potential of

microbial communities associated with different plant species tend to vary significantly (Dudley 1996, Pei et al. 2016). Owing to the symbiotic N_2-fixation via root symbioses, legume species can abate soil N limitation and often exhibited greater and continuous yield responses compared to non-legumes to eCO_2 over long period of time (Hebeisen et al. 1997, Lee et al. 2003, Rogers et al. 2006, van Groenigen et al. 2006). Relative to non-legume species (e.g. C3 grass in this study), this implies that legume-associate microbial communities may drive more organic matter (OM) input and higher N availability. Indeed, overall microbial metabolic patterns in this study were closely linked to soil total N content, aboveground and root biomass, and root biomass N content as suggested by the Mantel test.

Soil N status plays an important role in shaping microbial community composition and structure. A recent large-scale survey examined 25 grassland sites across the globe and showed that soil microbial community composition across these sites shifted in consistent ways with higher nutrients (N, P) (Leff et al. 2015). The high N condition tends to favor copiotrophic bacteria taxa and reduce the abundance of oligotrophic taxa (Leff et al. 2015). Similar results were also observed by Ramirez and colleagues who studied 28 soils from a broad range of ecosystems in North America using high-throughput pyrosequencing and showed that N addition consistently altered bacterial community composition, increasing the relative abundance of *Actinobacteria* and *Firmicutes* which are generally considered to be more copiotrophic, and decreasing relative abundance of the largely oligotrophic *Acidobacteria* phylum (Ramirez et al. 2012). In this study, total soil N content was approximately 1.5 time higher in the legume than in the C3 grass plots ($P < 0.05$), thus there might be more copiotrophic microorganisms in the legume than in

the C3 grass plots. As copiotrophic microorganism are more capable of utilizing labile organic substrates (Koch 2001, Ho et al. 2017), it may explain the overall significantly higher richness and metabolic potential of microbial communities in legume than C3 grass plots on the C sources provided on EcoPlate, all of which are labile, low molecular weight compounds (Garland 1997, Preston-Mafham et al. 2002). Knowing which types of bacteria are specialized in metabolize the labile C may be useful in the assessment of factors that control soil C balance, as microbial decomposition offsets input of plant-derived labile C (*i.e.* litter, decaying roots and root exudates). In addition, population size (biomass) was not likely contributed to the differences in metabolic potential between plant functional groups as greater total microbial and bacterial biomass were detected in the C3 grass than legume plot soils, showing an opposite trend to the microbial metabolic potential in these plots.

It has been reported that over-fertilization disrupts plant-microbe mutualisms, reduce microbial biomass and respiration (Leff et al. 2015, Klinger et al. 2016) which, therefore, may partially explain the significantly lower microbial metabolic potential in N-added legume plots than the control plots. Meanwhile, the microbial metabolic potential was significantly higher under eCO_2 than under aCO_2 in fertilized legume plots, therefore eCO_2 appears to counterbalance the N effects possibly through increasing plant-derived substrate availability and microorganisms capable of readily utilizing these C compounds. Our results showed minor to moderate changes in metabolic profiles of microbial communities in the C3 grass and legume plots in response to eCO_2 and eN, suggesting that community composition and structures may have moderately changed in response to these factors. However, it should be noted that EcoPlate contains a relatively

simple combination of C sources which has limited ability to represent and monitor the much more complexed C pool in the rhizosphere and bulk soils, and corresponding microbial metabolic potential. Such limitation may cause underestimation of possible changes in microbial community in response to eCO_2 and eN. Also, the Biolog technique is culture-dependent with biases towards fast-growing, easily culturable species (Smalla et al. 1998). Thus, Biolog method should not be seen as a stand-alone approach, but complemented with other approaches (e.g. classical and molecular) in the analysis of microbial communities.

Chapter 5: Pyrosequencing analysis of *amoA* genes for soil ammonia-oxidizing archaeal communities under elevated CO_2 and nitrogen deposition

5.1 Abstract

The recent discovery of archaeal *amoA* encoding the α-subunit of ammonia monooxygenase and its widespread distribution of ammonia oxidizing archaea (AOA) in marine, terrestrial and other environments (e.g. hot spring) indicate AOA may play an important role in the global N cycle. Yet, little is known regarding the effect of elevated CO_2 on community diversity, composition, and structure of AOA. Furthermore, the interactive effects of multiple factors (i.e., elevated CO_2, soil N level, temperature) on the abundance and community structure of AOA remain to be demonstrated. In this study, the AOA community structure and diversity were investigated in a grassland ecosystem subjected to ambient CO2 (aCO_2, 368 ppm), elevated CO_2 (eCO_2, 560 ppm), ambient nitrogen deposition (aN) or elevated nitrogen deposition (eN) treatments for 12-year, using barcoded 454 pyrosequencing coupled with GeoChip functional gene array targeting the archaeal *amoA* gene. Elevated CO_2 and N deposition alone and combined did not significantly alter the abundance of AOA. A total of 87 *amoA* OTUs (95% identity cutoff) were generated from 26,211 qualified reads. The diversity of AOA communities measured by OTU richness (Chao1), Pielou evenness, Shannon and phylogenetic hill number was significantly reduced by long-term elevated CO_2 but the CO_2 effects were confined within ambient N condition. PCoA, βMNTD and non-parametric dissimilarity tests revealed significant CO_2 effects on the community structure of AOA regardless of N deposition, but no effect of N deposition was observed. The relative abundance of

several AOA taxa were significantly correlated with plant root biomass, proportional soil moisture, and pH. In addition, significant positive correlations between several AOA taxa and soil nitrification rate were observed, indicating soil AOA may play a role in the nitrification process in grassland soil. These results are important in furthering our understanding of the global change impacts on AOA community structure in the long term.

Keywords: *amoA*; ammonia oxidizing archaea; AOA; community structure; elevated CO_2, N deposition

5.2 Introduction

Ammonia oxidation is the first as well as rate-limiting step in nitrification, converting ammonia to nitrite and then nitrate. It is of great importance to the global nitrogen cycle, economically of paramount importance to agricultural production, and contributes to ground water pollution and greenhouse gas emission (N_2O) (Stephen et al. 1998). Catalyzed by the enzyme ammonia monooxygenase, the ability to oxidize ammonia was originally found in a few groups bacteria phylogenetically associated to the β- and γ-*Proteobacteria*. For the past decade, metagenomic approaches and following lab incubation efforts (Treusch et al. 2004, Schleper et al. 2005, Leininger et al. 2006) have revealed the existence of unique ammonia monooxygenase α-subunit (*amoA*) genes derived from archaea (Treusch et al. 2004, Venter et al. 2004, Francis et al. 2005). *amoA-based* phylogenetic analyses have demonstrated that AOA are widely distributed in various environments and often outnumber their bacterial counterparts by orders of magnitudes (Beman and Francis 2006, Leininger et al. 2006, Di et al. 2009). Also, community composition and abundance of AOA have been shown to strongly correlate to soil nitrification potential (Gubry-Rangin et al. 2010, Radax et al. 2012, Xue et al. 2016). These results indicate that that AOA community may be actively involved in and play a more important role than these ammonia oxidizing bacteria (AOB) in nitrogen cycling.

AOA are phylogenetically associated to a newly defined archaeal phylum *Thaumarchaeota* and can be further classified into sub-clusters including *Nitrososphaera, Nitrosopumilus, Nitrosotalea, Nitrosocaldus,* and *Nitrososphaera* sister clusters (Spang et al. 2010, Pester et al. 2011, Pester et al. 2012). Insights into the diversity, structure, and

distribution of AOA communities have been gained by analyzing the archaeal-*amoA* gene family in various environments. *Nitrososphaera* cluster (also called group I.1b) often dominant the AOA community in soils, with the exception of *Nitrosotalea* cluster dominating low pH soils. AOA related to the *Nitrosopumilus* cluster (also called group I.1a) has been shown to be abundant in marine, freshwater, and sediments but absent or represent minor populations in soils (Pester et al. 2012). In addition, *Nitrosocaldus* cluster mainly consists of sequences from hot spring (Pester et al. 2012). Multiple environmental factors such as ammonium concentration, organic C levels, pH, moisture, temperature, and salinity have been documented to influence the community diversity and structure of AOA (Erguder et al. 2009, Biller et al. 2012, Hatzenpichler 2012, Cao et al. 2013). For example, *amoA*-based sequencing analyses targeting agriculture soil showed that pH was a major factor shaping AOA community composition and structure, and different AOA phylotypes are selected in soils of different pH with dominant populations *Nitrosopumilus* and *Nitrososphaera* cluster being negative and positive correlations with soil pH, respectively (Shen et al. 2012). In pristine forest soil, *amoA*-based analysis revealed a decreasing abundance of AOA with increasing soil moisture, suggesting that AOA may sensitive to anaerobic conditions (Szukics et al. 2010).

Elevated CO_2 stimulates plant net primary productivity and increases C/N ratio of plant litter (Cotrufo et al. 1998, Norby et al. 2001, He et al. 2010) which could result in slower carbon degradation and N mineralization. Also, soil pH and moisture have been shown to increase in response to elevated CO_2 (Reich et al. 2006). As a result, the subsequent AOA community and nitrification process may be strongly affected by elevated atmospheric CO_2. Yet, the response of AOA diversity and structure to elevated

CO_2 are poorly assessed, particularly for AOA communities in grassland, one of Earth's largest ecosystems. A previous GeoChip survey showed increased *amoA* abundance in response to elevated CO_2 in the BioCON grassland experiment, however, the phylogenetic association (either AOA or AOB) of these *amoA* probes was not clear (He et al. 2010). Also, limited by the relatively small *amoA* probe number designed on GeoChip, in-depth analyses of diversity and structure changes of AOA community in response to elevated CO_2 were not performed.

Natural ecosystems under long-term elevated CO_2 concentration are subjected to progressive N limitation due to the stimulated plant growth and immobilization of N compounds in biomass (Hu et al. 2001, Luo et al. 2004, Finzi et al. 2006, Tilman et al. 2006). Inorganic N fertilization could support long-term ecosystem responses to elevated CO_2, however, the utilization efficiency of inorganic nitrogen fertilizer largely depends on AOA (Stark et al. 2007). Previous study in an alkaline sandy loam (pH 8.3-8.7) using DGGE revealed no significant change of AOA community after 17 years of fertilization practices using a combination of fertilizer N, P and K (Shen et al. 2008). In contrast, it has been suggested that AOA are favored in ammonia-limited oligotrophic environments, indicating that N fertilization may inhibit their abundance (Erguder et al. 2009, Jia and Conrad 2009, Di et al. 2010). Consistently, long-term fertilization-induced decrease in pH and increase in nutrient supply (e.g. total N and SOM) have been shown to significantly shift AOA community and enzyme activities (Xue et al. 2016). It is of crucial interest to understand how the belowground AOA communities respond to the interactive effects of elevated CO_2 and N deposition.

The objective of the present study was to quantitatively assess the response of soil AOA to elevated CO_2 and/or N deposition using 454 pyrosequencing of archaeal-*amoA* gene amplicons coupled with GeoChip functional gene array data, and to determine the diversity and structure of soil AOA in the BioCON experimental site after 12-years of treatments (Reich et al. 2001). The following hypotheses were tested: (1) Higher soil moisture at elevated CO_2 would reduce *amoA* gene relative abundance as previously reported;(2) Greater plant-derived organic matter input under elevated CO_2 and/or N addition may stimulate soil microorganism growth and intensify competition for limiting nutrients, thus decrease AOA diversity. This study provides valuable insights into our understanding of microbial ecology of AOA in soil.

5.3 Materials and Methods

5.3.1 Site description and sample collection

A total of 20 bulk soil samples were taken in June 2009 from the BioCON 4 plant species plots under ambient and elevated CO_2 conditions for microbial community analysis. Same samples collecting procedure was used as described in Chapter 2.

In this study, the 4 plant species in each plot were randomly chosen from a pool of 16 species including, *Agropyron repens, Bromus inermis, Koeleria cristata, Poa pratensis, Andropogon gerardii, Bouteloua gracilis, Schizachyrium scoparium, Sorghastrum nutans, Amorpha canescens, Lespedeza capitata, Lupinus perennis, Petalostemum villosum, Achillea millefolium, Anemone cylindrica, Asclepias tuberosa,* and *Solidago rigida*. All of these plants are native or naturalized to the Cedar Creek

Ecosystem Science Reserve, and there was no specific functional classification of these plants in this study.

5.3.2 DNA extraction, purification, and quantification

Soil DNA was extracted by freeze-grinding mechanical lysis as described previously (Zhou et al. 1996) and was purified using a low melting agarose gel followed by phenol extraction for all 20 soil samples collected. DNA quality was assessed by the ratios of 260/280 nm, and 260/230 nm using a NanoDrop ND-1000 Spectrophotometer (NanoDrop Technologies Inc., Wilmington, DE), and final soil DNA concentrations were quantified with PicoGreen (Ahn et al. 1996) using a FLUOstar Optima (BMG Labtech, Jena, Germany).

5.3.3 PCR amplification and 454 pyrosequencing

Amplification was performed using the Arch-amoAF and Arch-amoAR (Arch-amoAF: STAATGGTCTGGCTTAGACG, and Arch-amoAR: GCGGCCATCCATCTGTATGT) with 8 replicates each, whose products are expected to be approximately 635-bp (Francis et al. 2005). A unique 8-mer barcode was added to each sample at the 5'-end of the forward primer. The barcode-primers were synthesized by Invitrogen (Carlsbad, CA) and used for the generation of PCR amplicons. Octuplicate 25 µl PCR reactions were performed as follows: 2.5 µl Promega GoTaq buffer, 0.25 µl GoTaq DNA polymerase, 2.5 µl Roche 25 mM $MgCl_2$, 2 µl Invitrogen 10 mM dNTP mix, 0.5 µl of each primer (10 pmol μl^{-1}), 0.25 µl New England BioLabs 10 mg ml^{-1}BSA, 1 µl of 25 ng μl^{-1} template, and 15.5 µl H_2O. Cycling conditions were an initial denaturation at 95°C for 4 min, 30 cycles of 94°C for 1 min, 53°C for 1 min, 72°C for 45 s, and a final extension at 72°C for 15 min. Replicated PCR products were pooled andthen subjected to gel purification using

the Qiagen Gel Purification Kit. After adapter ligation, amplicons were sequenced on an FLX 454 system (454 Life Sciences, Branford, CT) by Macrogen (Seoul, South Korea) using Lib-L kits and processed using the shotgun protocol.

5.3.4 Data analysis

Raw pyrosequencing reads were extracted from the *sff* file using the *sffinfo* tool from Roche 454. Two files, a *fasta* file containing the sequence and a *qual* file containing the quality information, were generated and then converted into a *fastq* file using the python script "faqual2fastq2.py" that comes with the UPARSE pipeline (Edgar 2013). The quality filtering, chimera removal, and OTU clustering were carried out using the UPARSE pipeline (Edgar 2013). Only the reads with perfectly matched barcodes and a maximum of 2 primer mismatches were kept for further analysis. Barcodes and primers were deleted from reads. The remaining reads were then truncated to 450 bp, and reads with expected errors > 0.5 were discarded. The program FrameBot (Wang et al. 2013) was used to correct potential frame shifts caused by sequencing errors and only reads whose translated proteins got mapped to reference archaeal-*amoA* protein sequences with > 30% identity were kept. The reads were then dereplicated, sorted, and clustered into candidate OTUs with an identity cutoff of 0.95, which is near the average nucleotide identity that approximately corresponds to the species cutoff of 16S rRNA genes (Konstantinidis and Tiedje 2005). Chimeric OTUs were then identified and removed by searching against the *amoA* reference sequences maintained by IEG galaxy pipeline (http://www.drive5.com/uchime/). Finally, qualified reads were mapped to OTU reference sequences for relative abundance calculation.

Taxonomic assignment for archaeal-*amoA* OTUs was carried out by searching OTU representative sequences against reference archaeal-*amoA* sequences with known taxonomic information. A minimum recalculated global identity cutoff of 80% was used to filter BLAST results. A lowest common ancestor algorithm was applied for taxonomic assignment by using CREST v1.0 software (Lanzen et al. 2012) with default parameters (minimum bit-score = 155, LCA range = 2%). Taxonomic information at genus level or higher was assigned. For phylogenetic analysis, representative OTU sequences were aligned by the MUSCLE program (Edgar 2004), and a phylogenetic tree was built by FASTTREE (Price et al. 2009). Significance tests for different taxonomic groups and OTUs were performed by response ratio analysis (Hedges et al. 1999) at 95% confidence interval level. Species richness, evenness, and diversity indices were calculated by the Mothur package (Schloss et al. 2009).

5.4 Results

5.4.1 Effects of eCO_2 and eN on plant biomass, soil N, and amoA gene abundance

The plant biomass (aboveground and root) and soil nitrogen levels (NO_3^- and NH_4^+) were collected and analyzed. Nitrogen addition significantly increased root biomass production under both aCO_2 and eCO_2 (+66.7%, $P = 0.01$), but no effect of elevated CO_2 on plant biomass was observed (Fig. 5.1A). Elevated CO_2 significantly increased deep-layer soil moisture content (42-59 cm and 83-100 cm) in unfertilized plots ($P < 0.001$, Fig. 5.1C) and increased soil pH in fertilized plots ($P = 0.02$, Fig. 5.1D). Soil nitrification was calculated based on changes in NO_3^- and NH_4^+ concentrations measured through one

month *in situ* incubation, which showed no significant response to elevated CO_2 or N addition (Fig. 5.1E).

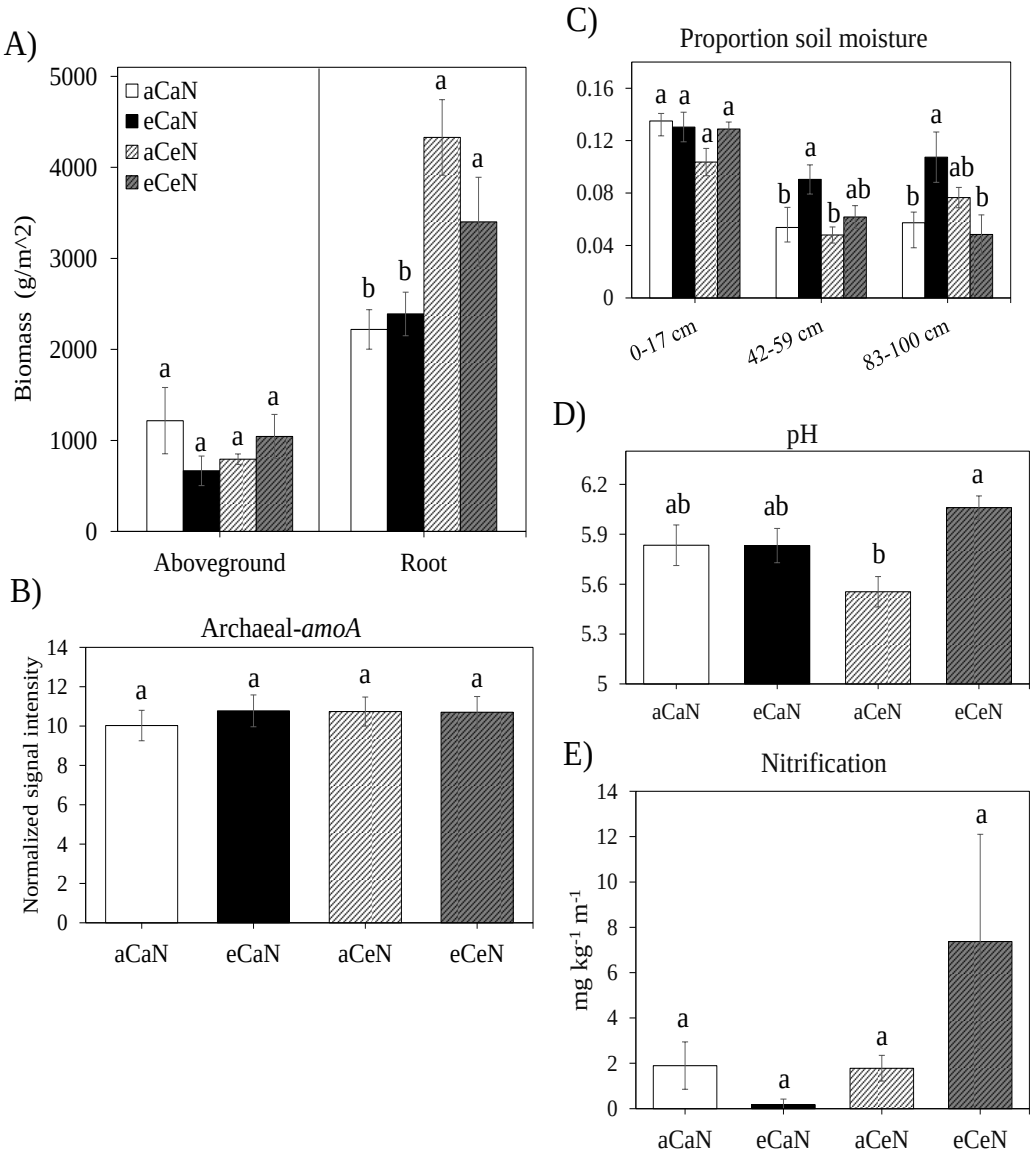

Fig. 5.1 Effects of eCO_2 and eN on plant biomass (A), *amoA* gene abundance (B), proportional soil moisture (C), soil pH (D), and soil nitrification rate (E). Both aboveground and root biomass were averaged from 3 years at the time of sampling, i.e. 2007-2009. Soil nitrification was calculated by NO_3^- and NH_4^+ concentrations measured using a semi-open core, one-month *in situ* incubation approach. The abundance of *amoA* genes was obtained from Geochip datasets by extracting probes mapped to archaeal-*amoA* genes. Statistical testing was performed by ANOVA followed by LSD with holm adjustment. aCaN: ambient CO_2, no N addition; eCaN: elevated CO_2, no N addition; aCeN: ambient CO_2, N added; eCeN: elevated CO_2, N added.

The abundance of *amoA* genes was assessed by extracting archaeal-*amoA* probes from GeoChip microarray profiling datasets, which the signal intensity of probes are proportional to the corresponding gene abundances (Wu et al. 2001). A total of 43 probes associated to archaeal-*amoA* on GeoChip were detected, and there was no significant difference for the abundance of *amoA* genes under different CO_2 and N levels (Fig. 5.1B). This suggested that neither eCO_2 nor eN had a significant influence on the abundance of archaeal-*amoA* genes in soils of this grassland ecosystem.

5.4.2 Sequencing data summary

Using 454 pyrosequencing, a total of 47,659 raw reverse reads targeting archaeal-*amoA* gene amplicons were obtained for the 20 samples, among which 28,585 were assigned to corresponding barcodes. After quality trimming, frameshift correction and chimera removal, 26,211 reads were clustered into 87 *amoA* OTUs at 95% identity cutoff, of which 64 (a total of 6,153 reads with 1,683; 1,781; 1,037 and 1,652 from aCaN, eCaN, aCeN and eCeN, respectively) were non-singleton OTUs. The number of sequences in each sample ranged from 115 to 546 (308 on average), resulting in 10 to 33 OTUs per sample. A random re-sampling effort of 115 reads per sample was made for further statistical analysis.

5.4.3 Significant eCO_2 and eN effects on overall AOA diversity and structure

To analyze the Archaeal-*amoA* community diversity and their responses to elevated CO_2 at different soil N condition, the OTU richness (Chao1), evenness, taxonomic and phylogenetic diversity indices were calculated (Table 5.1). A total of 40, 28, 39, and 30 OTUs were identified for samples under aCaN, eCaN, aCeN and eCeN, respectively, with the current sequencing effort. Elevated CO_2 significantly reduced the evenness and

taxonomic diversity of overall *amoA* community in unfertilized plots ($P < 0.05$), except OTU richness which showed no effect of CO_2 or N. Consistently, the phylogenetic diversity of *amoA* gene, which also considers the phylogenetic relationship among OTUs was significantly lower at elevated than ambient CO2 condition in unfertilized plot soils ($P < 0.05$, Table 5.1). No significant differences between fertilized and unfertilized samples were observed for OTU richness, evenness, and diversity at both taxonomic and phylogenetic levels were observed (Table 5.1). All these results suggested that the diversity of *amoA*-community was significantly altered by long-term elevated CO_2 but the CO_2 effects were confined within ambient N condition in this grassland ecosystem.

Table 5.1 The diversity of *amoA* genes in the grassland ecosystem under different CO_2 and N conditions. Shown are mean values (n=5) ± standard errors. Values labeled with different letters are significantly different ($P < 0.05$) according to ANOVA, followed by Fisher's least significant difference (LSD) test with Holm-Bonferroni adjustment.

Treatment	Chao1 richness	Shannon	Pielou evenness	Phylogenetic diversity (hill_0)
aCaN	20.80 ± 3.22 a	2.14 ± 0.24 a	0.76 ± 0.06 a	17.00 ± 2.30 a
eCaN	16.92 ± 5.94 a	1.26 ± 0.12 b	0.55 ± 0.04 b	9.80 ± 0.86 b
aCeN	20.89 ± 5.72 a	1.66 ± 0.29 ab	0.62 ± 0.06 ab	14.60 ± 2.80 ab
eCeN	17.47 ± 1.42 a	1.57 ± 0.15 ab	0.61 ± 0.05 ab	13.20 ± 0.80 ab

Long-term elevated CO_2 fertilization also significantly alter the overall archaeal *amoA*-community structure in the grassland soil ecosystem with greater influence in low than high N levels (Fig. S5.1). The overall community structural differences among all samples were assessed by both weighted (with relative abundance data)/unweighted (with richness data) UniFrac PCoA and βMNTD analyses. A well separation of elevated CO_2 samples from ambient CO_2 samples in unfertilized plots were observed by all the analyses (Fig. S5.1). A separation trend of elevated CO_2 samples in fertilized plots from ambient CO_2 samples in unfertilized plots could be observed with some overlaps (Fig. S5.1).

However, there was no clear separation for elevated CO_2 samples from ambient CO_2 samples in fertilized plots (Fig. S5.1). Further dissimilarity analysis also suggested that the overall community structure between ambient CO_2 and elevated CO_2 samples in unfertilized plots was significantly different (ADONIS: $F = 4.920$, $P = 0.015$; ANOSIM: $R = 0.472$, $P = 0$ 0.009; MRPP: $\delta = 0.421$, $P = 0.007$). And samples between ambient CO_2 and elevated CO_2 samples in fertilized plots were significantly different by ANOSIM ($R = 0.472$, $P = 0.009$) and (ADONIS: $F = 3.359$, $P = 0.041$), and marginally significant by MRPP ($\delta = 0.439$, $P = 0.054$).

5.4.4 The taxonomic and phylogenetic composition of archaeal-amoA genes

Compare to the 16S rRNA and bacterial-*amoA* genes, reference sequences for archaeal-*amoA* genes from cultivated microbial strains/species are still very limited, making it difficult to classify archaeal-*amoA* sequences into their taxonomic groups, especially at the lower taxonomic levels. By assigning taxonomic information to OTUs having a minimum of 95% sequence similarity with references in the *amoA* database, only 63 OTUs could be assigned to known taxonomic groups including *Nitrososphaera* subclusters 1.1, 3.1, 3.2, 3.3, 5.1, 6.1, 7, 8.1, 8.2, and 11; *Nitrososphaera* sister subcluster 1.1 and 2; and *Nitrosotalea* subcluster 1.1 (Fig. 5.2A).

The AOA community was dominated by *Nitrososphaera* cluster (98.4%) across all CO_2 and N levels, among which *Nitrososphaera* subcluster 8.2, an unclassified *Nitrososphaera* subcluster, subcluster 1.1 and 8.1 were most dominant, accounting for 45.7%, 22.3%, 7.6%, and 5.0% of the entire AOA community, respectively. Whereas, clusters related to *Nitrososphaera* sister and *Nitrosotalea* only accounted for 1.6% of the entire AOA community in this study. Elevated CO_2 significantly reduced the relative

abundances of *Nitrososphaera* subclusters 5.1, 8.1, and 11 in unfertilized plots, but increased *Nitrososphaera* subcluster 8.2 in fertilized plots ($P < 0.05$, Fig. 5.2B); whereas N fertilization significantly increased the relative abundance of *Nitrososphaera* subcluster 1.1 at elevated CO_2, but *Nitrososphaera* sister subcluster 1.1 at ambient CO_2 ($P < 0.05$, Fig. 5.2B). At OTU level, only 8 OTUs were significantly affected by elevated CO_2 and/or N deposition, which however quantitatively accounted for 57.5% of the AOA community ($P < 0.05$). All the 8 OTUs were assigned to *Nitrososphaera* cluster. The most dominant OTU (denovo642), belongs to *Nitrososphaera* subcluster 8.2 and accounted for 47.2% of the archaeal-*amoA* community, was more abundant under elevated than ambient CO_2 in unfertilized plots ($P < 0.05$, Fig. S5.2). Less dominant OTUs including denovo301 (0.8%), denovo33 (4.7%) and denovo840 (0.7%) had significant lower relative abundances with elevated CO_2 in unfertilized plots ($P < 0.05$, Fig. S5.2). No significant changes of relative abundances for any *amoA* groups at the OTU level were observed between ambient CO_2 and elevated CO_2 in fertilized plots.

A)

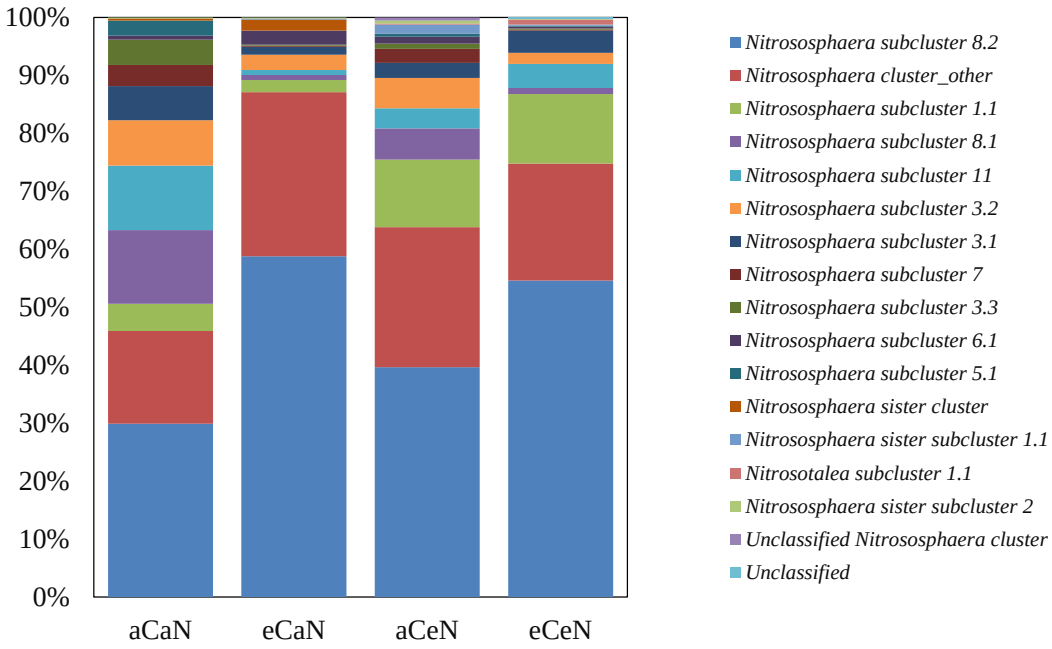

B)

	CO_2		N		CO_2*N		LSD			
	F	*p*	*F*	*p*	*F*	*p*	aCaN	eCaN	aCeN	eCeN
Nitrososphaera subcluster 1.1	0.12	0.74	6.58	**0.02**	0.20	0.66	ab	b	ab	a
Nitrososphaera subcluster 5.1	6.08	**0.03**	2.55	0.13	3.56	0.08	a	b	ab	ab
Nitrososphaera subcluster 7	5.92	**0.03**	0.27	0.61	0.27	0.61	a	a	a	a
Nitrososphaera subcluster 8.1	17.18	**0.00**	3.34	0.09	3.67	0.07	a	b	ab	b
Nitrososphaera subcluster 8.2	5.96	**0.03**	0.10	0.76	0.60	0.45	b	a	ab	ab
Nitrososphaera subcluster 11	3.74	0.07	0.77	0.39	4.90	**0.04**	a	b	b	ab
Nitrososphaera sister subcluster 1.1	3.16	0.09	5.23	**0.04**	5.23	**0.04**	b	ab	a	ab

Fig. 5.2 Phylogenetic composition of archaeal-*amoA* gene among different CO_2 and N conditions (A) and significantly changed AOA groups in response to CO_2 and N (B). Variations between different treatments were tested by ANOVA. Different letters denote significant differences among treatments from least-significant-difference (LSD) tests with holm adjustment. Only significant changed AOA groups were listed.

5.4.5 Linkage between archaeal amoA gene and environmental factors and soil nitrification rate

To examine the linkage between detected individual archaeal-amoA taxa and environmental factors, Spearman's rank correlation coefficient was performed. Changes in taxa were found to closely correlate to several of the selected environment properties including aboveground and root plant biomass, soil pH and proportional moisture (Table

S5.1). Root biomass significantly correlated with 7 out of the 16 AOA phylogenetic groups including *Nitrososphaera* subclusters 1.1, 6.1, 8.2, 11 and three *Nitrososphaera* sister clusters (Table S5.1, $P < 0.1$). Soil moisture, particularly at the depth of 42-59 cm, was significantly correlated with 5 AOA groups including *Nitrososphaera* subclusters 1.1, 3.2, 5.1, 6.1 and *Nitrososphaera* sister cluster (Table S5.1, $P < 0.1$).

Linkage between soil nitrification rate and individual archaeal-*amoA* phylogenetic groups were further analyzed based on Spearman's rank correlation coefficient (Table 5.2). A total of 4 AOA taxa including *Nitrososphaera* subclusters 8.2, 6.1, 3.1 and 3.2 were positively correlated with soil nitrification rate ($P < 0.05$), indicating soil ammonia oxidizing archaea were actively involved in the nitrification process in grassland soil.

5.5 Discussion

Given the numerically abundant and ubiquitous existence, understanding the diversity, composition, and structure of AOA communities is essential for predicting N dynamics in ecosystems. In this study, we used 454 pyrosequencing approach coupled with Geochip functional gene array to analyze AOA communities in grassland soils subjected to 12-year elevated CO_2 and N deposition. Our results showed that long-term eCO_2, N deposition, and their interactive effects did not change the abundance of archaeal-*amoA* genes, but significantly change the overall *amoA* diversity and structure of soil AOA communities. Environmental factors including plant root biomass, soil moisture and pH were significantly correlated with the abundances of several archaeal-*amoA* taxa. This

study provides novel insights into our understanding microbial ecology of AOA communities in grassland ecosystems.

The first objective of this study was to determine whether the abundance of AOA community will be altered in response to long-term elevated CO_2 and N deposition in this grassland ecosystem. Based on the signal intensity of archaeal-*amoA* probes detected by GeoChip, no significant differences in AOA abundance were observed under different CO_2 and N conditions. This result was in accordance with previous reports showing that inorganic N fertilization significantly increases the abundance of soil ammonia oxidizing bacteria (AOB) but not AOA (Shen et al. 2008, Di et al. 2009). Contrarily, negative effects of NO_3^- by fertilization on AOA community were also reported (Ying et al. 2017). It should be noted that relatively small N amendment level (4 g N m^{-2} yr^{-1}) was carried out in this experiment, which is less than the N addition in several other studies (up to 56 g N m^{-2} yr^{-1}) to simulate agricultural N fertilization (Zanetti et al. 1997, Reich et al. 2001). As a result, no significant differences in soil N content or pH were observed between unfertilized and fertilized soils in this study ($P > 0.05$).

Enhanced plant-derived organic matter input under elevated CO_2 was commonly found to stimulate belowground microbial biomass and alter community structure (He et al. 2010). However, changes in the AOA community abundance in response to the surplus of organic matter input is still debatable. Studies on AOA representatives *N. maritimus* and *N. yellowstonii* showed slow, or halted growth in the presence of additional organic substrates even at very low concentrations, suggesting a strong inhibition for AOA by organic matter (Falkowski et al. 2008). Similarly, a negative linear relationship between the $\delta^{13}C$ and archaeal-*amoA* gene was observed in the Duke Forest FACE experiment,

indicating a negative effect of elevated CO_2 on the growth ammonia oxidizing archaea (Long et al. 2012). However, other evidence had demonstrated that labile organic matter may have a positive effect on the growth of AOA (Stopnisek et al. 2010). Inconsistencies in these observations may relate to the potential ability of AOA to use both inorganic and organic material as C sources (Hallam et al. 2006, Zhang et al. 2010). Meanwhile, elevated CO_2 always increase soil moisture by increasing plant water using efficiency (Reich et al. 2006), an effect that observed in the unfertilized plots as well in this study. Studies on *amoA* gene in pristine forest soil revealed a decreasing abundance of AOA with increasing soil moisture, suggesting that AOA may sensitive to anaerobic conditions (Szukics et al. 2010). Together, the unchanged AOA abundance in response to elevated CO_2 in this study may be an effect of those mechanisms canceling each other. In addition, it should be noted that less than 100 archaeal-*amoA* probes were detected using GeoChip which limits its ability in quantifying the abundance of AOA in this study. Further studies such as quantitative PCR targeting the *amoA* genes are needed to confirm these results.

The results of PCoA, βMNTD and non-parametric dissimilarity tests generally agreed with each other showing that elevated CO_2 significantly influenced the diversity and structure of AOA community in this grassland ecosystem rather than N deposition. Long-term elevated CO_2 significantly decreased AOA community richness, taxonomic and phylogenetic diversity. Similar results were reported by previous studies at this site showing significantly decreased overall soil microbial richness, although no differences in overall functional diversity were observed in response to elevated CO_2 (He et al. 2010, He et al. 2012). However, an increase in overall functional community diversity was observed in response to elevated CO_2 (Chapter 3). These findings suggest the responses

of community diversity of different microbial phylogenetic and functional groups to global change factors are diverse. Meanwhile, varied responses of different taxonomic and phylogenetic groups of AOA to elevated CO_2 and N deposition were observed, contributing to the significant changes of the AOA community structure in response to elevated CO_2 and N deposition. Similarly, markedly different phylogenetic/functional structure of overall microbial community between ambient and elevated CO_2 were widely observed at BioCON (He et al. 2010, Deng et al. 2012, Xu et al. 2013, He et al. 2014, Tu et al. 2015). Our results also suggested that N deposition mitigated the effects of elevated CO_2 on the archaeal *amoA*-community. It appears that N deposition negated the elevated CO_2 effects, resulting in weaker CO_2 effects on AOA community diversity and structure at enriched than ambient N conditions. This may partially relate to the unresponsiveness of plant and soil factors to the combined effect of elevated CO_2 and N deposition. As community composition and structure of AOA correlate to soil nitrification potential (Gubry-Rangin et al. 2010, Radax et al. 2012, Xue et al. 2016), AOA community diversity and structure shifts under elevated CO_2 have the potential to alter N cycling in grassland soil.

AOA communities in this study were predominantly composed of *Nitrososphaera*, a finding consistent with other studies that have shown the dominance of this group of AOA in soils (Wessen et al. 2011, Jiang et al. 2014). In contrast, the *Nitrosotalea*-associate AOA have been observed mainly in acidic environments (Lehtovirta-Morley et al. 2011, Pester et al. 2012). Thus, it is not surprising for the presence of these groups in the slightly acidic BioCON soil, although their relative abundance were low (pH 5.3-6.3). In addition, studies on the only *Nitrososphaera* sister

cluster isolate '*Ca.* N. franklandus' revealed high ammonia tolerance and suggests potential contributions to nitrification in fertilized soils for this group of AOA (Lehtovirta-Morley et al. 2016). Consistently, significant N effect on the relative abundance of *Nitrososphaera* sister subcluster 1.1 was observed in our study where N deposition significantly increased their abundance.

Unlike AOB who rely on Calvin-Benson-Bassham (Calvin cycle) to fix carbon (Kowalchuk and Stephen 2001), AOA seems developed different carbon fixation strategies. Both autotrophic and heterotrophic life strategies were suggested through lab incubation and molecular analysis targeting AOA isolates (Ingalls et al. 2006, Agogue et al. 2008, Mussmann et al. 2011). These results raised uncertainties regarding the ecological function of AOA community in N cycling because under possible mixotrophic, even heterotrophic life styles, AOA may not gain energy through oxidation of ammonia to nitrite, and under which the ammonia oxidation potential of AOA may not be functional. Correlation test in this study revealed significant correlations between measured soil nitrification rate and individual archaeal-*amoA* phylogenetic groups, indicating soil AOA may actively involve in the nitrification process in this grassland soil.

In conclusion, this study comprehensively analyzed the abundance, diversity, and structure of ammonia oxidation archaea communities in a CO_2 enriched grassland ecosystem under different soil N conditions. Our results provided several valuable insights into the microbial ecology of AOA and their responses to long-term elevated CO_2 and/or N deposition. First, this study was conducted in a grassland ecosystem subjected to >12 years elevated CO_2 and N deposition treatments using multiple complementary approaches, providing reliable evidence that individual and interactive effects of these global change factors can significantly affect the diversity and structure of AOA

community but not their abundance. Second, AOA community composition was significantly correlated with selected environmental factors including plant root biomass and soil moisture. Finally, several individual archaeal-*amoA* phylogenetic groups may actively involve in the nitrification process in this grassland soil. As nitrification is the rate-limiting step in the N cycling of highly complex terrestrial ecosystems, shifts in the diversity and structure of AOA community may have a large influence on the N cycling in grassland ecosystem in the long term. However, additional experiments are needed on the potential nitrification rate and archaeal-*amoA* gene expression which could offer more detailed information about the response of AOA to global change such as elevated CO_2 and N deposition.

Chapter 6: Summary and Output

The atmospheric CO_2 concentration is continuously increasing, and scientific research demonstrates that this leads to huge changes to the global ecosystem, such as climate change. How and by what mechanisms long-term elevated CO_2 affects belowground microbial communities is a critical issue for ecology and global change biology. Furthermore, the interactive effects of elevated CO_2 with other environmental change factors, such as nitrogen (N) deposition, on belowground microbial communities, and their feedbacks on ecosystem function have been scarcely studied. Using integrated approaches including high-throughput functional gene array (GeoChip 3.0), 454 pyrosequencing, Illumina sequencing, biolog, and stable isotope-based microbial C-sequestration and N_2-fixation measurements, this study obtained insights into grassland soil microbial community diversity and their interactive responses to long-term elevated CO_2 and N deposition (12-year). Based on the observed results, several outcomes and/or mechanisms about microbial community responses to the treatment effects were revealed.

First, to study the interactive effects of elevated CO_2 with N deposition on belowground microbial communities, we assessed changes in soil microbial communities of two plant functional groups (C3 grass and legume) under elevated CO_2 on and/or N deposition. C3 grasses were chosen as the model due to their strong responses to elevated CO_2, and legumes were chosen due to their symbiotic N_2-fixation capability via root symbioses which may abate soil N limitation compared to non-legumes under elevated CO_2 over a long period of time. Due partially to the extreme complexity of soil microbial community and limitations of conventional molecular microbial ecology approaches for characterizing them, until now, no consistent results were obtained about how elevated

CO_2 affects the belowground microbial community structure and diversity (Janus et al. 2005, Lipson et al. 2005, Lipson et al. 2006, Lesaulnier et al. 2008, Castro et al. 2010, Dunbar et al. 2012, Eisenhauer et al. 2012, He et al. 2012). Using advanced Illumina platform, we did large scale sequencing of microbial 16S rRNA gene amplicons to examine the diversity and structure. Metagenomic sequencing analyses reveals marked divergence in the structure and composition of soil microbial communities at elevated CO_2 and N deposition, and between C3 grass and legume plots. Elevated CO_2 increased community phylogenetic diversity in C3 grass plots, while increased richness in legume plots. N deposition, on the other hand, increased community richness but only in C3 grass plots. No CO_2 and N interactive effects were observed on community diversity or richness. Further investigation suggested that less abundant groups rather than dominant taxa were mainly responsible for the changed community diversity and structure. In addition, our results suggested that copiotrophic-like bacteria appear to be more abundant in the legume than in the C3 grass plots, whereas oligotrophic-like bacteria appear to be more abundant in the C3 grass than in the legume plots. Changes in community diversity and composition were closely related to plant and soil properties including plant biomass, biomass N content and C/N ratio, soil ammonium and nitrate, pH, moisture, temperature, and soil C and N contents. Because the belowground microbial community is intimately linked to aboveground biodiversity (Wardle et al. 2004) and mediates ecosystem multifunctioning (Fierer et al. 2009, Wagg et al. 2014), these changes in microbial diversity and structure may lead to considerable ecosystem consequences in the future. Our results demonstrated that elevated CO_2 effects are contingent on N conditions and

plant functional groups, underscoring the difficulty toward predictive modeling of soil ecosystem under future climate scenarios and necessitating more detailed studies.

Second, we found that 12-year elevated CO_2 increased belowground microbial functional gene diversity, structure, and potential activities, but the magnitude of such effect depends on soil N levels and plant functional groups. Microbial functional genes in C3 grass plots had stronger responses to elevated CO_2 and N deposition than those in legume plots. And microbial functional genes related to C, N, S and P cycling in low fertility soils were stimulated more by elevated CO_2 than fertilized ones. Particularly, microbial genes related to chemically recalcitrant C degradation (e.g. phenol_oxidase, manganese peroxidase, vanillin dehydrogenase, vanillate monooxygenase, malate synthase, isocitrate lyase, endochitinase, acetylglucosaminidase) were selectively increased with elevated CO_2 in non-fertilized C3 grass plot soils only. These results suggest that microbial N-mining through decomposition of soil organic substrates could have increased with elevated CO_2 (Priming effect) and being stronger in low than high nutrient conditions in the grassland ecosystem of this study. Furthermore, the abundance of *ureC* gene for ammonification was increased with elevated CO_2 in non-fertilized C3 grass plot soils, resulting in a positive effect of elevated CO_2 on net N mineralization in these plots. Moreover, the abundance of *nifH* genes increased by 35.5% with elevated CO_2 in non-fertilized C3 grass plots, suggesting more N could have been fixed in these plots. The combination of these effects may increase soil N availability and contribute to the long-term stimulation of elevated CO_2 on plant productivity, but persistent turnover of chemically recalcitrant C by microbes also accelerates soil C loss under elevated CO_2 particularly when N is limited, offering a

partial explanation for the lack of C accumulation in the C3 grass plot soils at this site despite 12 years of CO_2-induced increases in NPP (Reich and Hobbie 2013). N deposition, on the other hand, reduced genes involved in both labile and recalcitrant C decomposition (mainly in C3 grass plots), suggesting a decrease in SOM decomposition in these plots. N deposition also reduced the abundance of *nifH* genes. Together, N deposition may contribute to C accumulation but reduce biological N-gain through microbial N-mining and N-fixation in the long-term. To what extent, these changes in microbial functional potential will alter total C and N budgets in this grassland ecosystem requires further study.

Third, DNA-based technologies (e.g., RFLP, DGGE, and Geochip) are limited to directly reflecting the actual activity of active microbial populations (McGrath et al. 2010, Simon and Daniel 2011, Franzosa et al. 2015). Therefore, we further measured belowground microbial C utilization profile using cultivation-based Biolog EcoPlate. We found that community composition of soil microbes in the C3 grass plot soils was significantly different from those in the legume plot soils based on the C utilization rate. And microbial communities in legume plots had significantly higher metabolic potential than in C3 grass plots for decomposing organic substrates. Elevated CO_2 and N deposition didn't significantly alter metabolic potential of microorganisms in the C3 grass plots. Overall microbial metabolic activities significantly increased with elevated CO_2 by 20.6% in the fertilized legume plots, while there was no evidence for a CO_2 effect in the non-fertilized legume soils. These results demonstrated that elevated CO_2 effects on active microbial metabolic activities are contingent on N conditions, and such effect differs between plant functional groups. Meanwhile, PLFA analysis showed both total

microbial and bacterial biomass were significantly lower in legume than in C3 grass plots, showing an opposite trend to the microbial metabolic potential in these plots. Thus, differences in microbial metabolic potential among treatments and between plant functional groups were not due to population size (biomass) but likely attributed to changes in community structure and/or enzymatic activities of belowground microbes.

Fourth, the recently discovered ammonia oxidizing archaea (AOA) community has been shown to be widely distributed, more abundant than its bacterial counterparts, ammonia oxidizing bacteria (AOB), and may play an important role in the global N cycle. Yet, little is known regarding the effect of elevated CO_2 on their community diversity, composition, and structure. Furthermore, the interactive effects of multiple factors (i.e., elevated CO_2, soil N level, temperature) on the abundance and community structure of AOA remain to be demonstrated. Using barcoded 454 pyrosequencing coupled with GeoChip functional gene array targeting the archaeal *amoA* gene, the AOA community structure and diversity were investigated in this study. Although elevated CO_2 and N deposition alone and combined did not significantly alter the abundance of AOA. The taxonomic and phylogenetic diversity of AOA communities were significantly reduced by long-term elevated CO_2 but the CO_2 effects were confined within ambient N condition. Elevated CO_2 also significantly altered the community structure of AOA regardless of N deposition, but no main effect of N deposition on AOA community diversity and structure were observed. The relative abundance of several AOA taxa were significantly correlated with plant root biomass, proportional soil moisture, and pH. In addition, significant positive correlations between AOA taxa and soil nitrification rate were observed, indicating soil ammonia oxidizing archaea were actively involved in the nitrification

process in grassland soil. These results are important in furthering our understanding of the global change impacts on AOA community structure in the long term.

In addition, based on the archaeal *amoA* gene sequences obtained from this study, we also constructed high-density functional gene arrays (FGAs) containing more archaeal *amoA* genes probes for better monitoring AOA community dynamics in natural environments.

In conclusion, this study advances our understanding of (i) the diversity of grassland microbial communities, (ii) the responses of soil microbial communities to changes in atmospheric CO_2 and N deposition, and (iii) the mechanistic linkages among aboveground plant and belowground microbial communities and associated ecosystem processes. These results have important implications for feedback responses of ecosystems to atmospheric CO_2 and N deposition.

Those results from this study and other associated projects that I have involved are largely reflected in my publications (published, in press, in preparation) as they are listed below:

1. **Feifei Liu**, Kai Xue, Bo Wu, Qun Gao, Zhili He, Liyou Wu, Sarah Hobbie, Peter Reich, Jizhong Zhou. Contingency in belowground microbial functional responses to rising atmospheric CO_2 at contrast nitrogen conditions. *Preparing for submission.*
2. **Feifei Liu,** Bo Wu, Renmao Tian, Daliang Ning, Sarah Hobbie, Peter Reich, Jizhong Zhou. Shifts of phylogenetic composition and structure of soil microbial communities in response to elevated carbon dioxide and nitrogen deposition. *Preparing for submission.*
3. **Feifei Liu** et al. Pyrosequencing analysis of *amoA* genes for soil ammonia-oxidizing archaea communities under elevated CO2 and nitrogen deposition conditions. *Draft.*
4. **Feifei Liu** et al. Dynamic responses of soil microbial communities to elevated CO_2. *Draft.*
5. Michelle Q. Carter , Kai Xue, **Feifei Liu**, Liyou Wu, Jacqueline W. Louie, Robert E. Mandrell, Jizhong Zhou. Functional Metagenomics of Escherichia coli O157:H7

Interactions with Spinach Indigenous Microorganisms during Biofilm Formation. *Plos One, 05 September 2012*.

6. Kai Xue, Jianping Xie, Aifen Zhou, **Feifei Liu,** Dejun Li, Liyou Wu, Ye Deng, Zhili He, Joy Van Nostrand, Yiqi Luo, Jizhong Zhou. Warming alters expressions of microbial functional genes important to ecosystem functioning. *Front. Microbiol. 06 May 2016*.
7. Christopher Penton, Caiyun Yang, **Feifei Liu,** Liyou Wu, Qiong Wang, Jin Zhang, Yujia Qin, Ye Deng, Christopher L Hemme, Tianling Zheng, Edward A.G. Schuur, James M. Tiedje, Jizhong Zhou "NifH- Harboring Bacterial Community Composition Across an Alaskan Permafrost Thaw Gradient. *Front. Microbiol. 2016*.
8. Bo Wu, **Feifei Liu,** Lina Shen, Ye Deng, Liyou Wu, Michael Weiser, Mike E. Kaspari, Brian J. Enquist, Robert B. Waide, and James H. Brown, Shouwen Chen*, and Jizhong Zhou, and Zhili He*. The diversity and biogeographic distribution of N_2O-reducing microbial communities in forest soils along a temperature gradient. *Functional Ecology*. *In revision*
9. Chongqing Wen; Liyou Wu; Yujia Qin; Joy Van Nostrand; Bo Sun; Kai Xue; Ye Deng; **Feifei Liu**; Jizhong Zhou. Evaluation of the Reproducibility of Amplicon Sequencing with Illumina MiSeq Platform. *PLoS ONE. 2017*
10. Penton C.R., Yang C., Tiedje J., **Liu F**., Ma J., Yuan M., Zhang J., Xue K., Van Nostrand J., Yuan T., Wu L., He X., Schuur E.A.G., Zhou J. 2012. Diversity of soil fungal communities across a permafrost thawing gradient in an Arctic tundra. *In prep.*
11. Penton C.R., Pham A., St. Louis D., **Liu F.**, Zhang J., Schuur E.A.G., Tiedje J. 2012. Fungal community shifts due to artificial warming in grassland and tundra ecosystems. *In prep.*
12. Penton C.R., St. Louis D., Pham A., **Liu F**., Zhang J., Schuur E.A.G., Tiedje J. 2012. Changes in N functional communities as a response to warming in grassland and tundra ecosystems through pyrosequencing of *nifH*, *nirS*, *nirK*, *nosZ*, and *amoA* genes. *In prep.*

References

Adair, E. C., P. B. Reich, J. J. Trost and S. E. Hobbie (2011). "Elevated CO2 stimulates grassland soil respiration by increasing carbon inputs rather than by enhancing soil moisture." Global Change Biology **17**(12): 3546-3563.

Agogue, H., M. Brink, J. Dinasquet and G. J. Herndl (2008). "Major gradients in putatively nitrifying and non-nitrifying Archaea in the deep North Atlantic." Nature **456**(7223): 788-U772.

Ahn, S. J., J. Costa and J. R. Emanuel (1996). "PicoGreen quantitation of DNA: Effective evaluation of samples pre- or post-PCR." Nucleic Acids Research **24**(13): 2623-2625.

Ahn, S. J., J. Costa and J. Rettig Emanuel (1996). "PicoGreen Quantitation of DNA: Effective Evaluation of Samples Pre-or Psost-PCR." Nucleic Acids Research **24**(13): 2623-2625.

Ainsworth, E. A. and S. P. Long (2005). "What have we learned from 15 years of free-air CO2 enrichment (FACE)? A meta-analytic review of the responses of photosynthesis, canopy." New Phytologist **165**(2): 351-371.

Amthor, J. S. (1995). "Terrestrial Higher-Plant Response to Increasing Atmospheric [Co2] in Relation to the Global Carbon-Cycle." Global Change Biology **1**(4): 243-274.

Austin, E. E., H. F. Castro, K. E. Sides, C. W. Schadt and A. T. Classen (2009). "Assessment of 10 years of CO2 fumigation on soil microbial communities and function in a sweetgum plantation." Soil Biology & Biochemistry **41**(3): 514-520.

Beman, J. M. and C. A. Francis (2006). "Diversity of ammonia-oxidizing archaea and bacteria in the sediments of a hypernutrified subtropical estuary: Bahia del Tobari, Mexico." Applied and Environmental Microbiology **72**(12): 7767-7777.

Berthrong, S. T., C. M. Yeager, L. Gallegos-Graves, B. Steven, S. A. Eichorst, R. B. Jackson and C. R. Kuske (2014). "Nitrogen Fertilization Has a Stronger Effect on Soil Nitrogen-Fixing Bacterial Communities than Elevated Atmospheric CO2." Applied and Environmental Microbiology **80**(10): 3103-3112.

Biller, S. J., A. C. Mosier, G. F. Wells and C. A. Francis (2012). "Global Biodiversity of Aquatic Ammonia-Oxidizing Archaea is Partitioned by Habitat." Frontiers in microbiology **3**: 252.

Blagodatskaya, E., S. Blagodatsky, M. Dorodnikov and Y. Kuzyakov (2010). "Elevated atmospheric CO2 increases microbial growth rates in soil: results of three CO2 enrichment experiments." Global Change Biology **16**(2): 836-848.

Bremer, C., G. Braker, D. Matthies, A. Reuter, C. Engels and R. Conrad (2007). "Impact of plant functional group, plant species, and sampling time on the composition of nirK-Type denitrifier communities in soil." Applied and Environmental Microbiology **73**(21): 6876-6884.

Butterly, C. R., L. A. Phillips, J. L. Wiltshire, A. E. Franks, R. D. Armstrong, D. L. Chen, P. M. Mele and C. X. Tang (2016). "Long-term effects of elevated CO2 on carbon and nitrogen functional capacity of microbial communities in three contrasting soils." Soil Biology & Biochemistry **97**: 157-167.

Cao, H. L., J. C. Auguet and J. D. Gu (2013). "Global Ecological Pattern of Ammonia-Oxidizing Archaea." Plos One **8**(2).

Carney, K. M., B. A. Hungate, B. G. Drake and J. P. Megonigal (2007). "Altered soil microbial community at elevated CO2 leads to loss of soil carbon." Proceedings of the National Academy of Sciences of the United States of America **104**(12): 4990-4995.

Carrillo, Y., F. A. Dijkstra, E. Pendall, D. LeCain and C. Tucker (2014). "Plant rhizosphere influence on microbial C metabolism: the role of elevated CO2, N availability and root stoichiometry." Biogeochemistry **117**(2-3): 229-240.

Castro, H. F., A. T. Classen, E. E. Austin, R. J. Norby and C. W. Schadt (2010). "Soil Microbial Community Responses to Multiple Experimental Climate Change Drivers." Applied and Environmental Microbiology **76**(4): 999-1007.

Chao, A. (1984). "Non-parametric estimation of the number of classes in a population." Scandinavian Journal of Statistics **11**: 5.

Chao, A., C. H. Chiu and L. Jost (2010). "Phylogenetic diversity measures based on Hill numbers." Philosophical Transactions of the Royal Society B-Biological Sciences **365**(1558): 3599-3609.

Chapin, F. S., E. S. Zavaleta, V. T. Eviner, R. L. Naylor, P. M. Vitousek, H. L. Reynolds, D. U. Hooper, S. Lavorel, O. E. Sala, S. E. Hobbie, M. C. Mack and S. Diaz (2000). "Consequences of changing biodiversity." Nature **405**(6783): 234-242.

Chen, R. R., M. Senbayram, S. Blagodatsky, O. Myachina, K. Dittert, X. G. Lin, E. Blagodatskaya and Y. Kuzyakov (2014). "Soil C and N availability determine the priming effect: microbial N mining and stoichiometric decomposition theories." Global Change Biology **20**(7): 2356-2367.

Cheng, W., Kuzyakov, Y (2005). Root Effects on Soil Organic Matter Decomposition. Roots and Soil Management: Interactions between Roots and the Soil. R. Zobel, Wright, S. Madison, WI., American Society of Agronomy, Crop Science Society of America, Soil Science Society of America**:** 119–143.

Cho, B. C. and F. Azam (1988). "Major Role of Bacteria in Biogeochemical Fluxes in the Oceans Interior." Nature **332**(6163): 441-443.

Chung, H. G., D. R. Zak and E. A. Lilleskov (2006). "Fungal community composition and metabolism under elevated CO2 and O-3." Oecologia **147**(1): 143-154.

Chung, H. G., D. R. Zak, P. B. Reich and D. S. Ellsworth (2007). "Plant species richness, elevated CO2, and atmospheric nitrogen deposition alter soil microbial community composition and function." Global Change Biology **13**(5): 980-989.

Clarke, K. R. and M. Ainsworth (1993). "A Method of Linking Multivariate Community Structure to Environmental Variables." Marine Ecology Progress Series **92**(3): 205-219.

Collins, B., J. V. McArthur and R. R. Sharitz (2004). "Plant effects on microbial assemblages and remediation of acidic coal pile runoff in mesocosm treatment wetlands." Ecological Engineering **23**(2): 107-115.

Colwell, R. K. and J. A. Coddington (1994). "Estimating Terrestrial Biodiversity through Extrapolation." Philosophical Transactions of the Royal Society of London Series B-Biological Sciences **345**(1311): 101-118.

Cotrufo, M. F., M. J. I. Briones and P. Ineson (1998). "Elevated CO2 affects field decomposition rate and palatability of tree leaf litter: Importance of changes in substrate quality." Soil Biology & Biochemistry **30**(12): 1565-1571.

Cotrufo, M. F. and A. Gorissen (1997). "Elevated CO2 enhances below-ground C allocation in three perennial grass species at different levels of N availability." New Phytologist **137**(3): 421-431.

Craine, J. M., C. Morrow and N. Fierer (2007). "Microbial nitrogen limitation increases decomposition." Ecology **88**(8): 2105-2113.

Craine, J. M., P. B. Reich, G. D. Tilman, D. Ellsworth, J. Fargione, J. Knops and S. Naeem (2003). "The role of plant species in biomass production and response to elevated CO2 and N." Ecology Letters **6**(7): 623-630.

Craine, J. M., D. A. Wedin, F. S. Chapin and P. B. Reich (2003). "Relationship between the structure of root systems and resource use for 11 North American grassland plants." Plant Ecology **165**(1): 85-100.

Deng, Y., Z. He, M. Xu, Y. Qin, J. D. Van Nostrand, L. Wu, B. A. Roe, G. Wiley, S. E. Hobbie, P. B. Reich and J. Zhou (2012). "Elevated carbon dioxide alters the structure of soil microbial communities." Appl Environ Microbiol **78**(8): 2991-2995.

Di, H. J., K. C. Cameron, J. P. Shen, C. S. Winefield, M. O'Callaghan, S. Bowatte and J. Z. He (2009). "Nitrification driven by bacteria and not archaea in nitrogen-rich grassland soils." Nature Geoscience **2**(9): 621-624.

Di, H. J., K. C. Cameron, J. P. Shen, C. S. Winefield, M. O'Callaghan, S. Bowatte and J. Z. He (2010). "Ammonia-oxidizing bacteria and archaea grow under contrasting soil nitrogen conditions." Fems Microbiology Ecology **72**(3): 386-394.

Diaz, S., J. P. Grime, J. Harris and E. Mcpherson (1993). "Evidence of a Feedback Mechanism Limiting Plant-Response to Elevated Carbon-Dioxide." Nature **364**(6438): 616-617.

Dijkstra, F. A., N. E. Bader, D. W. Johnson and W. X. Cheng (2009). "Does accelerated soil organic matter decomposition in the presence of plants increase plant N availability?" Soil Biology & Biochemistry **41**(6): 1080-1087.

Dixon, P. (2003). "VEGAN, a package of R functions for community ecology." Journal of Vegetation Science **14**(6): 927-930.

Drigo, B., G. A. Kowalchuk and J. A. van Veen (2008). "Climate change goes underground: effects of elevated atmospheric CO(2) on microbial community structure and activities in the rhizosphere." Biology and Fertility of Soils **44**(5): 667-679.

Drigo, B., J. A. Van Veen and G. A. Kowalchuk (2009). "Specific rhizosphere bacterial and fungal groups respond differently to elevated atmospheric CO2." Isme Journal **3**(10): 1204-1217.

Drissner, D., H. Blum, D. Tscherko and E. Kandeler (2007). "Nine years of enriched CO2 changes the function and structural diversity of soil microorganisms in a grassland." European Journal of Soil Science **58**(1): 260-269.

Dudley, S. A. (1996). "Differing selection on plant physiological traits in response to environmental water availability: A test of adaptive hypotheses." Evolution **50**(1): 92-102.

Dunbar, J., S. A. Eichorst, L. Gallegos-Graves, S. Silva, G. Xie, N. W. Hengartner, R. D. Evans, B. A. Hungate, R. B. Jackson, J. P. Megonigal, C. W. Schadt, R. Vilgalys, D. R. Zak and C. R. Kuske (2012). "Common bacterial responses in six ecosystems exposed to 10 years of elevated atmospheric carbon dioxide." Environmental Microbiology **14**(5): 1145-1158.

Dunbar, J., S. A. Eichorst, L. V. Gallegos-Graves, S. Silva, G. Xie, N. W. Hengartner, R. D. Evans, B. A. Hungate, R. B. Jackson, J. P. Megonigal, C. W. Schadt, R. Vilgalys, D. R. Zak and C. R. Kuske (2012). "Common bacterial responses in six ecosystems exposed to 10 years of elevated atmospheric carbon dioxide." Environmental Microbiology **14**(5): 1145-1158.

Ebersberger, D., N. Werrnbter, P. A. Niklaus and E. Kandeler (2004). "Effects of long term CO2 enrichment on microbial community structure in calcareous grassland." Plant and Soil **264**(1-2): 313-323.

Edgar, R. C. (2004). "MUSCLE: multiple sequence alignment with high accuracy and high throughput." Nucleic Acids Research **32**(5): 1792-1797.

Edgar, R. C. (2010). "Search and clustering orders of magnitude faster than BLAST." Bioinformatics **26**(19): 2460-2461.

Edgar, R. C. (2013). "UPARSE: highly accurate OTU sequences from microbial amplicon reads." Nature methods.

Edgar, R. C., B. J. Haas, J. C. Clemente, C. Quince and R. Knight (2011). "UCHIME improves sensitivity and speed of chimera detection." Bioinformatics **27**(16): 2194-2200.

Eichorst, S. A., C. R. Kuske and T. M. Schmidt (2011). "Influence of Plant Polymers on the Distribution and Cultivation of Bacteria in the Phylum Acidobacteria." Applied and Environmental Microbiology **77**(2): 586-596.

Eisenhauer, N., S. Cesarz, R. Koller, K. Worm and P. B. Reich (2012). "Global change belowground: impacts of elevated CO2, nitrogen, and summer drought on soil food webs and biodiversity." Global Change Biology **18**(2): 435-447.

Erguder, T. H., N. Boon, L. Wittebolle, M. Marzorati and W. Verstraete (2009). "Environmental factors shaping the ecological niches of ammonia-oxidizing archaea." Fems Microbiology Reviews **33**(5): 855-869.

Falkowski, P. G., T. Fenchel and E. F. Delong (2008). "The microbial engines that drive Earth's biogeochemical cycles." Science **320**(5879): 1034-1039.

Feng, Y. Z., X. G. Lin, Y. M. Wang, J. Zhang, T. T. Mao, R. Yin and J. G. Zhu (2009). "Free-air CO2 enrichment (FACE) enhances the biodiversity of purple phototrophic bacteria in flooded paddy soil." Plant and Soil **324**(1-2): 317-328.

Field, C. B., R. B. Jackson and H. A. Mooney (1995). "Stomatal Responses to Increased Co2 - Implications from the Plant to the Global-Scale." Plant Cell and Environment **18**(10): 1214-1225.

Fierer, N. and J. P. Schimel (2003). "A proposed mechanism for the pulse in carbon dioxide production commonly observed following the rapid rewetting of a dry soil." Soil Science Society of America Journal **67**(3): 798-805.

Fierer, N., J. P. Schimel and P. A. Holden (2003). "Variations in microbial community composition through two soil depth profiles." Soil Biology & Biochemistry **35**(1): 167-176.

Fierer, N., M. S. Strickland, D. Liptzin, M. A. Bradford and C. C. Cleveland (2009). "Global patterns in belowground communities." Ecology Letters **12**(11): 1238-1249.

Finzi, A. C., D. J. Moore, E. H. DeLucia, J. Lichter, K. S. Hofmockel, R. B. Jackson, H. S. Kim, R. Matamala, H. R. McCarthy, R. Oren, J. S. Pippen and W. H. Schlesinger (2006). "Progressive nitrogen limitation of ecosystem processes under elevated CO2 in a warm-temperate forest." Ecology **87**(1): 15-25.

Finzi, A. C., R. J. Norby, C. Calfapietra, A. Gallet-Budynek, B. Gielen, W. E. Holmes, M. R. Hoosbeek, C. M. Iversen, R. B. Jackson, M. E. Kubiske, J. Ledford, M. Liberloo, R. Oren, A. Polle, S. Pritchard, D. R. Zak, W. H. Schlesinger and R. Ceulemans (2007). "Increases in nitrogen uptake rather than nitrogen-use efficiency support higher rates of temperate forest productivity under elevated CO2." Proceedings of the National Academy of Sciences of the United States of America **104**(35): 14014-14019.

Francis, C. A., J. M. Beman and M. M. M. Kuypers (2007). "New processes and players in the nitrogen cycle: the microbial ecology of anaerobic and archaeal ammonia oxidation." Isme Journal **1**(1): 19-27.

Francis, C. A., K. J. Roberts, J. M. Beman, A. E. Santoro and B. B. Oakley (2005). "Ubiquity and diversity of ammonia-oxidizing archaea in water columns and sediments of the ocean." Proc Natl Acad Sci U S A **102**(41): 14683-14688.

Francis, C. A., K. J. Roberts, J. M. Beman, A. E. Santoro and B. B. Oakley (2005). "Ubiquity and diversity of ammonia-oxidizing archaea in water columns and sediments of the ocean." Proceedings of the National Academy of Sciences of the United States of America **102**(41): 14683-14688.

Franzosa, E. A., T. Hsu, A. Sirota-Madi, A. Shafquat, G. Abu-Ali, X. C. Morgan and C. Huttenhower (2015). "Sequencing and beyond: integrating molecular 'omics' for microbial community profiling." Nature Reviews Microbiology **13**(6): 360-372.

Garland, J. L. (1996). "Analytical approaches to the characterization of samples of microbial communities using patterns of potential C source utilization." Soil Biology & Biochemistry **28**(2): 213-221.

Garland, J. L. (1997). "Analysis and interpretation of community-level physiological profiles in microbial ecology." Fems Microbiology Ecology **24**(4): 289-300.

Garland, J. L. and A. L. Mills (1991). "Classification and Characterization of Heterotrophic Microbial Communities on the Basis of Patterns of Community-Level Sole-Carbon-Source Utilization." Applied and Environmental Microbiology **57**(8): 2351-2359.

Gleeson, S. K. and D. Tilman (1992). "Plant Allocation and the Multiple Limitation Hypothesis." American Naturalist **139**(6): 1322-1343.

Grayston, S. J., S. Q. Wang, C. D. Campbell and A. C. Edwards (1998). "Selective influence of plant species on microbial diversity in the rhizosphere." Soil Biology & Biochemistry **30**(3): 369-378.

Gryta, A., M. Frac and K. Oszust (2014). "The Application of the Biolog EcoPlate Approach in Ecotoxicological Evaluation of Dairy Sewage Sludge." Applied Biochemistry and Biotechnology **174**(4): 1434-1443.

Gubry-Rangin, C., G. W. Nicol and J. I. Prosser (2010). "Archaea rather than bacteria control nitrification in two agricultural acidic soils." Fems Microbiology Ecology **74**(3): 566-574.

Guckert, J. B., G. J. Carr, T. D. Johnson, B. G. Hamm, D. H. Davidson and Y. Kumagai (1996). "Community analysis by Biolog: Curve integration for statistical analysis of activated sludge microbial habitats." Journal of Microbiological Methods **27**(2-3): 183-197.

Hallam, S. J., T. J. Mincer, C. Schleper, C. M. Preston, K. Roberts, P. M. Richardson and E. F. DeLong (2006). "Pathways of carbon assimilation and ammonia oxidation suggested by environmental genomic analyses of marine Crenarchaeota." Plos Biology **4**(4): e95.

Hatzenpichler, R. (2012). "Diversity, Physiology, and Niche Differentiation of Ammonia-Oxidizing Archaea." Applied and Environmental Microbiology **78**(21): 7501-7510.

He, Z., Y. Piceno, Y. Deng, M. Xu, Z. Lu, T. DeSantis, G. Andersen, S. E. Hobbie, P. B. Reich and J. Zhou (2012). "The phylogenetic composition and structure of soil microbial communities shifts in response to elevated carbon dioxide." ISME J **6**(2): 259-272.

He, Z., J. Xiong, A. D. Kent, Y. Deng, K. Xue, G. Wang, L. Wu, J. D. Van Nostrand and J. Zhou (2014). "Distinct responses of soil microbial communities to elevated CO2 and O3 in a soybean agro-ecosystem." ISME J **8**(3): 714-726.

He, Z., M. Xu, Y. Deng, S. Kang, L. Kellogg, L. Wu, J. D. Van Nostrand, S. E. Hobbie, P. B. Reich and J. Zhou (2010). "Metagenomic analysis reveals a marked divergence in the structure of belowground microbial communities at elevated CO2." Ecol Lett **13**(5): 564-575.

He, Z. L., Y. Deng, J. D. Van Nostrand, Q. C. Tu, M. Y. Xu, C. L. Hemme, X. Y. Li, L. Y. Wu, T. J. Gentry, Y. F. Yin, J. Liebich, T. C. Hazen and J. Z. Zhou (2010). "GeoChip 3.0 as a high-throughput tool for analyzing microbial community composition, structure and functional activity." Isme Journal **4**(9): 1167-1179.

He, Z. L., Y. Piceno, Y. Deng, M. Y. Xu, Z. M. Lu, T. DeSantis, G. Andersen, S. E. Hobbie, P. B. Reich and J. Z. Zhou (2012). "The phylogenetic composition and structure of soil microbial communities shifts in response to elevated carbon dioxide." Isme Journal **6**(2): 259-272.

He, Z. L., M. Y. Xu, Y. Deng, S. H. Kang, L. Kellogg, L. Y. Wu, J. D. Van Nostrand, S. E. Hobbie, P. B. Reich and J. Z. Zhou (2010). "Metagenomic analysis reveals a marked divergence in the structure of belowground microbial communities at elevated CO2." Ecology Letters **13**(5): 564-575.

He, Z. L. and J. Z. Zhou (2008). "Empirical evaluation of a new method for calculating signal-to-noise ratio for microarray data analysis." Applied and Environmental Microbiology **74**(10): 2957-2966.

Heath, J., E. Ayres, M. Possell, R. D. Bardgett, H. I. J. Black, H. Grant, P. Ineson and G. Kerstiens (2005). "Rising atmospheric CO2 reduces sequestration of root-derived soil carbon." Science **309**(5741): 1711-1713.

Hebeisen, T., A. Luscher, S. Zanetti, B. U. Fischer, U. A. Hartwig, M. Frehner, G. R. Hendrey, H. Blum and J. Nosberger (1997). "Growth response of Trifolium

repens L and Lolium perenne L as monocultures and bi-species mixture to free air CO2 enrichment and management." Global Change Biology **3**(2): 149-160.
Hector, A. and R. Bagchi (2007). "Biodiversity and ecosystem multifunctionality." Nature **448**(7150): 188-190.
Hector, A. and R. Hooper (2002). "Darwin and the First Ecological Experiment." Science **295**(5555): 639-640.
Hedges, L. V., J. Gurevitch and P. S. Curtis (1999). "The meta-analysis of response ratios in experimental ecology." Ecology **80**(4): 1150-1156.
Ho, A., D. P. Di Lonardo and P. L. E. Bodelier (2017). "Revisiting life strategy concepts in environmental microbial ecology." Fems Microbiology Ecology **93**(3).
Hoosbeek, M. R., M. Lukac, D. van Dam, D. L. Godbold, E. J. Velthorst, F. A. Biondi, A. Peressotti, M. F. Cotrufo, P. de Angelis and G. Scarascia-Mugnozza (2004). "More new carbon in the mineral soil of a poplar plantation under Free Air Carbon Enrichment (POPFACE): Cause of increased priming effect?" Global Biogeochemical Cycles **18**(1).
Hu, S., F. S. Chapin, M. K. Firestone, C. B. Field and N. R. Chiariello (2001). "Nitrogen limitation of microbial decomposition in a grassland under elevated CO2." Nature **409**(6817): 188-191.
Hu, S. J., M. K. Firestone and F. S. Chapin (1999). "Soil microbial feedbacks to atmospheric CO2 enrichment." Trends in Ecology & Evolution **14**(11): 433-437.
Hungate, B. A., J. S. Dukes, M. R. Shaw, Y. Q. Luo and C. B. Field (2003). "Nitrogen and climate change." Science **302**(5650): 1512-1513.
Hungate, B. A., E. A. Holland, R. B. Jackson, F. S. Chapin, H. A. Mooney and C. B. Field (1997). "The fate of carbon in grasslands under carbon dioxide enrichment." Nature **388**(6642): 576-579.
Inauen, N., C. Korner and E. Hiltbrunner (2012). "No growth stimulation by CO2 enrichment in alpine glacier forefield plants." Global Change Biology **18**(3): 985-999.
Ingalls, A. E., S. R. Shah, R. L. Hansman, L. I. Aluwihare, G. M. Santos, E. R. M. Druffel and A. Pearson (2006). "Quantifying archaeal community autotrophy in the mesopelagic ocean using natural radiocarbon." Proceedings of the National Academy of Sciences of the United States of America **103**(17): 6442-6447.
Inouye, R. S. and D. Tilman (1988). "Convergence and Divergence of Old-Field Plant-Communities Along Experimental Nitrogen Gradients." Ecology **69**(4): 995-1004.
IPCC (2007). Climate Change 2007: The Physical Science Basis. Contribution of Working Group I to the Fourth Assessment Report of the Intergovernmental Panel on Climate Change. Cambridge, United Kingdom and New York, NY, USA, Cambridge University Press.
Janssen, P. H. (2006). "Identifying the dominant soil bacterial taxa in libraries of 16S rRNA and 16S rRNA genes." Applied and Environmental Microbiology **72**(3): 1719-1728.
Janus, L., N. Angeloni, J. McCormack, S. Rier, N. Tuchman and J. Kelly (2005). "Elevated Atmospheric CO2 Alters Soil Microbial Communities Associated

with Trembling Aspen (Populus tremuloides) Roots." Microbial Ecology **50**(1): 102-109.
Janus, L. R., N. L. Angeloni, J. McCormack, S. T. Rier, N. C. Tuchman and J. J. Kelly (2005). "Elevated atmospheric CO2 alters soil microbial communities associated with trembling aspen (Populus tremuloides) roots." Microbial Ecology **50**(1): 102-109.
Jastrow, J. D., R. M. Miller, R. Matamala, R. J. Norby, T. W. Boutton, C. W. Rice and C. E. Owensby (2005). "Elevated atmospheric carbon dioxide increases soil carbon." Global Change Biology **11**(12): 2057-2064.
Jia, Z. J. and R. Conrad (2009). "Bacteria rather than Archaea dominate microbial ammonia oxidation in an agricultural soil." Environmental Microbiology **11**(7): 1658-1671.
Jiang, H. C., L. Q. Huang, Y. Deng, S. Wang, Y. Zhou, L. Liu and H. L. Dong (2014). "Latitudinal Distribution of Ammonia-Oxidizing Bacteria and Archaea in the Agricultural Soils of Eastern China." Applied and Environmental Microbiology **80**(18): 5593-5602.
Jin, V. L. and R. D. Evans (2007). "Elevated CO2 increases microbial carbon substrate use and nitrogen cycling in Mojave Desert soils." Global Change Biology **13**(2): 452-465.
Johnson, D. W. (2006). "Progressive N limitation in forests: Review and implications for long-term responses to elevated CO2." Ecology **87**(1): 64-75.
Jones, T. H., L. J. Thompson, J. H. Lawton, T. M. Bezemer, R. D. Bardgett, T. M. Blackburn, K. D. Bruce, P. F. Cannon, G. S. Hall, S. E. Hartley, G. Howson, C. G. Jones, C. Kampichler, E. Kandeler and D. A. Ritchie (1998). "Impacts of rising atmospheric carbon dioxide on model terrestrial ecosystems." Science **280**(5362): 441-443.
Jorgensen, B. B. and A. Boetius (2007). "Feast and famine - microbial life in the deep-sea bed." Nature Reviews Microbiology **5**(10): 770-781.
Jossi, M., N. Fromin, S. Tarnawski, F. Kohler, F. Gillet, M. Aragno and J. Hamelin (2006). "How elevated pCO(2) modifies total and metabolically active bacterial communities in the rhizosphere of two perennial grasses grown under field conditions." Fems Microbiology Ecology **55**(3): 339-350.
Joyce, C. B., M. Simpson and M. Casanova (2016). "Future wet grasslands: ecological implications of climate change." Ecosystem Health and Sustainability **2**(9): e01240-n/a.
Kandeler, E., D. Tscherko, R. D. Bardgett, P. J. Hobbs, C. Kampichler and T. H. Jones (1998). "The response of soil microorganisms and roots to elevated CO2 and temperature in a terrestrial model ecosystem." Plant and Soil **202**(2): 251-262.
Kenarova, A., M. Encheva, V. Chipeva, N. Chipev, P. Hristova and P. Moncheva (2013). "Physiological diversity of bacterial communities from different soil locations on Livingston Island, South Shetland archipelago, Antarctica." Polar Biology **36**(2): 223-233.
Klinger, C. R., J. A. Lau and K. D. Heath (2016). "Ecological genomics of mutualism decline in nitrogen-fixing bacteria." Proceedings of the Royal Society B-Biological Sciences **283**(1826).
Koch, A. L. (2001). "Oligotrophs versus copiotrophs." Bioessays **23**(7): 657-661.

Kong, Y. (2011). "Btrim: A fast, lightweight adapter and quality trimming program for next-generation sequencing technologies." Genomics **98**(2): 152-153.
Konstantinidis, K. T. and J. M. Tiedje (2005). "Genomic insights that advance the species definition for prokaryotes." Proceedings of the National Academy of Sciences of the United States of America **102**(7): 2567-2572.
Korner, C. and J. A. Arnone (1992). "Responses to Elevated Carbon-Dioxide in Artificial Tropical Ecosystems." Science **257**(5077): 1672-1675.
Korner, C., R. Asshoff, O. Bignucolo, S. Hattenschwiler, S. G. Keel, S. Pelaez-Riedl, S. Pepin, R. T. W. Siegwolf and G. Zotz (2005). "Carbon flux and growth in mature deciduous forest trees exposed to elevated CO2." Science **309**(5739): 1360-1362.
Kowalchuk, G. A. and J. R. Stephen (2001). "Ammonia-oxidizing bacteria: A model for molecular microbial ecology." Annual Review of Microbiology **55**: 485-529.
Kuzyakov, Y. and G. Domanski (2000). "Carbon input by plants into the soil. Review." Journal of Plant Nutrition and Soil Science-Zeitschrift Fur Pflanzenernahrung Und Bodenkunde **163**(4): 421-431.
Kuzyakov, Y., J. K. Friedel and K. Stahr (2000). "Review of mechanisms and quantification of priming effects." Soil Biology & Biochemistry **32**(11-12): 1485-1498.
Lal, R. (2004). "Soil carbon sequestration impacts on global climate change and food security." Science **304**(5677): 1623-1627.
Langille, M. G. I., J. Zaneveld, J. G. Caporaso, D. McDonald, D. Knights, J. A. Reyes, J. C. Clemente, D. E. Burkepile, R. L. V. Thurber, R. Knight, R. G. Beiko and C. Huttenhower (2013). "Predictive functional profiling of microbial communities using 16S rRNA marker gene sequences." Nature Biotechnology **31**(9): 814-+.
Lanzen, A., S. L. Jorgensen, D. H. Huson, M. Gorfer, S. H. Grindhaug, I. Jonassen, L. Ovreas and T. Urich (2012). "CREST - Classification Resources for Environmental Sequence Tags." Plos One **7**(11).
Lauro, F. M., D. McDougald, T. Thomas, T. J. Williams, S. Egan, S. Rice, M. Z. DeMaere, L. Ting, H. Ertan, J. Johnson, S. Ferriera, A. Lapidus, I. Anderson, N. Kyrpides, A. C. Munk, C. Detter, C. S. Han, M. V. Brown, F. T. Robb, S. Kjelleberg and R. Cavicchioli (2009). "The genomic basis of trophic strategy in marine bacteria." Proceedings of the National Academy of Sciences of the United States of America **106**(37): 15527-15533.
Lee, T. D., P. B. Reich and M. G. Tjoelker (2003). "Legume presence increases photosynthesis and N concentrations of co-occurring non-fixers but does not modulate their responsiveness to carbon dioxide enrichment." Oecologia **137**(1): 22-31.
Lee, T. D., M. G. Tjoelker, D. S. Ellsworth and P. B. Reich (2001). "Leaf gas exchange responses of 13 prairie grassland species to elevated CO2 and increased nitrogen supply." New Phytologist **150**(2): 405-418.
Lee, T. D., M. G. Tjoelker, P. B. Reich and M. P. Russelle (2003). "Contrasting growth response of an N-2-fixing and non-fixing forb to elevated CO2: dependence on soil N supply." Plant and Soil **255**(2): 475-486.

Leff, J. W., S. E. Jones, S. M. Prober, A. Barberan, E. T. Borer, J. L. Firn, W. S. Harpole, S. E. Hobbie, K. S. Hofmockel, J. M. H. Knops, R. L. McCulley, K. La Pierre, A. C. Risch, E. W. Seabloom, M. Schutz, C. Steenbock, C. J. Stevens and N. Fierer (2015). "Consistent responses of soil microbial communities to elevated nutrient inputs in grasslands across the globe." Proceedings of the National Academy of Sciences of the United States of America **112**(35): 10967-10972.

Lehtovirta-Morley, L. E., J. Ross, L. Hink, E. B. Weber, C. Gubry-Rangin, C. Thion, J. I. Prosser and G. W. Nicol (2016). "Isolation of 'Candidatus Nitrosocosmicus franklandus', a novel ureolytic soil archaeal ammonia oxidiser with tolerance to high ammonia concentration." Fems Microbiology Ecology **92**(5).

Lehtovirta-Morley, L. E., K. Stoecker, A. Vilcinskas, J. I. Prosser and G. W. Nicol (2011). "Cultivation of an obligate acidophilic ammonia oxidizer from a nitrifying acid soil." Proceedings of the National Academy of Sciences of the United States of America **108**(38): 15892-15897.

Leininger, S., T. Urich, M. Schloter, L. Schwark, J. Qi, G. W. Nicol, J. I. Prosser, S. C. Schuster and C. Schleper (2006). "Archaea predominate among ammonia-oxidizing prokaryotes in soils." Nature **442**(7104): 806-809.

Lesaulnier, C., D. Papamichail, S. McCorkle, B. Ollivier, S. Skiena, S. Taghavi, D. Zak and D. van der Lelie (2008). "Elevated atmospheric CO2 affects soil microbial diversity associated with trembling aspen." Environmental Microbiology **10**(4): 926-941.

Liang, Y. T., Z. L. He, L. Y. Wu, Y. Deng, G. H. Li and J. Z. Zhou (2010). "Development of a Common Oligonucleotide Reference Standard for Microarray Data Normalization and Comparison across Different Microbial Communities." Applied and Environmental Microbiology **76**(4): 1088-1094.

Lichter, J., S. A. Billings, S. E. Ziegler, D. Gaindh, R. Ryals, A. C. Finzi, R. B. Jackson, E. A. Stemmler and W. H. Schlesinger (2008). "Soil carbon sequestration in a pine forest after 9 years of atmospheric CO(2) enrichment." Global Change Biology **14**(12): 2910-2922.

Lima-Bittencourt, C. I., P. S. Costa, M. P. Reis, A. B. Santos, F. A. R. Barbosa, J. L. Valentin, F. L. Thompson, E. Chartone-Souza and A. M. A. Nascimento (2014). "A survey on cultivable heterotrophic bacteria inhabiting a thermally unstratified water column in an Atlantic Rainforest lake." Peerj **2**.

Lipson, D., M. Blair, G. Barron-Gafford, K. Grieve and R. Murthy (2006). "Relationships Between Microbial Community Structure and Soil Processes Under Elevated Atmospheric Carbon Dioxide." Microbial Ecology **51**(3): 302-314.

Lipson, D. A., R. F. Wilson and W. C. Oechel (2005). "Effects of elevated atmospheric CO2 on soil microbial biomass, activity, and diversity in a chaparral ecosystem." Applied and Environmental Microbiology **71**(12): 8573-8580.

Llado, S., L. Zifcakova, T. Vetrovsky, I. Eichlerova and P. Baldrian (2016). "Functional screening of abundant bacteria from acidic forest soil indicates the metabolic potential of Acidobacteria subdivision 1 for polysaccharide decomposition." Biology and Fertility of Soils **52**(2): 251-260.

Long, S. P., E. A. Ainsworth, A. Rogers and D. R. Ort (2004). "Rising atmospheric carbon dioxide: Plants face the future." Annual Review of Plant Biology **55**: 591-628.

Long, X., C. R. Chen, Z. H. Xu, R. Oren and J. Z. He (2012). "Abundance and community structure of ammonia-oxidizing bacteria and archaea in a temperate forest ecosystem under ten-years elevated CO2." Soil Biology & Biochemistry **46**: 163-171.

Lukac, M., C. Calfapietra and D. L. Godbold (2003). "Production, turnover and mycorrhizal colonization of root systems of three Populus species grown under elevated CO2 (POPFACE)." Global Change Biology **9**(6): 838-848.

Lukac, M., A. Lagomarsino, M. C. Moscatelli, P. De Angelis, M. F. Cotrufo and D. L. Godbold (2009). "Forest soil carbon cycle under elevated CO2 - a case of increased throughput?" Forestry **82**(1): 75-86.

Luo, Y., B. Su, W. S. Currie, J. S. Dukes, A. C. Finzi, U. Hartwig, B. Hungate, R. E. McMurtrie, R. Oren, W. J. Parton, D. E. Pataki, M. R. Shaw, D. R. Zak and C. B. Field (2004). "Progressive nitrogen limitation of ecosystem responses to rising atmospheric carbon dioxide." Bioscience **54**(8): 731-739.

Luo, Y., B. O. Su, W. S. Currie, J. S. Dukes, A. Finzi, U. Hartwig, B. Hungate, R. E. M. Murtrie, R. A. M. Oren, W. J. Parton, D. E. Pataki, M. R. Shaw, D. R. Zak and C. B. Field (2004). "Progressive Nitrogen Limitation of Ecosystem Responses to Rising Atmospheric Carbon Dioxide." BioScience **54**(8): 731-739.

Luo, Y. Q., D. F. Hui and D. Q. Zhang (2006). "Elevated CO2 stimulates net accumulations of carbon and nitrogen in land ecosystems: A meta-analysis." Ecology **87**(1): 53-63.

Lyons, M. M., J. E. Ward, H. Gaff, R. E. Hicks, J. M. Drake and F. C. Dobbs (2010). "Theory of island biogeography on a microscopic scale: organic aggregates as islands for aquatic pathogens." Aquatic Microbial Ecology **60**(1): 1-13.

Magoc, T. and S. L. Salzberg (2011). "FLASH: fast length adjustment of short reads to improve genome assemblies." Bioinformatics **27**(21): 2957-2963.

Mastrogianni, A., E. M. Papatheodorou, N. Monokrousos, U. Menkissoglu-Spiroudi and G. P. Stamou (2014). "Reclamation of lignite mine areas with Triticum aestivum: The dynamics of soil functions and microbial communities." Applied Soil Ecology **80**: 51-59.

McCann, K. S. (2000). "The diversity-stability debate." Nature **405**(6783): 228-233.

McCarthy, H. R., R. Oren, K. H. Johnsen, A. Gallet-Budynek, S. G. Pritchard, C. W. Cook, S. L. LaDeau, R. B. Jackson and A. C. Finzi (2010). "Re-assessment of plant carbon dynamics at the Duke free-air CO2 enrichment site: interactions of atmospheric [CO2] with nitrogen and water availability over stand development." New Phytologist **185**(2): 514-528.

McGrath, K. C., R. Mondav, R. Sintrajaya, B. Slattery, S. Schmidt and P. M. Schenk (2010). "Development of an Environmental Functional Gene Microarray for Soil Microbial Communities." Applied and Environmental Microbiology **76**(21): 7161-7170.

Meier, C. L., K. N. Suding and W. D. Bowman (2008). "Carbon flux from plants to soil: roots are a below-ground source of phenolic secondary compounds in an alpine ecosystem." Journal of Ecology **96**(3): 421-430.

Mendes, L. W., E. E. Kuramae, A. A. Navarrete, J. A. van Veen and S. M. Tsai (2014). "Taxonomical and functional microbial community selection in soybean rhizosphere." Isme Journal **8**(8): 1577-1587.

Mussmann, M., I. Brito, A. Pitcher, J. S. S. Damste, R. Hatzenpichler, A. Richter, J. L. Nielsen, P. H. Nielsen, A. Muller, H. Daims, M. Wagner and I. M. Head (2011). "Thaumarchaeotes abundant in refinery nitrifying sludges express amoA but are not obligate autotrophic ammonia oxidizers." Proceedings of the National Academy of Sciences of the United States of America **108**(40): 16771-16776.

Norby, R. J., K. Kobayashi and B. K. Kimball (2001). "Rising CO2 - future ecosystems - Commentary." New Phytologist **150**(2): 215-221.

Norby, R. J., J. Ledford, C. D. Reilly, N. E. Miller and E. G. O'Neill (2004). "Fine-root production dominates response of a deciduous forest to atmospheric CO2 enrichment." Proceedings of the National Academy of Sciences of the United States of America **101**(26): 9689-9693.

Norby, R. J., J. M. Warren, C. M. Iversen, B. E. Medlyn and R. E. McMurtrie (2010). "CO2 enhancement of forest productivity constrained by limited nitrogen availability." Proceedings of the National Academy of Sciences of the United States of America **107**(45): 19368-19373.

Oren, R., D. S. Ellsworth, K. H. Johnsen, N. Phillips, B. E. Ewers, C. Maier, K. V. R. Schafer, H. McCarthy, G. Hendrey, S. G. McNulty and G. G. Katul (2001). "Soil fertility limits carbon sequestration by forest ecosystems in a CO2-enriched atmosphere." Nature **411**(6836): 469-472.

Palmroth, S., R. Oren, H. R. McCarthy, K. H. Johnsen, A. C. Finzi, J. R. Butnor, M. G. Ryan and W. H. Schlesinger (2006). "Aboveground sink strength in forests controls the allocation of carbon below ground and its [CO2] - induced enhancement." Proceedings of the National Academy of Sciences of the United States of America **103**(51): 19362-19367.

Parsons, W. F. J., J. G. Bockheim and R. L. Lindroth (2008). "Independent, interactive, and species-specific responses of leaf litter decomposition to elevated CO(2) and O(3) in a northern hardwood forest." Ecosystems **11**(4): 505-519.

Pei, Z. Q., D. Eichenberg, H. Bruelheide, W. Krober, P. Kuhn, Y. Li, G. von Oheimb, O. Purschke, T. Scholten, F. Buscot and J. L. M. Gutknecht (2016). "Soil and tree species traits both shape soil microbial communities during early growth of Chinese subtropical forests." Soil Biology & Biochemistry **96**: 180-190.

Peralta, A. L. and M. M. Wander (2008). "Soil organic matter dynamics under soybean exposed to elevated [CO2]." Plant and Soil **303**(1-2): 69-81.

Pester, M., T. Rattei, S. Flechl, A. Grongroft, A. Richter, J. Overmann, B. Reinhold-Hurek, A. Loy and M. Wagner (2012). "amoA-based consensus phylogeny of ammonia-oxidizing archaea and deep sequencing of amoA genes from soils of four different geographic regions." Environmental Microbiology **14**(2): 525-539.

Pester, M., C. Schleper and M. Wagner (2011). "The Thaumarchaeota: an emerging view of their phylogeny and ecophysiology." Current Opinion in Microbiology **14**(3): 300-306.

Phillips, R. P., E. S. Bernhardt and W. H. Schlesinger (2009). "Elevated CO2 increases root exudation from loblolly pine (Pinus taeda) seedlings as an N-mediated response." Tree Physiology **29**(12): 1513-1523.

Phillips, R. P., A. C. Finzi and E. S. Bernhardt (2011). "Enhanced root exudation induces microbial feedbacks to N cycling in a pine forest under long-term CO2 fumigation." Ecology Letters **14**(2): 187-194.

Pollierer, M. M., R. Langel, C. Korner, M. Maraun and S. Scheu (2007). "The underestimated importance of belowground carbon input for forest soil animal food webs." Ecology Letters **10**(8): 729-736.

Preston-Mafham, J., L. Boddy and P. F. Randerson (2002). "Analysis of microbial community functional diversity using sole-carbon-source utilisation profiles - a critique." Fems Microbiology Ecology **42**(1): 1-14.

Price, M. N., P. S. Dehal and A. P. Arkin (2009). "FastTree: computing large minimum evolution trees with profiles instead of a distance matrix." Molecular biology and evolution **26**(7): 1641-1650.

Pritchard, S. G., A. E. Strand, M. L. McCormack, M. A. Davis, A. C. Finzi, R. B. Jackson, R. Matamala, H. H. Rogers and R. Oren (2008). "Fine root dynamics in a loblolly pine forest are influenced by free-air-CO2-enrichment: a six-year-minirhizotron study." Global Change Biology **14**(3): 588-602.

Quast, C., E. Pruesse, P. Yilmaz, J. Gerken, T. Schweer, P. Yarza, J. Peplies and F. O. Glockner (2013). "The SILVA ribosomal RNA gene database project: improved data processing and web-based tools." Nucleic Acids Research **41**(D1): D590-D596.

Radax, R., F. Hoffmann, H. T. Rapp, S. Leininger and C. Schleper (2012). "Ammonia-oxidizing archaea as main drivers of nitrification in cold-water sponges." Environmental Microbiology **14**(4): 909-923.

Ramette, A. and J. M. Tiedje (2007). "Multiscale responses of microbial life to spatial distance and environmental heterogeneity in a patchy ecosystem." Proceedings of the National Academy of Sciences of the United States of America **104**(8): 2761-2766.

Ramirez, K. S., J. M. Craine and N. Fierer (2010). "Nitrogen fertilization inhibits soil microbial respiration regardless of the form of nitrogen applied." Soil Biology & Biochemistry **42**(12): 2336-2338.

Ramirez, K. S., J. M. Craine and N. Fierer (2012). "Consistent effects of nitrogen amendments on soil microbial communities and processes across biomes." Global Change Biology **18**(6): 1918-1927.

Reed, S. C., C. C. Cleveland and A. R. Townsend (2011). "Functional Ecology of Free-Living Nitrogen Fixation: A Contemporary Perspective." Annual Review of Ecology, Evolution, and Systematics, Vol 42 **42**: 489-512.

Reich, P. B. and S. E. Hobbie (2013). "Decade-long soil nitrogen constraint on the CO2 fertilization of plant biomass." Nature Climate Change **3**(3): 278-282.

Reich, P. B., S. E. Hobbie, T. Lee, D. S. Ellsworth, J. B. West, D. Tilman, J. M. H. Knops, S. Naeem and J. Trost (2006). "Nitrogen limitation constrains sustainability of ecosystem response to CO2." Nature **440**(7086): 922-925.

Reich, P. B., B. A. Hungate and Y. Q. Luo (2006). "Carbon-nitrogen interactions in terrestrial ecosystems in response to rising atmospheric carbon dioxide." Annual Review of Ecology Evolution and Systematics **37**: 611-636.

Reich, P. B., J. Knops, D. Tilman, J. Craine, D. Ellsworth, M. Tjoelker, T. Lee, D. Wedin, S. Naeem and D. Bahauddin (2001). "Plant diversity enhances

ecosystem responses to elevated CO2 and nitrogen deposition." Nature **410**(6830): 809-810.
Reich, P. B., J. Knops, D. Tilman, J. Craine, D. Ellsworth, M. Tjoelker, T. Lee, D. Wedin, S. Naeem, D. Bahauddin, G. Hendrey, S. Jose, K. Wrage, J. Goth and W. Bengston (2001). "Plant diversity enhances ecosystem responses to elevated CO2 and nitrogen deposition." Nature **410**(6839): 809-812.
Reich, P. B., D. Tilman, J. Craine, D. Ellsworth, M. G. Tjoelker, J. Knops, D. Wedin, S. Naeem, D. Bahauddin, J. Goth, W. Bengtson and T. D. Lee (2001). "Do species and functional groups differ in acquisition and use of C, N and water under varying atmospheric CO2 and N availability regimes? A field test with 16 grassland species." New Phytologist **150**(2): 435-448.
Reich, P. B., D. Tilman, S. Naeem, D. S. Ellsworth, J. Knops, J. Craine, D. Wedin and J. Trost (2004). "Species and functional group diversity independently influence biomass accumulation and its response to CO2 and N." Proceedings of the National Academy of Sciences of the United States of America **101**(27): 10101-10106.
Ridl, J., M. Kolar, M. Strejcek, H. Strnad, P. Stursa, J. Paces, T. Macek and O. Uhlik (2016). "Plants Rather than Mineral Fertilization Shape Microbial Community Structure and Functional Potential in Legacy Contaminated Soil." Frontiers in Microbiology **7**.
Rogers, A., Y. Gibon, M. Stitt, P. B. Morgan, C. J. Bernacchi, D. R. Ort and S. P. Long (2006). "Increased C availability at elevated carbon dioxide concentration improves N assimilation in a legume." Plant Cell and Environment **29**(8): 1651-1658.
Roller, B. R. K. and T. M. Schmidt (2015). "The physiology and ecological implications of efficient growth." Isme Journal **9**(7): 1481-1487.
Roller, B. R. K., S. F. Stoddard and T. M. Schmidt (2016). "Exploiting rRNA operon copy number to investigate bacterial reproductive strategies." Nature Microbiology **1**(11).
Saarsalmi, A., M. Kukkola, M. Moilanen and M. Arola (2006). "Long-term effects of ash and N fertilization on stand growth, tree nutrient status and soil chemistry in a Scots pine stand." Forest Ecology and Management **235**(1-3): 116-128.
Sadowsky, M. J. and M. Schortemeyer (1997). "Soil microbial responses to increased concentrations of atmospheric CO2." Global Change Biology **3**(3): 217-224.
Schleper, C., G. Jurgens and M. Jonuscheit (2005). "Genomic studies of uncultivated archaea." Nature Reviews Microbiology **3**(6): 479-488.
Schlesinger, W. H. and J. Lichter (2001). "Limited carbon storage in soil and litter of experimental forest plots under increased atmospheric CO2." Nature **411**(6836): 466-469.
Schloss, P. D., S. L. Westcott, T. Ryabin, J. R. Hall, M. Hartmann, E. B. Hollister, R. A. Lesniewski, B. B. Oakley, D. H. Parks and C. J. Robinson (2009). "Introducing mothur: open-source, platform-independent, community-supported software for describing and comparing microbial communities." Applied and Environmental Microbiology **75**(23): 7537-7541.
Schneider, M. K., A. Luscher, M. Richter, U. Aeschlimann, U. A. Hartwig, H. Blum, E. Frossard and J. Nosberger (2004). "Ten years of free-air CO2 enrichment altered

the mobilization of N from soil in Lolium perenne L. swards." Global Change Biology **10**(8): 1377-1388.
Scurlock, J. M. O. and D. O. Hall (1998). "The global carbon sink: a grassland perspective." Global Change Biology **4**(2): 229-233.
Shaw, M. R., E. S. Zavaleta, N. R. Chiariello, E. E. Cleland, H. A. Mooney and C. B. Field (2002). "Grassland responses to global environmental changes suppressed by elevated CO2." Science **298**(5600): 1987-1990.
Shen, J. P., L. M. Zhang, H. J. Di and J. Z. He (2012). "A review of ammonia-oxidizing bacteria and archaea in Chinese soils." Frontiers in Microbiology **3**.
Shen, J. P., L. M. Zhang, Y. G. Zhu, J. B. Zhang and J. Z. He (2008). "Abundance and composition of ammonia-oxidizing bacteria and ammonia-oxidizing archaea communities of an alkaline sandy loam." Environmental Microbiology **10**(6): 1601-1611.
Simon, C. and R. Daniel (2011). "Metagenomic Analyses: Past and Future Trends." Applied and Environmental Microbiology **77**(4): 1153-1161.
Sinsabaugh, R. L., M. E. Gallo, C. Lauber, M. P. Waldrop and D. R. Zak (2005). "Extracellular enzyme activities and soil organic matter dynamics for northern hardwood forests receiving simulated nitrogen deposition." Biogeochemistry **75**(2): 201-215.
Smalla, K., U. Wachtendorf, H. Heuer, W. T. Liu and L. Forney (1998). "Analysis of BIOLOG GN substrate utilization patterns by microbial communities." Applied and Environmental Microbiology **64**(4): 1220-1225.
Souza, L., R. T. Belote, P. Kardol, J. F. Weltzin and R. J. Norby (2010). "CO2 enrichment accelerates successional development of an understory plant community." Journal of Plant Ecology **3**(1): 33-39.
Spang, A., R. Hatzenpichler, C. Brochier-Armanet, T. Rattei, P. Tischler, E. Spieck, W. Streit, D. A. Stahl, M. Wagner and C. Schleper (2010). "Distinct gene set in two different lineages of ammonia-oxidizing archaea supports the phylum Thaumarchaeota." Trends in Microbiology **18**(8): 331-340.
Stark, C., L. M. Condron, A. Stewart, H. J. Di and M. O'Callaghan (2007). "Influence of organic and mineral amendments on microbial soil properties and processes." Applied Soil Ecology **35**(1): 79-93.
Stephen, J. R., G. A. Kowalchuk, M. A. V. Bruns, A. E. McCaig, C. J. Phillips, T. M. Embley and J. I. Prosser (1998). "Analysis of beta-subgroup proteobacterial ammonia oxidizer populations in soil by denaturing gradient gel electrophoresis analysis and hierarchical phylogenetic probing." Applied and Environmental Microbiology **64**(8): 2958-2965.
Stocker, T. F., D. Qin, G.-K. Plattner, M. Tignor, S.K. Allen, J. Boschung, A. Nauels, Y. Xia, V. Bex and P.M. (2013). Climate Change 2013: The Physical Science Basis. Working Group I Contribution to the Fifth Assessment Report of the Intergovernmental Panel on Climate Change. Cambridge, United Kingdom and New York, NY, USA, Cambridge University Press.
Stopnisek, N., C. Gubry-Rangin, S. Hofferle, G. W. Nicol, I. Mandic-Mulec and J. I. Prosser (2010). "Thaumarchaeal Ammonia Oxidation in an Acidic Forest Peat Soil Is Not Influenced by Ammonium Amendment." Applied and Environmental Microbiology **76**(22): 7626-7634.

Szukics, U., G. C. J. Abell, V. Hodl, B. Mitter, A. Sessitsch, E. Hackl and S. Zechmeister-Boltenstern (2010). "Nitrifiers and denitrifiers respond rapidly to changed moisture and increasing temperature in a pristine forest soil." Fems Microbiology Ecology **72**(3): 395-406.

Talhelm, A. F., K. S. Pregitzer and D. R. Zak (2009). "Species-specific responses to atmospheric carbon dioxide and tropospheric ozone mediate changes in soil carbon." Ecology Letters **12**(11): 1219-1228.

Tilman, D., P. B. Reich and J. M. Knops (2006). "Biodiversity and ecosystem stability in a decade-long grassland experiment." Nature **441**(7093): 629-632.

Treusch, A. H., A. Kletzin, G. Raddatz, T. Ochsenreiter, A. Quaiser, G. Meurer, S. C. Schuster and C. Schleper (2004). "Characterization of large-insert DNA libraries from soil for environmental genomic studies of Archaea." Environmental Microbiology **6**(9): 970-980.

Tu, Q. C., M. T. Yuan, Z. L. He, Y. Deng, K. Xue, L. Y. Wu, S. E. Hobbie, P. B. Reich and J. Z. Zhou (2015). "Fungal Communities Respond to Long-Term CO2 Elevation by Community Reassembly." Applied and Environmental Microbiology **81**(7): 2445-2454.

van Ginkel, J. H., A. Gorissen and D. Polci (2000). "Elevated atmospheric carbon dioxide concentration: effects of increased carbon input in a Lolium perenne soil on microorganisms and decomposition." Soil Biology & Biochemistry **32**(4): 449-456.

van Groenigen, K. J., X. Qi, C. W. Osenberg, Y. Q. Luo and B. A. Hungate (2014). "Faster Decomposition Under Increased Atmospheric CO2 Limits Soil Carbon Storage." Science **344**(6183): 508-509.

van Groenigen, K. J., J. Six, B. A. Hungate, M. A. de Graaff, N. van Breemen and C. van Kessel (2006). "Element interactions limit soil carbon storage." Proceedings of the National Academy of Sciences of the United States of America **103**(17): 6571-6574.

Venter, J. C., K. Remington, J. F. Heidelberg, A. L. Halpern, D. Rusch, J. A. Eisen, D. Y. Wu, I. Paulsen, K. E. Nelson, W. Nelson, D. E. Fouts, S. Levy, A. H. Knap, M. W. Lomas, K. Nealson, O. White, J. Peterson, J. Hoffman, R. Parsons, H. Baden-Tillson, C. Pfannkoch, Y. H. Rogers and H. O. Smith (2004). "Environmental genome shotgun sequencing of the Sargasso Sea." Science **304**(5667): 66-74.

Wagg, C., S. F. Bender, F. Widmer and M. G. A. van der Heijden (2014). "Soil biodiversity and soil community composition determine ecosystem multifunctionality." Proceedings of the National Academy of Sciences.

Waldrop, M. P. and D. R. Zak (2006). "Response of oxidative enzyme activities to nitrogen deposition affects soil concentrations of dissolved organic carbon." Ecosystems **9**(6): 921-933.

Walther, G.-R., E. Post, P. Convey, A. Menzel, C. Parmesan, T. J. C. Beebee, J.-M. Fromentin, O. Hoegh-Guldberg and F. Bairlein (2002). "Ecological responses to recent climate change." Nature **416**(6879): 389-395.

Wang, Q., J. F. Quensen, J. A. Fish, T. Kwon Lee, Y. Sun, J. M. Tiedje and J. R. Cole (2013). "Ecological Patterns of nifH Genes in Four Terrestrial Climatic Zones

Explored with Targeted Metagenomics Using FrameBot, a New Informatics Tool." mBio **4**(5).

Wardle, D. A., R. D. Bardgett, J. N. Klironomos, H. Setälä, W. H. Van Der Putten and D. H. Wall (2004). "Ecological linkages between aboveground and belowground biota." Science **304**(5677): 1629-1633.

Weber, K. P. and R. L. Legge (2009). "One-dimensional metric for tracking bacterial community divergence using sole carbon source utilization patterns." Journal of Microbiological Methods **79**(1): 55-61.

Wessen, E., M. Soderstrom, M. Stenberg, D. Bru, M. Hellman, A. Welsh, F. Thomsen, L. Klemedtson, L. Philippot and S. Hallin (2011). "Spatial distribution of ammonia-oxidizing bacteria and archaea across a 44-hectare farm related to ecosystem functioning." Isme Journal **5**(7): 1213-1225.

Wild, B., J. Schnecker, R. J. E. Alves, P. Barsukov, J. Barta, P. Capek, N. Gentsch, A. Gittel, G. Guggenberger, N. Lashchinskiy, R. Mikutta, O. Rusalimova, H. Santruckova, O. Shibistova, T. Urich, M. Watzka, G. Zrazhevskaya and A. Richter (2014). "Input of easily available organic C and N stimulates microbial decomposition of soil organic matter in arctic permafrost soil." Soil Biology & Biochemistry **75**: 143-151.

Wu, L. Y., X. Liu, C. W. Schadt and J. Z. Zhou (2006). "Microarray-based analysis of subnanogram quantities of microbial community DNAs by using whole-community genome amplification." Applied and Environmental Microbiology **72**(7): 4931-4941.

Wu, L. Y., D. K. Thompson, G. S. Li, R. A. Hurt, J. M. Tiedje and J. Z. Zhou (2001). "Development and evaluation of functional gene arrays for detection of selected genes in the environment." Applied and Environmental Microbiology **67**(12): 5780-5790.

Wu, L. Y., C. Q. Wen, Y. J. Qin, H. Q. Yin, Q. C. Tu, J. D. Van Nostrand, T. Yuan, M. T. Yuan, Y. Deng and J. Z. Zhou (2015). "Phasing amplicon sequencing on Illumina Miseq for robust environmental microbial community analysis." Bmc Microbiology **15**.

Wu, X. Q., W. M. Yuan, X. J. Tian, B. Fan, X. Fang, J. R. Ye and X. L. Ding (2013). "Specific and Functional Diversity of Endophytic Bacteria from Pine Wood Nematode Bursaphelenchus Xylophilus with Different Virulence." International Journal of Biological Sciences **9**(1): 34-44.

Xiong, J. B., Z. L. He, S. J. Shi, A. Kent, Y. Deng, L. Y. Wu, J. D. Van Nostrand and J. Z. Zhou (2015). "Elevated CO2 shifts the functional structure and metabolic potentials of soil microbial communities in a C-4 agroecosystem." Scientific Reports **5**.

Xiong, J. B., L. Y. Wu, S. X. Tu, J. D. Van Nostrand, Z. L. He, J. Z. Zhou and G. J. Wang (2010). "Microbial Communities and Functional Genes Associated with Soil Arsenic Contamination and the Rhizosphere of the Arsenic-Hyperaccumulating Plant Pteris vittata L." Applied and Environmental Microbiology **76**(21): 7277-7284.

Xu, M. Y., Z. L. He, Y. Deng, L. Y. Wu, J. D. van Nostrand, S. E. Hobbie, P. B. Reich and J. Z. Zhou (2013). "Elevated CO2 influences microbial carbon and nitrogen cycling." Bmc Microbiology **13**.

Xue, C., X. Zhang, C. Zhu, J. Zhao, P. Zhu, C. Peng, N. Ling and Q. R. Shen (2016). "Quantitative and compositional responses of ammonia-oxidizing archaea and bacteria to long-term field fertilization." Scientific Reports **6**.

Xue, K., L. Y. Wu, Y. Deng, Z. L. He, J. Van Nostrand, P. G. Robertson, T. M. Schmidt and J. Z. Zhou (2013). "Functional Gene Differences in Soil Microbial Communities from Conventional, Low-Input, and Organic Farmlands." Applied and Environmental Microbiology **79**(4): 1284-1292.

Ying, J. Y., X. X. Li, N. N. Wang, Z. C. Lan, J. Z. He and Y. F. Bai (2017). "Contrasting effects of nitrogen forms and soil pH on ammonia oxidizing microorganisms and their responses to long-term nitrogen fertilization in a typical steppe ecosystem." Soil Biology & Biochemistry **107**: 10-18.

Yu, H. L., Q. Gao, Z. Q. Shao, A. N. Ying, Y. Y. Sun, J. W. Liu, W. Mao and B. Zhang (2016). "Decreasing Nitrogen Fertilizer Input Had Little Effect on Microbial Communities in Three Types of Soils." Plos One **11**(3).

Zak, D. R., K. S. Pregitzer, P. S. Curtis and W. E. Holmes (2000). "Atmospheric CO2 and the composition and function of soil microbial communities." Ecological Applications **10**(1): 47-59.

Zak, D. R., K. S. Pregitzer, P. S. Curtis, J. A. Teeri, R. Fogel and D. L. Randlett (1993). "Elevated Atmospheric Co2 and Feedback between Carbon and Nitrogen Cycles." Plant and Soil **151**(1): 105-117.

Zak, D. R., K. S. Pregitzer, P. S. Curtis, C. S. Vogel, W. E. Holmes and J. Lussenhop (2000). "Atmospheric CO2, soil-N availability, and allocation of biomass and nitrogen by Populus tremuloides." Ecological Applications **10**(1): 34-46.

Zak, D. R., K. S. Pregitzer, J. S. King and W. E. Holmes (2000). "Elevated atmospheric CO2, fine roots and the response of soil microorganisms: a review and hypothesis." New Phytologist **147**(1): 201-222.

Zanetti, S., U. A. Hartwig, C. vanKessel, A. Luscher, T. Hebeisen, M. Frehner, B. U. Fischer, G. R. Hendrey, H. Blum and J. Nosberger (1997). "Does nitrogen nutrition restrict the CO2 response of fertile grassland lacking legumes?" Oecologia **112**(1): 17-25.

Zavaleta, E. S., J. R. Pasari, K. B. Hulvey and G. D. Tilman (2010). "Sustaining multiple ecosystem functions in grassland communities requires higher biodiversity." Proceedings of the National Academy of Sciences.

Zehr, J. P., B. D. Jenkins, S. M. Short and G. F. Steward (2003). "Nitrogenase gene diversity and microbial community structure: a cross‐system comparison." Environmental Microbiology **5**(7): 539-554.

Zhang, L. M., P. R. Offre, J. Z. He, D. T. Verhamme, G. W. Nicol and J. I. Prosser (2010). "Autotrophic ammonia oxidation by soil thaumarchaea." Proceedings of the National Academy of Sciences of the United States of America **107**(40): 17240-17245.

Zhang, Y., X. Liu, J. Cong, H. Lu, Y. Sheng, X. Wang, D. Li, X. Liu, H. Yin, J. Zhou and Y. Deng (2017). "The microbially mediated soil organic carbon loss under degenerative succession in an alpine meadow." Mol Ecol.

Zhou, J., M. A. Bruns and J. M. Tiedje (1996). "DNA recovery from soils of diverse composition." Applied and Environmental Microbiology **62**(2): 316-322.

Zhou, J. Z., M. A. Bruns and J. M. Tiedje (1996). "DNA recovery from soils of diverse composition." Applied and Environmental Microbiology **62**(2): 316-322.
Zhou, J. Z., S. Kang, C. W. Schadt and C. T. Garten (2008). "Spatial scaling of functional gene diversity across various microbial taxa." Proceedings of the National Academy of Sciences of the United States of America **105**(22): 7768-7773.

Appendix A: Supplementary Tables

Table S3.1 Effects of eCO_2 and eN on additional plant and soil attributes.

Table S3.2. Unique and overlapped genes among treatments in C3 grass and legume plots.

Table S3.3 Overall microbial functional gene diversity at different CO_2 and N levels.

Table S5.1 Correlation test between phylogenetic archaeal-*amoA* groups and environmental factors and soil nitrification rate.

Table S3.1 Effects of eCO_2 and eN on additional plant and soil attributes.

		Variables	Mean ± SE			
			aCaN	eCaN	aCeN	eCeN
C3 grass	Soil	pH	5.65 ± 0.12	5.49 ± 0.10	5.68 ± 0.11	5.58 ± 0.11
		Moisture	0.27 ± 0.03 **b**	0.46 ± 0.11 **a**	0.24 ± 0.03 **b**	0.16 ± 0.03 **b**
		Temperature (°C)	20.62 ± 0.44	20.72 ± 0.4	21.08 ± 0.46	20.81 ± 0.45
		Total C (%)	0.4 ± 0.15	0.56 ± 0.20	0.67 ± 0.22	0.52 ± 0.15
		Total N (%)	0.04 ± 0.02	0.07 ± 0.02	0.07 ± 0.02	0.06 ± 0.02
	Plant	Aboveground C/N	36.25 ± 4.43 **b**	46.17 ± 1.43 **a**	32.98 ± 2.76 **bc**	26.04 ± 1.50 **c**
		Root C/N	41.97 ± 5.05 **a**	42.82 ± 3.81 **a**	32.25 ± 2.33 **ab**	27.59 ± 2.80 **b**
Legume	Soil	pH	5.53 ± 0.14	5.71 ± 0.13	5.33 ± 0.25	5.62 ± 0.03
		Moisture	0.20 ± 0.01	0.21 ± 0.04	0.20 ± 0.01	0.25 ± 0.05
		Temperature (°C)	19.55 ± 0.68	20.12 ± 0.67	19.68 ± 0.54	18.99 ± 0.22
		Total C (%)	0.7 ± 0.02	0.69 ± 0.05	0.86 ± 0.11	0.76 ± 0.06
		Total N (%)	0.08 ± 0.01	0.09 ± 0.01	0.08 ± 0.01	0.09 ± 0.01
	Plant	Aboveground C/N	27.14 ± 3.63	22.46 ± 2.75	30.40 ± 4.94	29.54 ± 7.24
		Root C/N	20.30 ± 0.58	18.11 ± 1.34	20.13 ± 2.00	15.86 ± 1.31

1. Values labeled with different letters are significantly different ($P < 0.05$) according to ANOVA, followed by Fisher's least significant difference (LSD) test with Holm-Bonferroni adjustment. Shown are mean values (n=3) ± standard errors.
2. All plant and soil properties were data collected from the sampling year (2009). And soil moisture was the combination of all three measured proportions (0-17cm, 42-59cm and 83-100cm).
3. Abbreviations: aCaN: ambient CO_2 and ambient N; eCaN: elevated CO_2 and ambient N; aCeN: ambient CO_2 and enriched N; eCeN: elevated CO_2 and enriched N.

Table S3.2 Unique and overlapped genes among treatments in C3 grass and legume plots.

		aCaN	eCaN	aCeN	eCeN
C3 grass	aCaN	**394(11.92%)**	2733(51.18%)	1929(46.96%)	2117(48.77%)
	eCaN		**1201(25.19%)**	2328(45.03%)	2587(48.52%)
	aCeN			**245(8.97%)**	1948(49.50%)
	eCeN				**363(11.52%)**
Legume	aCaN	**448(19.67%)**	1261(46.31%)	1416(49.75%)	1558(48.92%)
	eCaN		**158(9.26%)**	1227(49.82%)	1355(48.12%)
	aCeN			**258(13.00%)**	1470(49.35%)
	eCeN				**540(21.91%)**

1. The gene only existed in one treatment was a unique gene (**Bold**), and gene existed in two treatments was overlapped gene. Abbreviations: aCaN: ambient CO_2 and ambient N; eCaN: elevated CO_2 and ambient N; aCeN: ambient CO_2 and enriched N; eCeN: elevated CO_2 and enriched N.

Table S3.3 Overall microbial functional gene diversity at different CO_2 and N levels

		aCaN	eCaN	aCeN	eCeN
C3 grass	1/*D*	2648.48 ± 287.57 **b**	3975.55 ± 176.13 **a**	2308.92 ± 74.00 **b**	2384.84 ± 342.10 **b**
	No. of probes	2669 ± 290 **b**	4012 ± 179 **a**	2323 ± 77 **b**	2406 ± 349 **b**
Legume	1/*D*	1798.94 ± 308.08	1380.85 ± 135.66	1615.25 ± 83.13	1962.36 ± 161.00
	No. of probes	1811 ± 311	1388 ± 137	1623 ± 84	1975 ± 163

1. Values labeled with different letters are significantly different ($p < 0.05$) according to ANOVA, followed by Fisher's least significant difference (LSD) test with Holm-Bonferroni adjustment. Shown are mean values (n=3) ± standard errors. Values labeled with stars (*) indicate significant ($p < 0.05$) F ratios: *, $p < 0.05$; **, $p < 0.01$.

Table S5.1 Correlation test between phylogenetic archaeal-*amoA* groups and environmental factors and soil nitrification rate.

	Aboveground biomass		Root biomass		pH		Moisture (0-17 cm)		Moisture (42-59 cm)		Moisture (83-100 cm)		Nitrification	
	rho	*p*	*rho*	*p*	*rho*	*p*	*rho*	*p*	*rho*	*p*	*rho*	*p*	*rho*	*p*
Nitrososphaera subcluster 1.1	0.34	0.14	0.24	**0.04**	0.33	0.16	-0.06	0.81	-0.51	**0.02**	-0.46	**0.04**	-0.37	0.10
Nitrososphaera subcluster 3.1	-0.01	0.96	0.01	0.96	0.16	0.51	0.37	0.10	-0.02	0.93	-0.01	0.97	0.51	**0.02**
Nitrososphaera subcluster 3.2	-0.22	0.35	-0.12	0.61	-0.07	0.77	0.54	**0.01**	0.31	**0.09**	0.09	0.70	0.47	**0.04**
Nitrososphaera subcluster 3.3	-0.23	0.34	0.07	0.76	-0.15	0.54	0.26	0.28	-0.07	0.76	0.01	0.97	0.25	0.29
Nitrososphaera subcluster 5.1	0.13	0.60	-0.11	0.65	0.08	0.75	0.05	0.84	-0.35	**0.06**	-0.16	0.50	0.16	0.50
Nitrososphaera subcluster 6.1	0.16	0.50	0.23	**0.03**	0.33	0.16	-0.19	0.41	-0.52	**0.02**	0.12	0.62	0.42	**0.07**
Nitrososphaera subcluster 7	0.24	0.31	-0.20	0.40	-0.21	0.38	0.01	0.96	-0.15	0.53	-0.19	0.42	-0.08	0.75
Nitrososphaera subcluster 8.1	-0.05	0.84	-0.22	**0.03**	-0.09	0.70	0.22	0.36	-0.04	0.87	-0.18	0.45	0.04	0.87
Nitrososphaera subcluster 8.2	-0.12	0.63	0.12	0.63	0.27	0.25	0.13	0.58	0.24	0.31	-0.15	0.52	0.16	**0.05**
Nitrososphaera subcluster 11	0.01	0.96	-0.12	**0.06**	-0.06	0.79	0.21	0.39	-0.01	0.95	-0.24	0.31	-0.16	0.50
Nitrososphaera cluster other	-0.01	0.98	-0.34	0.15	-0.05	0.82	-0.27	0.25	0.02	0.94	0.27	0.24	0.33	0.16
Nitrososphaera sister cluster other	-0.12	0.60	-0.38	**0.07**	0.04	0.88	0.32	0.18	0.41	**0.07**	0.11	0.64	-0.08	0.72
Nitrososphaera sister subcluster 1.1	-0.06	0.80	0.58	**0.01**	-0.29	0.22	-0.32	0.17	-0.26	0.27	0.15	0.53	-0.05	0.82
Nitrososphaera sister subcluster 2	-0.23	0.34	0.30	**0.05**	-0.45	**0.04**	-0.05	0.84	0.02	0.94	0.14	0.55	0.00	1.00
Nitrosotalea subcluster 1.1	0.30	0.19	-0.21	0.38	0.03	0.91	-0.28	0.22	-0.16	0.51	-0.11	0.65	0.37	0.11
Unclassified	0.14	0.56	0.26	0.27	0.10	0.68	0.06	0.80	-0.02	0.93	-0.24	0.31	0.34	0.14

Appendix B: Supplementary Figures

Fig. S2.1 Changes in selected environmental variables under eCO_2 and eN. AB: aboveground biomass; RB: root biomass; AB-N: aboveground biomass N content; AB-C/N: aboveground biomass C/N ratio; R-N: root N content; R-C/N: root C/N ratio.

Fig. S2.2 PCoA plot of communities of C3 grass and legume plots under four different CO_2 and N levels.

Fig. S2.3 Classes with different abundance levels among treatments within C3 grass and legume plots.

Fig. S2.4 Genera with different abundance levels among treatments within C3 grass plots.

Fig. S2.5 Genera with different abundance levels among treatments within legume plots.

Fig. S2.6 Spearman's rank correlation coefficient rho of selected classes (with different abundance levels among treatments) with environmental attributes.

Fig. S2.7 Spearman's rank correlation coefficient rho of selected genera (with different abundance levels among treatments) with environmental attributes.

Fig. S2.8 Variation partitioning analysis (VPA) of microbial community structure explained by plant properties, soil geochemical variables, CO_2, and N.

Fig. S2.9 Relative difference of each genus between treatment and control as a function of genus abundance rank in control.

Fig. S3.1 Multivariate regression tree (MRT) analysis to illustrate the relative contributions of plant functional group (C3 grass and legume), eCO_2 and eN in shaping microbial functional composition and structure derived from GeoChip 3.0.

Fig. S3.2 Elevated CO_2 and eN effects on genes in C3 grass plots involved in N cycle (a), C fixation and CH_4 processes (b), and P/S cycles (c). The processes involved in N cycle include ammonification (1), Anammox (2), assimilatory N reduction (3), denitrification (4), dissimilatory N reduction (5), nitrification (6), and N fixation (7). Bars labeled with different letters are significantly different ($P < 0.05$) according to ANOVA, followed by Fisher's least significant difference (LSD) test with Holm-Bonferroni adjustment.

Fig. S3.3 Elevated CO_2 and eN effects on genes in legume plots involved in N cycle (a), C fixation and CH_4 processes (b), and P/S cycles (c). The processes involved in N cycle include ammonification (1), Anammox (2), assimilatory N reduction (3), denitrification (4), dissimilatory N reduction (5), nitrification (6), and N fixation (7). Bars labeled with

different letters are significantly different ($P < 0.05$) according to ANOVA, followed by Fisher's least significant difference (LSD) test with Holm-Bonferroni adjustment.

Fig. S3.4 Significance of correlations between individual or all genes involved in C degradation and SCF or HR (a); genes involved in C fixation and ^{13}C sequestration strength (b); *nifH* gene involved in N fixation and ^{15}N fixation across samples at aN plots (c); genes involved in ammonification or nitrification and soil N processes (d). Significance is represented by ** when $p<0.05$ and * when $p<0.10$.

Fig. S3.5 Quantitative ^{13}C and ^{15}N enrichment in soils from C3 grass and legume plots at CO_2 and N treatments.

Fig. S4.1 Effects of eCO_2 and eN on microbial metabolic diversity represented by Richness, Shannon, and Evenness. Boxes labeled with different letters are significantly different ($P < 0.05$) according to ANOVA, followed by Fisher's least significant difference (LSD) test with Holm-Bonferroni adjustment. Abbreviations: aCaN: ambient CO_2 and no fertilization; eCaN: elevated CO_2 and no fertilization; aCeN: ambient CO_2 and fertilized; eCeN: elevated CO_2 and fertilized.

Fig. S4.2 DCA analysis of microbial communities based on metabolic diversity obtained through Biolog EcoPlate after 156h incubation. Abbreviations: aCaN: ambient CO_2 and no fertilization; eCaN: elevated CO_2 and no fertilization; aCeN: ambient CO_2 and fertilized; eCeN: elevated CO_2 and fertilized.

Fig. S5.1 UniFrac PCoA and βMNTD analyses of the archaeal-*amoA* community. Gray: aCaN; Red: aCeN; Blue: eCeN; Green: eCaN.

Fig. S5.2 Detection frequency and relative abundances of archaeal-*amoA* genes at OTU level in the four CO_2 and N conditions. Phylogenetic tree was constructed based on neighbor-joining criterion. Rings from inner to outer represents aCaN, eCaN, aCeN, and eCeN conditions, respectively. * in red, blue and green represent significant CO_2, N and their interactive effects, respectively (* $p < 0.05$, ** $p < 0.01$, ***$p < 0.001$, ANOVA test).

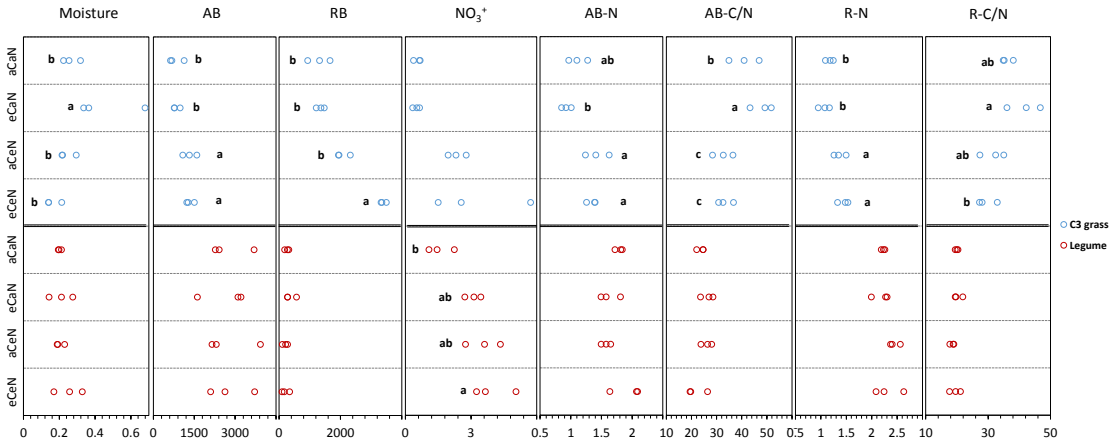

Fig. S2.1 Changes in selected environmental variables under eCO_2 and eN. AB: aboveground biomass; RB: root biomass; AB-N: aboveground biomass N content; AB-C/N: aboveground biomass C/N ratio; R-N: root N content; R-C/N: root C/N ratio.

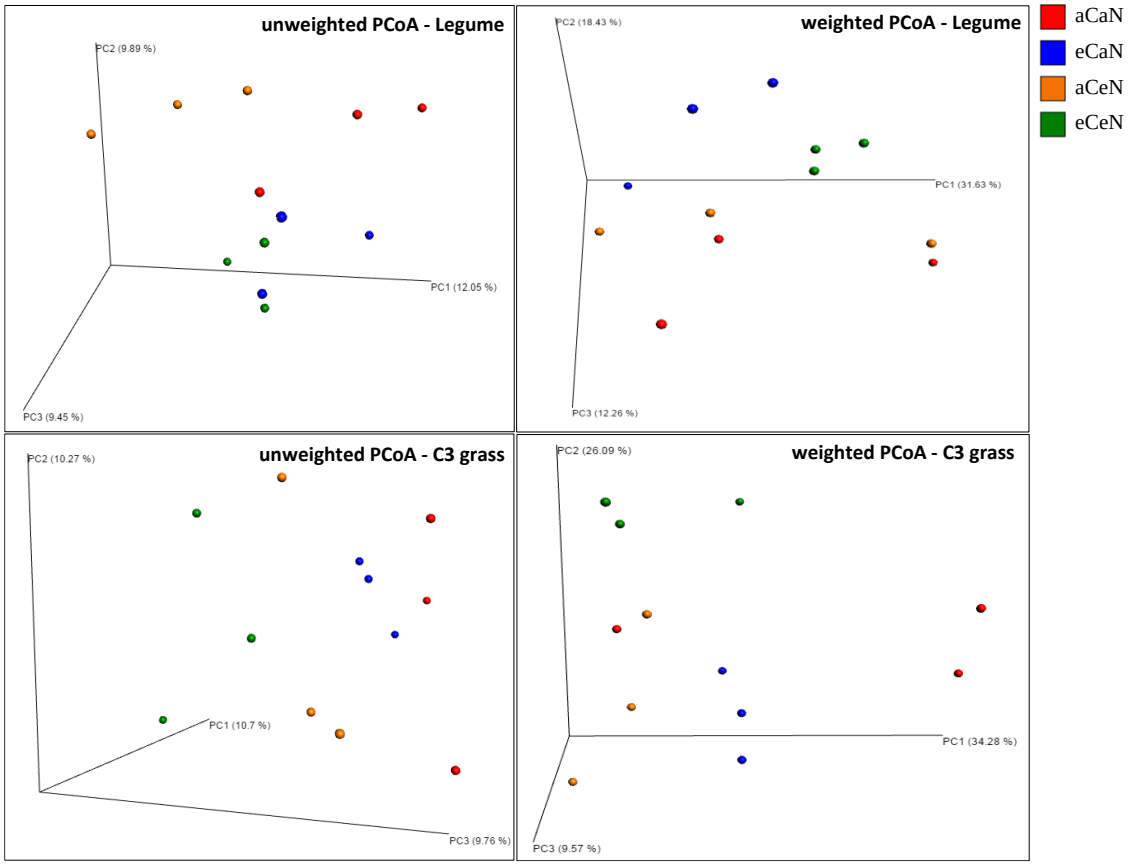

Fig. S2.2 PCoA plot of communities of C3 grass and legume plots under four different CO_2 and N levels. Each point corresponds to a sample.

		a	ab	b	bc	c		
	Class	aCaN	eCaN	aCeN	eCeN	abundance (%)	Treatment effects vs. aCaN	
C3	*Actinobacteria*					10.714%	Decreased with eCaN	
	Thermoleophilia					8.147%		
	Acidimicrobiia					1.097%	Decreased with aCeN	
	Planctomycetes BD7-11					0.005%		
	Gammaproteobacteria					1.726%	Increased with eCaN	
	Chlamydiae					0.112%		
	Verrucomicrobia UA11					0.002%		
	Bellilinea					0.002%		
	Deltaproteobacteria					1.582%	None	
	Phycisphaerae					0.666%		
	Nitrospira					0.353%		
	Melainabacteria					0.032%		
	Erysipelotrichia					0.029%		
Le	*Deltaproteobacteria*					1.858%	Decreased with eCaN	
	Phycisphaerae					0.582%		
	Chloroflexi JG30-KF-CM66					0.065%		
	Chloroflexi TK10					0.370%	Decreased with eCeN	
	Chloroflexi Gitt-GS-136					0.181%		
	Actinobacteria TakashiAC-B11					0.025%		
	Thermoleophilia					5.582%	Decreased with eCaN & eCeN	
	Chloroflexi JG37-AG-4					0.839%		
	Thermoplasmata					0.006%		
	Acidimicrobiia					0.963%	Decreased with aCeN	
	Acidobacteria subgroup 22					0.008%	Increased with eCaN	
	Acidobacteria subgroup 26					0.003%		
	Gammaproteobacteria					2.618%	Increased with eCeN	
	Bacteroidetes VC2.1 Bac22					0.002%		
	Latescibacteria bacterium					0.005%	Increased with eCaN & eCeN	
	Melainabacteria					0.035%	Increased with aCeN	
	Verrucomicrobia Incertae Sedis					0.006%		
	Acidobacteria subgroup 6					14.982%	None	
	Nitrospira					0.582%		
	Chlamydiae					0.170%		
	Caldilineae					0.041%		
	Planctomycetes vadinHA49					0.019%		

Fig. S2.3 Classes with different abundance levels among treatments within C3 grass and legume plots. The color panel under 'aCaN', 'eCaN', 'aCeN' and 'eCeN' reflects the relative abundance level at each treatment by LSD test. Red toned cells, (a); Blush toned cells, (ab); White toned cells, (b); Sapphire toned cells, (bc); and Blue toned cells, (c).

	Kingdom	Phylum	Class	Order	Family	Genus	aCaN	eCaN	aCeN	eCeN	Abundance (%)	Treatment effects vs. aCaN
	Bacteria	Actinobacteria	Thermoleophilia	Solirubrobacterales	Patulibacteraceae	Patulibacter					0.882%	Decreased with eCaN
	Bacteria	Actinobacteria	Actinobacteria	Micromonosporales	Micromonosporaceae	Virgisporangium					0.026%	
	Bacteria	Acidobacteria	Acidobacteria	Acidobacteria Subgroup 5	Acidobacteria Subgroup 5	Acidobacteria Subgroup 5					0.092%	
	Bacteria	Acidobacteria	Acidobacteria	Subgroup 17	Acidobacteria Subgroup 17	Acidobacteria Subgroup 17					0.043%	
	Bacteria	Actinobacteria	Actinobacteria	Frankiales	Frankiales	Frankiales					0.024%	
	Bacteria	Bacteroidetes	Sphingobacteriia	Sphingobacteriales	Sphingobacteriales env.OPS 17	Sphingobacteriales env.OPS 17					0.018%	
	Bacteria	Cyanobacteria	Cyanobacteria	SubsectionIV	FamilyI	FamilyI					0.010%	Decreased with eCeN
	Bacteria	Acidobacteria	Holophagae	Acidobacteria Subgroup 7	Acidobacteria Subgroup 7	Acidobacteria Subgroup 7					0.006%	
	Bacteria	Cyanobacteria	Cyanobacteria	SubsectionIV	FamilyI	Nostoc					0.003%	
	Bacteria	Proteobacteria	Betaproteobacteria	Hydrogenophilales	Hydrogenophilaceae	Hydrogenophilaceae					0.002%	
	Bacteria	Proteobacteria	Alphaproteobacteria	Rhizobiales	Hyphomicrobiaceae	Hyphomicrobiaceae					0.002%	
	Bacteria	Proteobacteria	Betaproteobacteria	Burkholderiales	Comamonadaceae	Albidiferax					0.001%	
	Bacteria	Bacteroidetes	Sphingobacteriia	Sphingobacteriales	Sphingobacteriales	Sphingobacteriales					0.056%	
	Bacteria	Actinobacteria	Acidimicrobiia	Acidimicrobiales	Acidimicrobiales	Acidimicrobiales					0.017%	
	Bacteria	Chloroflexi	Chloroflexia	Herpetosiphonales	Herpetosiphonaceae	Herpetosiphon					0.003%	
	Bacteria	Proteobacteria	Betaproteobacteria	Rhodocyclales	Rhodocyclaceae	Denitratisoma					0.002%	Decreased with eCaN & eCeN
	Bacteria	Proteobacteria	Alphaproteobacteria	Sphingomonadales	Sphingomonadaceae	Polymorphobacter					0.002%	
	Bacteria	Cyanobacteria	Cyanobacteria	SubsectionIII	FamilyI	Leptolyngbya					0.001%	
	Bacteria	Acidobacteria	Acidobacteria	Acidobacteria Subgroup 18	Acidobacteria Subgroup 18	Acidobacteria Subgroup 18					0.001%	
	Bacteria	Bacteroidetes	Flavobacteriia	Flavobacteriales	Cryomorphaceae	Fluviicola					0.001%	
	Bacteria	Proteobacteria	Betaproteobacteria	Nitrosomonadales	Nitrosomonadaceae	Nitrosomonadaceae					0.993%	
	Bacteria	Proteobacteria	Alphaproteobacteria	Rickettsiales	Rickettsiales Incertae Sedis	Captivus					0.006%	Decreased with aCeN
	Bacteria	Proteobacteria	Betaproteobacteria	Rhodocyclales	Rhodocyclaceae	Methyloversatilis					0.003%	
	Bacteria	Acidobacteria	Acidobacteria	Subgroup 4	Acidobacteria Subgroup 4	Acidobacteria Subgroup 4					0.216%	
	Bacteria	Proteobacteria	Alphaproteobacteria	Rhizobiales	Hyphomicrobiaceae	Hyphomicrobium					0.199%	
	Bacteria	Firmicutes	Bacilli	Bacillales	Paenibacillaceae	Paenibacillus					0.198%	
	Bacteria	Proteobacteria	Alphaproteobacteria	Rhizobiales	Rhizobiales Incertae Sedis	Bauldia					0.179%	
	Bacteria	Planctomycetes	Planctomycetacia	Planctomycetales	Planctomycetaceae	Planctomyces					0.095%	
	Bacteria	Firmicutes	Bacilli	Bacillales	Paenibacillaceae	Cohnella					0.025%	
	Bacteria	Planctomycetes	Planctomycetacia	Planctomycetales	Planctomycetaceae	Pir4 lineage					0.022%	
	Bacteria	Proteobacteria	Deltaproteobacteria	Deltaproteobacteria	Deltaproteobacteria	Deltaproteobacteria					0.021%	
	Bacteria	Proteobacteria	Alphaproteobacteria	Caulobacterales	Hyphomonadaceae	Hirschia					0.019%	
	Bacteria	Proteobacteria	Alphaproteobacteria	Rickettsiales	Holosporaceae	Holosporaceae					0.018%	
	Bacteria	Planctomycetes	Phycisphaerae	Pla1 lineage	Pla1 lineage	Pla1 lineage					0.017%	
C3	Bacteria	Proteobacteria	Alphaproteobacteria	Rhodospirillales	Rhodospirillales	Rhodospirillales					0.016%	
	Bacteria	Chlamydiae	Chlamydiae	Chlamydiales	Simkaniaceae	Rhabdochlamydia					0.013%	
	Bacteria	Proteobacteria	Betaproteobacteria	Burkholderiales	Comamonadaceae	Ideonella					0.012%	
	Bacteria	Actinobacteria	Actinobacteria	Corynebacteriales	Nocardiaceae	Smaragdicoccus					0.007%	
	Bacteria	Proteobacteria	Betaproteobacteria	Burkholderiales	Burkholderiaceae	Glomeribacter					0.006%	
	Bacteria	Proteobacteria	Proteobacteria TA18	Proteobacteria TA18	Proteobacteria TA18	Proteobacteria TA18					0.005%	
	Bacteria	Chloroflexi	Ktedonobacteria	Ktedonobacterales	Ktedonobacterales	Ktedonobacterales					0.005%	
	Bacteria	Verrucomicrobia	Verrucomicrobiae	Verrucomicrobiales	Verrucomicrobiaceae	Prosthecobacter					0.003%	
	Bacteria	Planctomycetes	Phycisphaerae	Phycisphaerae WD2101	Phycisphaerae WD2101	Phycisphaerae WD2101					0.003%	
	Bacteria	Proteobacteria	Betaproteobacteria	Burkholderiales	Comamonadaceae	Brachymonas					0.003%	
	Bacteria	Proteobacteria	Deltaproteobacteria	Myxococcales	Polyangiaceae	Polyangium					0.003%	
	Bacteria	Gemmatimonadetes	Gemmatimonadetes	Gemmatimonadetes	Gemmatimonadetes	Gemmatimonadetes					0.002%	
	Bacteria	Verrucomicrobia	UA11	Verrucomicrobia UA11	Verrucomicrobia UA11	Verrucomicrobia UA11					0.002%	Increased with eCaN
	Bacteria	Proteobacteria	Deltaproteobacteria	Deltaproteobacteria	Deltaproteobacteria	Deltaproteobacteria					0.002%	
	Bacteria	Elusimicrobia	Elusimicrobia	Lineage IIc	Lineage IIc	Lineage IIc					0.002%	
	Bacteria	Chloroflexi	Bellilinea	Bellilinea	Bellilinea	Bellilinea					0.002%	
	Bacteria	Proteobacteria	Deltaproteobacteria	Syntrophobacterales	Syntrophaceae	Syntrophaceae					0.001%	
	Bacteria	Proteobacteria	Deltaproteobacteria	Myxococcales	Nannocystaceae	Nannocystis					0.001%	
	Bacteria	Proteobacteria	Gammaproteobacteria	Xanthomonadales	Nevskiaceae	Nevskia					0.001%	
	Bacteria	Proteobacteria	Gammaproteobacteria	Xanthomonadales	Xanthomonadaceae	Metallibacterium					0.001%	
	Bacteria	Proteobacteria	Alphaproteobacteria	Rhizobiales	Hyphomicrobiaceae	Prosthecomicrobium					0.001%	
	Bacteria	Proteobacteria	Deltaproteobacteria	Myxococcales	Myxococcales	Myxococcales					0.001%	
	Bacteria	Actinobacteria	Actinobacteria	Streptomycetales	Streptomycetaceae	Streptacidiphilus					0.0003%	
	Bacteria	Armatimonadetes	Armatimonadia	Armatimonadales	Armatimonadaceae	Armatimonas					0.0003%	
	Bacteria	Bacteroidetes	Cytophagia	Cytophagales	Cyclobacteriaceae	Cyclobacteriaceae					0.0003%	
	Bacteria	Cyanobacteria	Cyanobacteria	SubsectionIII	FamilyI	Crinalium					0.0003%	
	Bacteria	Gemmatimonadetes	Gemmatimonadetes	Gemmatimonadales	Gemmatimonadaceae	Gemmatimonadaceae					0.0003%	
	Bacteria	Planctomycetes	Phycisphaerae	Phycisphaerae	Phycisphaerae	Phycisphaerae					0.0003%	
	Bacteria	Proteobacteria	Alphaproteobacteria	Rhodobacterales	Rhodobacteraceae	Defluviimonas					0.0003%	
	Bacteria	Proteobacteria	Alphaproteobacteria	Rickettsiales	Mitochondria	Mitochondria					0.0003%	
	Bacteria	Proteobacteria	Alphaproteobacteria	Rickettsiales	Rickettsiaceae	Orientia					0.0003%	
	Bacteria	Proteobacteria	Deltaproteobacteria	Desulfuromonadales	Desulfuromonadaceae	Desulfuromonas					0.0003%	
	Bacteria	Proteobacteria	Gammaproteobacteria	Chromatiales	Chromatiaceae	Nitrosococcus					0.0003%	
	Bacteria	Proteobacteria	Gammaproteobacteria	Xanthomonadales	Xanthomonadaceae	Rudaea					0.0003%	
	Bacteria	Firmicutes	Bacilli	Bacillales	Thermoactinomycetaceae	Kroppenstedtia					0.0003%	

(a)

	Kingdom	Phylum	Class	Order	Family	Genus	aCaN	eCaN	aCeN	eCeN	Abundance (%)	Treatment effects vs. aCaN
							a	ab	b	bc	c	
C3	Bacteria	Actinobacteria	Actinobacteria	Corynebacteriales	Mycobacteriaceae	Mycobacterium					0.960%	
	Bacteria	Actinobacteria	Thermoleophilia	Solirubrobacterales	Solirubrobacterales	Solirubrobacterales					0.765%	
	Bacteria	Actinobacteria	Actinobacteria	Micromonosporales	Micromonosporaceae	Micromonosporaceae					0.506%	
	Bacteria	Proteobacteria	Alphaproteobacteria	Rhizobiales	Hyphomicrobiaceae	Devosia					0.362%	
	Bacteria	Actinobacteria	Actinobacteria	Pseudonocardiales	Pseudonocardiaceae	Amycolatopsis					0.301%	
	Bacteria	Proteobacteria	Gammaproteobacteria	Xanthomonadales	Xanthomonadaceae	Dokdonella					0.097%	
	Bacteria	Actinobacteria	Actinobacteria	Micromonosporales	Micromonosporaceae	Planosporangium					0.096%	
	Bacteria	Proteobacteria	Alphaproteobacteria	Rhizobiales	Xanthobacteraceae	Labrys					0.096%	
	Bacteria	Actinobacteria	Actinobacteria	Pseudonocardiales	Pseudonocardiaceae	Kibdelosporangium					0.084%	
	Bacteria	Actinobacteria	Actinobacteria	Streptosporangiales	Thermomonosporaceae	Actinomadura					0.045%	
	Bacteria	Actinobacteria	Actinobacteria	Catenulisporales	Catenulisporaceae	Catenulispora					0.022%	
	Bacteria	Actinobacteria	Actinobacteria	Micrococcales	Intrasporangiaceae	Intrasporangiaceae					0.014%	
	Bacteria	Actinobacteria	Actinobacteria	Corynebacteriales	Corynebacteriales	Corynebacteriales					0.012%	
	Bacteria	Proteobacteria	Alphaproteobacteria	Sphingomonadales	Sphingomonadales	Sphingomonadales					0.010%	
	Bacteria	Verrucomicrobia	Spartobacteria	Chthoniobacterales	Chthoniobacterales	Chthoniobacterales					0.005%	Increased with eCeN
	Bacteria	Actinobacteria	Thermoleophilia	Gaiellales	Gaiellales	Solirubrobacter					0.003%	
	Bacteria	Actinobacteria	Actinobacteria	Frankiales	Frankiaceae	Frankiaceae					0.002%	
	Bacteria	Actinobacteria	Actinobacteria	Micrococcales	Micrococcaceae	Micrococcaceae					0.002%	
	Bacteria	Planctomycetes	Planctomycetacia	Planctomycetales	Planctomycetaceae	Schlesneria					0.002%	
	Bacteria	Cyanobacteria	Cyanobacteria ML635J-21	Cyanobacteria ML635J-21	Cyanobacteria ML635J-21	Cyanobacteria ML635J-21					0.001%	
	Bacteria	Proteobacteria	Betaproteobacteria	Burkholderiales	Comamonadaceae	Hydrogenophaga					0.001%	
	Bacteria	Proteobacteria	Alphaproteobacteria	Rhodospirillales	Rhodospirillaceae	Thalassospira					0.001%	
	Bacteria	Chlamydiae	Chlamydiae	Chlamydiales	Simkaniaceae	Simkaniaceae					0.001%	
	Bacteria	Planctomycetes	Planctomycetes	Planctomycetes	Planctomycetes	Planctomycetes					0.001%	
	Bacteria	Actinobacteria	Actinobacteria	Corynebacteriales	Corynebacteriaceae	Corynebacteriaceae					0.0003%	
	Bacteria	Bacteroidetes	Bacteroidia	Bacteroidales	Porphyromonadaceae	Dysgonomonas					0.0003%	
	Bacteria	Proteobacteria	Alphaproteobacteria	Caulobacterales	Hyphomonadaceae	Hyphomonadaceae					0.0003%	
	Bacteria	Proteobacteria	Alphaproteobacteria	Rhizobiales	Aurantimonadaceae	Aurantimonadaceae					0.0003%	
	Bacteria	Proteobacteria	Alphaproteobacteria	Rhizobiales	Rhodobiaceae	Rhodobiaceae					0.0003%	
	Bacteria	Proteobacteria	Betaproteobacteria	Burkholderiales	Comamonadaceae	Simplicispira					0.0003%	
	Bacteria	Actinobacteria	Actinobacteria	Propionibacteriales	Nocardioidaceae	Kribbella					0.092%	
	Bacteria	Proteobacteria	Gammaproteobacteria	Gammaproteobacteria NKB5	Gammaproteobacteria NKB5	Gammaproteobacteria NKB5					0.068%	
	Bacteria	Proteobacteria	Gammaproteobacteria	Legionellales	Legionellaceae	Legionella					0.063%	
	Bacteria	Chlamydiae	Chlamydiae	Chlamydiales	Parachlamydiaceae	Protochlamydia					0.029%	Increased with eCaN & eCeN
	Bacteria	Planctomycetes	Phycisphaerae	Phycisphaerales	Phycisphaeraceae	Phycisphaeraceae					0.011%	
	Bacteria	Acidobacteria	Acidobacteria	Acidobacteria Subgroup 3	Acidobacteria Subgroup 3	Acidobacteria Subgroup 3					0.010%	
	Bacteria	Proteobacteria	Deltaproteobacteria	Oligoflexales	Oligoflexaceae	Oligoflexaceae					0.004%	
	Bacteria	Proteobacteria	Gammaproteobacteria	Xanthomonadales	Xanthomonadales	Xanthomonadales					0.001%	
	Bacteria	Proteobacteria	Betaproteobacteria	Burkholderiales	Oxalobacteraceae	Oxalobacteraceae					0.074%	
	Bacteria	Actinobacteria	Actinobacteria	Streptosporangiales	Thermomonosporaceae	Actinoallomurus					0.069%	
	Bacteria	Chloroflexi	Ktedonobacteria	Ktedonobacteria	Ktedonobacteria	Ktedonobacteria					0.012%	
	Bacteria	Proteobacteria	Gammaproteobacteria	Xanthomonadales	Xanthomonadaceae	Dyella					0.006%	
	Bacteria	Acidobacteria	Acidobacteria	Acidobacteriales	Acidobacteriaceae Subgroup 1	Telmatobacter					0.006%	
	Bacteria	Proteobacteria	Alphaproteobacteria	Rhizobiales	Methylocystaceae	Methylocystaceae					0.005%	
	Bacteria	Proteobacteria	Betaproteobacteria	Rhodocyclales	Rhodocyclaceae	Azospira					0.003%	
	Bacteria	Proteobacteria	Betaproteobacteria	Burkholderiales	Alcaligenaceae	Bordetella					0.002%	Increased with aCeN
	Bacteria	Proteobacteria	Alphaproteobacteria	Rhizobiales	Methylocystaceae	Methylocystis					0.002%	
	Bacteria	Armatimonadetes	Armatimonadia	Armatimonadales	Armatimonadales	Armatimonadales					0.002%	
	Bacteria	Proteobacteria	Alphaproteobacteria	Rickettsiales	Rickettsiaceae	Rickettsiaceae					0.001%	
	Bacteria	Actinobacteria	Actinobacteria	Pseudonocardiales	Pseudonocardiaceae	Goodfellowiella					0.001%	
	Bacteria	Proteobacteria	Gammaproteobacteria	Legionellales	Legionellaceae	Legionellaceae					0.001%	
	Archaea	esearchaeota (DHVEG	euryarchaeote	euryarchaeote	euryarchaeote	euryarchaeote					0.001%	
	Bacteria	Proteobacteria	Gammaproteobacteria	Enterobacteriales	Enterobacteriaceae	Serratia					0.001%	
	Bacteria	Actinobacteria	Thermoleophilia	Gaiellales	Gaiellales	Gaiellales					0.0003%	
	Bacteria	Actinobacteria	Actinobacteria	Pseudonocardiales	Pseudonocardiaceae	Pseudonocardia					1.090%	
	Bacteria	Proteobacteria	Alphaproteobacteria	Rhizobiales	Phyllobacteriaceae	Mesorhizobium					0.308%	
	Bacteria	Actinobacteria	Actinobacteria	Micromonosporales	Micromonosporaceae	Dactylosporangium					0.236%	
	Bacteria	Nitrospirae	Nitrospira	Nitrospirales	Nitrospiraceae	Nitrospira					0.215%	
	Bacteria	Actinobacteria	Actinobacteria	Frankiales	Geodermatophilaceae	Modestobacter					0.168%	
	Bacteria	Actinobacteria	Actinobacteria	Micromonosporales	Micromonosporaceae	Micromonospora					0.083%	
	Bacteria	Bacteroidetes	Cytophagia	Cytophagales	Cytophagaceae	Cytophagaceae					0.075%	
	Bacteria	Proteobacteria	Alphaproteobacteria	Rhodospirillales	Acetobacteraceae	Acidiphilium					0.072%	
	Bacteria	Actinobacteria	Actinobacteria	Frankiales	Geodermatophilaceae	Blastococcus					0.055%	
	Bacteria	Proteobacteria	Alphaproteobacteria	Caulobacterales	Hyphomonadaceae	Woodsholea					0.027%	
	Bacteria	Firmicutes	Erysipelotrichia	Erysipelotrichales	Erysipelotrichaceae	Asteroleplasma					0.026%	
	Bacteria	Proteobacteria	Gammaproteobacteria	Xanthomonadales	Xanthomonadaceae	Arenimonas					0.021%	
	Bacteria	Proteobacteria	Gammaproteobacteria	Xanthomonadales	Xanthomonadaceae	Luteibacter					0.020%	None
	Bacteria	Actinobacteria	Actinobacteria	Streptosporangiales	Streptosporangiaceae	Nonomuraea					0.017%	
	Bacteria	Actinobacteria	Actinobacteria	Micrococcales	Micrococcaceae	Micrococcus					0.012%	
	Bacteria	Bacteroidetes	Sphingobacteriia	Sphingobacteriales	Chitinophagaceae	Niabella					0.012%	
	Bacteria	Proteobacteria	Alphaproteobacteria	Rhodospirillales	Rhodospirillaceae	Defluviicoccus					0.012%	
	Bacteria	Proteobacteria	Gammaproteobacteria	Xanthomonadales	Xanthomonadaceae	Lysobacter					0.010%	
	Bacteria	Actinobacteria	Actinobacteria	Pseudonocardiales	Pseudonocardiaceae	Saccharopolyspora					0.010%	
	Bacteria	Actinobacteria	Actinobacteria	Micrococcales	Microbacteriaceae	Herbiconiux					0.009%	
	Bacteria	Actinobacteria	Actinobacteria	Micrococcales	Microbacteriaceae	Marisediminicola					0.005%	
	Bacteria	Candidate division OP3	uncultured bacterium	uncultured bacterium	uncultured bacterium	OP3					0.003%	
	Bacteria	Proteobacteria	Alphaproteobacteria	Rhodospirillales	Acetobacteraceae	Rubritepida					0.002%	
	Bacteria	Proteobacteria	Gammaproteobacteria	Xanthomonadales	Xanthomonadaceae	Tahibacter					0.002%	
	Bacteria	Actinobacteria	Actinobacteria	Pseudonocardiales	Pseudonocardiaceae	Saccharothrix					0.001%	

(b)

Fig. S2.4 Genera with different abundance levels among treatments within C3 grass plots. The color panel under 'aCaN', 'eCaN', 'aCeN' and 'eCeN' reflects the relative abundance level at each treatment by LSD test. Red toned cells, (a); Blush toned cells, (ab); White toned cells, (b); Sapphire toned cells, (bc); and Blue toned cells, (c).

	Kingdom	Phylum	Class	Order	Family	Genus	aCaN	eCaN	aCeN	eCeN	Abundance (%)	Treatment effects vs. aCaN
	Bacteria	Actinobacteria	Thermoleophilia	Solirubrobacterales	Solirubrobacterales	Solirubrobacterales	a				0.377%	
	Bacteria	Proteobacteria	Deltaproteobacteria	Myxococcales	Haliangiaceae	Haliangium	a				0.329%	
	Bacteria	Proteobacteria	Deltaproteobacteria	Myxococcales	Polyangiaceae	Sorangium	a				0.115%	
	Bacteria	Proteobacteria	Deltaproteobacteria	Bdellovibrionales	Bdellovibrionaceae	Bdellovibrio	a				0.081%	
	Bacteria	Bacteroidetes	Sphingobacteriia	Sphingobacteriales	Sphingobacteriales	Sphingobacteriales	a				0.055%	
	Bacteria	Armatimonadetes	Chthonomonadetes	Chthonomonadales	Chthonomonadaceae	Chthonomonas	a				0.052%	Decreased with eCaN
	Bacteria	Elusimicrobia	Elusimicrobia	Lineage IV	Lineage IV	Lineage IV	a				0.004%	
	Bacteria	Armatimonadetes	Armatimonadia	Armatimonadales	Armatimonadales	Armatimonadales	a				0.002%	
	Bacteria	Cyanobacteria	Melainabacteria	Vampirovibrionales	Vampirovibrionales	Vampirovibrionales	a				0.002%	
	Bacteria	Gemmatimonadetes	Gemmatimonadetes	Gemmatimonadales	Gemmatimonadaceae	Gemmatimonadaceae	a				0.002%	
	Bacteria	Proteobacteria	Gammaproteobacteria	Thiotrichales	Thiotrichales	Thiotrichales	a				0.001%	
	Bacteria	Actinobacteria	Acidimicrobiia	Acidimicrobiales	Acidimicrobiales	Acidimicrobiales	a	ab			0.646%	
	Bacteria	Planctomycetes	Planctomycetacia	Planctomycetales	Planctomycetaceae	Singulisphaera	a	ab			0.166%	
	Bacteria	Actinobacteria	TakashiAC-B11	TakashiAC-B11	TakashiAC-B11	TakashiAC-B11	a	ab			0.025%	
	Bacteria	Actinobacteria	Actinobacteria	Frankiales	Frankiales	Frankiales	ab	b	a	c	0.022%	
	Bacteria	Bacteroidetes	Cytophagia	Cytophagales	Cytophagaceae	Sporocytophaga	a	ab			0.015%	Decreased with eCeN
	Bacteria	Bacteroidetes	Cytophagia	Cytophagales	Cytophagaceae	Cytophaga	a	ab			0.007%	
	Bacteria	Proteobacteria	Alphaproteobacteria	Rhodobacterales	Rhodobacteraceae	Paracocccus	a	ab	a		0.003%	
	Bacteria	Proteobacteria	Alphaproteobacteria	Rhizobiales	Methylocystaceae	Methylocystis	a	ab	b	c	0.001%	
	Bacteria	Chloroflexi	Ktedonobacteria	Ktedonobacterales	Ktedonobacteraceae	Ktedonobacter	a	ab	ab		0.001%	
	Bacteria	Chloroflexi	Chloroflexi	Chloroflexi	Chloroflexi	Chloroflexi	a	ab	ab		0.839%	
	Bacteria	Planctomycetes	Phycisphaerae	Phycisphaerae WD2101 soil group	Phycisphaerae WD2101 soil group	Phycisphaerae WD2101 soil group	a		ab		0.461%	
	Bacteria	Actinobacteria	Actinobacteria	Frankiales	Frankiaceae	Jatrophihabitans	a		ab		0.306%	
	Bacteria	Planctomycetes	Planctomycetacia	Planctomycetales	Planctomycetaceae	Gemmata	a		ab		0.198%	
	Bacteria	Actinobacteria	Actinobacteria	Frankiales	Cryptosporangiaceae	Cryptosporangium	a	b	ab	c	0.045%	
	Bacteria	Chloroflexi	Ktedonobacteria	Ktedonobacteria	Ktedonobacteria	Ktedonobacteria	a		ab		0.018%	
	Archaea	Euryarchaeota	Thermoplasmata	Thermoplasmatales	Marine Group II	Marine Group II	a		ab		0.006%	Decreased with eCaN & eCeN
	Bacteria	Actinobacteria	Actinobacteria	Propionibacteriales	Propionibacteriales	Propionibacteriales	a		ab		0.002%	
	Bacteria	Proteobacteria	Betaproteobacteria	Burkholderiales	Comamonadaceae	Hydrogenophaga	a				0.002%	
	Bacteria	Actinobacteria	Actinobacteria	Streptosporangiales	Thermomonosporaceae	Spirillospora	a				0.001%	
	Bacteria	Actinobacteria	Actinobacteria	Frankiales	Frankiaceae	Frankiaceae	a		a		0.001%	
	Bacteria	Firmicutes	Bacilli	Bacillales	Paenibacillaceae	Paenibacillaceae	a				0.001%	
	Bacteria	Planctomycetes	Phycisphaerae	Phycisphaerales	Phycisphaeraceae	Phycisphaeraceae	a				0.001%	
	Bacteria	Firmicutes	Bacilli	Lactobacillales	Carnobacteriaceae	Carnobacterium	a				0.0003%	
	Bacteria	Acidobacteria	Acidobacteria	Acidobacteria AT-s3-28	Acidobacteria AT-s3-28	Acidobacteria AT-s3-28	a	ab			0.007%	
	Bacteria	Armatimonadetes	Armatimonadetes	Armatimonadetes	Armatimonadetes	Armatimonadetes	ab	b	a	c	0.005%	Decreased with eCeN
	Bacteria	Firmicutes	Negativicutes	Selenomonadales	Veillonellaceae	Sporomusa	a	ab			0.001%	
	Bacteria	Proteobacteria	Alphaproteobacteria	Rhizobiales	Hyphomicrobiaceae	Rhodoplanes		a			0.536%	
	Bacteria	Proteobacteria	Betaproteobacteria	Betaproteobacteria,	Betaproteobacteria	Betaproteobacteria		a			0.103%	
	Bacteria	Bacteroidetes	Cytophagia	Cytophagales	Cytophagaceae	Adhaeribacter		a			0.098%	
Le	Bacteria	Bacteroidetes	Sphingobacteriia	Sphingobacteriales	Chitinophagaceae	Chitinophagaceae		a			0.086%	
	Bacteria	Proteobacteria	Gammaproteobacteria	Legionellales	Coxiellaceae	Coxiella		a			0.027%	
	Bacteria	Proteobacteria	Alphaproteobacteria	Rhizobiales	Beijerinckiaceae	Beijerinckiaceae		a	a		0.024%	
	Bacteria	Proteobacteria	Alphaproteobacteria	Rickettsiales	Holosporaceae	Holosporaceae		a			0.023%	
	Bacteria	Proteobacteria	Alphaproteobacteria	Rhizobiales	Hyphomicrobiaceae	Rhodomicrobium		a			0.017%	
	Bacteria	Acidobacteria	Holophagae	Holophagae Subgroup 10	Holophagae Subgroup 10	Holophagae Subgroup 10	ab	a	b	c	0.016%	
	Bacteria	Proteobacteria	Gammaproteobacteria	Xanthomonadales	Xanthomonadaceae	Tahibacter		a			0.011%	
	Bacteria	Actinobacteria	Actinobacteria	Streptosporangiales	Streptosporangiaceae	Microbispora		a			0.010%	
	Bacteria	Proteobacteria	Betaproteobacteria	Burkholderiales	Burkholderiales	Burkholderiales		a			0.009%	
	Bacteria	Proteobacteria	Alphaproteobacteria	Caulobacterales	Caulobacteraceae	Asticcacaulis		a			0.009%	Increased with eCaN
	Bacteria	Proteobacteria	Betaproteobacteria	Burkholderiales	Comamonadaceae	Ottowia		a	a		0.006%	
	Bacteria	Proteobacteria	Alphaproteobacteria	Rhizobiales	Rhizobiales	Rhizobiales		a			0.005%	
	Bacteria	Actinobacteria	Actinobacteria	Micromonosporales	Micromonosporaceae	Hamadaea		a			0.004%	
	Bacteria	Planctomycetes	Phycisphaerae	Phycisphaerae	Phycisphaerae	Phycisphaerae		a			0.004%	
	Bacteria	Acidobacteria	Acidobacteria Subgroup 26	Acidobacteria Subgroup 26	Acidobacteria Subgroup 26	Acidobacteria Subgroup 26		a			0.003%	
	Bacteria	Chloroflexi	Caldilineae	Caldilineales	Caldilineaceae	Litorilinea		a			0.003%	
	Bacteria	Proteobacteria	Alphaproteobacteria	Rhizobiales	Xanthobacteraceae	Starkeya		a			0.001%	
	Bacteria	Proteobacteria	Alphaproteobacteria	Rhizobiales	Bartonellaceae	Bartonella		a			0.001%	
	Bacteria	Actinobacteria	Actinobacteria	Streptosporangiales	Nocardiopsaceae	Streptomonospora		a			0.001%	
	Bacteria	Actinobacteria	Actinobacteria	Corynebacteriales	Tsukamurellaceae	Tsukamurella		a			0.0003%	
	Bacteria	Actinobacteria	Actinobacteria	Propionibacteriales	Propionibacteriaceae	Microlunatus		a			0.0003%	
	Bacteria	Actinobacteria	Actinobacteria	Streptosporangiales	Streptosporangiaceae	Sinosporangium		a			0.0003%	
	Bacteria	Proteobacteria	Alphaproteobacteria	Rhizobiales	Bradyrhizobiaceae	Bradyrhizobiaceae		ab	ab	a	0.128%	
	Archaea	Thaumarchaeota	Thaumarchaeota (SCG)	Thaumarchaeota (SCG)	Thaumarchaeota (SCG)	Thaumarchaeota (SCG)		ab		a	0.106%	
	Bacteria	Proteobacteria	Deltaproteobacteria	Myxococcales	Myxococcales	Myxococcales		ab		a	0.089%	
	Bacteria	Proteobacteria	Gammaproteobacteria	Xanthomonadales	Xanthomonadaceae	Arenimonas				a	0.059%	
	Bacteria	Chlamydiae	Chlamydiae	Chlamydiales	Parachlamydiaceae	Metachlamydia		ab		a	0.025%	
	Bacteria	Chlamydiae	Chlamydiae	Chlamydiales	Chlamydiales	Chlamydiales		ab		a	0.018%	
	Bacteria	Acidobacteria	Acidobacteria	Acidobacteria Subgroup 3	Acidobacteria Subgroup 3	Acidobacteria Subgroup 3				a	0.017%	
	Archaea	Thaumarchaeota	Thaumarchaeota (SCG)	Unknown Order	Unknown Family	Nitrososphaera				a	0.015%	
	Bacteria	Actinobacteria	Actinobacteria	Streptosporangiales	Streptosporangiaceae	Nonomuraea		ab	a	a	0.013%	
	Bacteria	Acidobacteria	Acidobacteria Subgroup 22	Acidobacteria Subgroup 22	Acidobacteria Subgroup 22	Acidobacteria Subgroup 22		ab		a	0.008%	Increased with eCeN
	Bacteria	Proteobacteria	Deltaproteobacteria	Bdellovibrionales	Bacteriovoracaceae	Bacteriovorax		ab	a	a	0.006%	
	Bacteria	Proteobacteria	Betaproteobacteria	Rhodocyclales	Rhodocyclaceae	Rhodocyclaceae				a	0.005%	
	Bacteria	Proteobacteria	Alphaproteobacteria	Rhizobiales	Rhizobiales Incertae Sedis	Phreatobacter		ab	a	a	0.001%	
	Bacteria	Acidobacteria	Acidobacteria	Acidobacteria Subgroup 17	Acidobacteria Subgroup 17	Acidobacteria Subgroup 17		ab	a	a	0.001%	
	Bacteria	Bacteroidetes	Flavobacteriia	Flavobacteriales	Flavobacteriaceae	Epilithonimonas				a	0.001%	
	Bacteria	Proteobacteria	Gammaproteobacteria	Order Incertae Sedis	Family Incertae Sedis	Marinicella				a	0.0003%	
	Bacteria	Proteobacteria	Alphaproteobacteria	Rhodobacterales	Rhodobacteraceae	Leisingera				a	0.0003%	
	Bacteria	Acidobacteria	Acidobacteria	Acidobacteriales	Acidobacteriaceae Gp 1	Bryocella				a	0.0003%	
	Bacteria	Actinobacteria	Actinobacteria	Micrococcales	Microbacteriaceae	Galbitalea				a	0.0003%	

(a)

	Kingdom	Phylum	Class	Order	Family	Genus	aCaN	eCaN	aCeN	eCeN	Abundance (%)	Treatment effects vs. aCaN
							a	ab	b	bc	c	
Le	Bacteria	Acidobacteria	Acidobacteria	Subgroup 4	Acidobacteria Subgroup 4	Acidobacteria Subgroup 4					5.806%	Increased with eCaN & eCeN
	Bacteria	Acidobacteria	Holophagae	Holophagae	Holophagae	Holophagae					0.044%	
	Bacteria	Proteobacteria	Alphaproteobacteria	Rhizobiales	Phyllobacteriaceae	Phyllobacteriaceae					0.037%	
	Bacteria	Proteobacteria	Alphaproteobacteria	Rhodospirillales	Rhodospirillales	Rhodospirillales					0.021%	
	Bacteria	Verrucomicrobia	Spartobacteria	Chthoniobacterales	Chthoniobacterales	Chthoniobacterales					0.020%	
	Bacteria	Proteobacteria	Gammaproteobacteria	Legionellales	Coxiellaceae	Coxiellaceae					0.008%	
	Bacteria	Elusimicrobia	Elusimicrobia	Lineage IIa	Lineage IIa	Lineage IIa					0.007%	
	Bacteria	Proteobacteria	Gammaproteobacteria	Gammaproteobacteria	Gammaproteobacteria	Gammaproteobacteria					0.005%	
	Bacteria	Latescibacteria	Latescibacteria	Latescibacteria	Latescibacteria	Latescibacteria					0.005%	
	Bacteria	Proteobacteria	Alphaproteobacteria	Rhizobiales	Methylocystaceae	Methylocystaceae					0.004%	
	Bacteria	Actinobacteria	Actinobacteria	Corynebacteriales	Mycobacteriaceae	Mycobacterium					0.876%	Increased with aCeN
	Bacteria	Proteobacteria	Betaproteobacteria	Burkholderiales	Oxalobacteraceae	Noviherbaspirillum					0.260%	
	Bacteria	Actinobacteria	Actinobacteria	Pseudonocardiales	Pseudonocardiaceae	Amycolatopsis					0.108%	
	Bacteria	Actinobacteria	Thermoleophilia	Gaiellales	Gaiellales	Gaiellales					0.030%	
	Bacteria	Proteobacteria	Gammaproteobacteria	Enterobacteriales	Enterobacteriaceae	Pantoea					0.026%	
	Bacteria	Cyanobacteria	Melainabacteria	Obscuribacterales	Obscuribacterales	Obscuribacterales					0.025%	
	Bacteria	Proteobacteria	Betaproteobacteria	Burkholderiales	Comamonadaceae	Pseudorhodoferax					0.016%	
	Bacteria	Proteobacteria	Alphaproteobacteria	Rhodospirillales	Acetobacteraceae	Rhodopila					0.008%	
	Bacteria	Proteobacteria	Alphaproteobacteria	Alphaproteobacteria	Alphaproteobacteria	Alphaproteobacteria					0.008%	
	Bacteria	Actinobacteria	Actinobacteria	Micrococcales	Microbacteriaceae	Marisediminicola					0.006%	
	Bacteria	Proteobacteria	Betaproteobacteria	Burkholderiales	Comamonadaceae	Leptothrix					0.006%	
	Bacteria	Verrucomicrobia	Verrucomicrobia Incertae Sedis	Unknown Order	Unknown Family	Methylacidiphilum					0.006%	
	Bacteria	Proteobacteria	Betaproteobacteria	Burkholderiales	Oxalobacteraceae	Oxalicibacterium					0.005%	
	Bacteria	Proteobacteria	Betaproteobacteria	Burkholderiales	Comamonadaceae	Rubrivivax					0.004%	
	Bacteria	Proteobacteria	Alphaproteobacteria	Rhizobiales	Rhodobiaceae	Rhodoligotrophos					0.003%	
	Bacteria	Proteobacteria	Alphaproteobacteria	Rhizobiales	Rhizobiaceae	Shinella					0.003%	
	Bacteria	Proteobacteria	Alphaproteobacteria	Rhizobiales	Brucellaceae	Brucellaceae					0.002%	
	Bacteria	Cyanobacteria	Cyanobacteria	SubsectionIII	FamilyI	FamilyI					0.002%	
	Bacteria	Firmicutes	Bacilli	Bacillales	Bacillaceae	Oceanobacillus					0.002%	
	Archaea	Thaumarchaeota	SAGMCG-1	Unknown Order	Unknown Family	Nitrosotalea					0.001%	
	Bacteria	Planctomycetes	Planctomycetacia	Planctomycetales	Planctomycetaceae	Nostocoida					0.001%	
	Bacteria	Actinobacteria	Actinobacteria	Propionibacteriales	Nocardioidaceae	Nocardioidaceae					0.001%	
	Bacteria	Actinobacteria	Actinobacteria	Pseudonocardiales	Pseudonocardiaceae	Thermocrispum					0.001%	
	Bacteria	Verrucomicrobia	Spartobacteria	Chthoniobacterales	Chthoniobacterales DA101 soil	Chthoniobacterales DA101 soil					0.001%	
	Bacteria	Proteobacteria	Betaproteobacteria	Burkholderiales	Comamonadaceae	Tepidimonas					0.001%	
	Bacteria	Proteobacteria	Betaproteobacteria	Burkholderiales	Comamonadaceae	Schlegelella					0.0003%	
	Bacteria	Gemmatimonadetes	Gemmatimonadetes	Gemmatimonadales	Gemmatimonadaceae	Gemmatimonas					0.538%	None
	Bacteria	Nitrospirae	Nitrospira	Nitrospirales	Nitrospiraceae	Nitrospira					0.483%	
	Bacteria	Actinobacteria	Actinobacteria	Micromonosporales	Micromonosporaceae	Actinoplanes					0.462%	
	Bacteria	Proteobacteria	Alphaproteobacteria	Rhizobiales	Rhizobiales Incertae Sedis	Bauldia					0.155%	
	Bacteria	Proteobacteria	Alphaproteobacteria	Rhizobiales	Hyphomicrobiaceae	Pedomicrobium					0.150%	
	Bacteria	Acidobacteria	Acidobacteria	Subgroup 5	Acidobacteria Subgroup 5	Acidobacteria Subgroup 5					0.090%	
	Bacteria	Actinobacteria	Actinobacteria	Micromonosporales	Micromonosporaceae	Micromonospora					0.076%	
	Bacteria	Actinobacteria	Actinobacteria	Micrococcales	Microbacteriaceae	Curtobacterium					0.063%	
	Bacteria	Proteobacteria	Alphaproteobacteria	Caulobacterales	Hyphomonadaceae	Woodsholea					0.054%	
	Bacteria	Actinobacteria	Actinobacteria	Frankiales	Geodermatophilaceae	Blastococcus					0.038%	
	Bacteria	Chlamydiae	Chlamydiae	Chlamydiales	Parachlamydiaceae	Protochlamydia					0.038%	
	Bacteria	Actinobacteria	Actinobacteria	Streptosporangiales	Thermomonosporaceae	Actinoallomurus					0.037%	
	Bacteria	Chlamydiae	Chlamydiae	Chlamydiales	Parachlamydiaceae	Parachlamydiaceae					0.036%	
	Bacteria	Actinobacteria	Acidimicrobiia	Acidimicrobiales	Acidimicrobiaceae	CL500-29 marine group					0.024%	
	Bacteria	Proteobacteria	Deltaproteobacteria	Myxococcales	Polyangiaceae	Polyangiaceae					0.021%	
	Bacteria	Proteobacteria	Deltaproteobacteria	Bdellovibrionales	Bacteriovoracaceae	Peredibacter					0.017%	
	Bacteria	Proteobacteria	Alphaproteobacteria	Rhodospirillales	Rhodospirillaceae	Defluviicoccus					0.015%	
	Bacteria	Actinobacteria	Actinobacteria	Micrococcales	Microbacteriaceae	Frigoribacterium					0.009%	
	Bacteria	Proteobacteria	Deltaproteobacteria	Oligoflexales	Oligoflexales	Oligoflexales					0.008%	
	Bacteria	Proteobacteria	Alphaproteobacteria	Rickettsiales	Rickettsiales Incertae Sedis	Captivus					0.007%	
	Bacteria	Planctomycetes	Planctomycetacia	Planctomycetales	Planctomycetaceae	Blastopirellula					0.006%	
	Bacteria	Actinobacteria	Actinobacteria	Kineosporiales	Kineosporiaceae	Kineosporiaceae					0.005%	
	Bacteria	Proteobacteria	Alphaproteobacteria	Rickettsiales	Mitochondria	Pseudogymnoascus					0.005%	
	Bacteria	Acidobacteria	Acidobacteria	Acidobacteria Subgroup 15	Acidobacteria Subgroup 15	Acidobacteria Subgroup 15					0.005%	
	Bacteria	Verrucomicrobia	Verrucomicrobiae	Verrucomicrobiales	Verrucomicrobiaceae	Roseimicrobium					0.004%	
	Bacteria	Bacteroidetes	Cytophagia	Cytophagales	Cyclobacteriaceae	Cyclobacteriaceae					0.004%	
	Bacteria	Firmicutes	Bacilli	Bacillales	Planococcaceae	Planococcus					0.003%	
	Bacteria	Actinobacteria	Actinobacteria	Micrococcales	Cellulomonadaceae	Cellulomonadaceae					0.003%	
	Bacteria	Firmicutes	Clostridia	Thermoanaerobacterales	Thermodesulfobiaceae	Coprothermobacter					0.003%	
	Bacteria	Bacteroidetes	Bacteroidia	Bacteroidales	Porphyromonadaceae	Dysgonomonas					0.003%	
	Bacteria	Actinobacteria	Actinobacteria	Micromonosporales	Micromonosporaceae	Pilimelia					0.002%	
	Bacteria	Proteobacteria	Gammaproteobacteria	Enterobacteriales	Enterobacteriaceae	Serratia					0.002%	
	Bacteria	Bacteroidetes	Sphingobacteriia	Sphingobacteriales	Sphingobacteriaceae	Solitalea					0.002%	
	Bacteria	Acidobacteria	Acidobacteria	Acidobacteria Subgroup 18	Acidobacteria Subgroup 18	Acidobacteria Subgroup 18					0.001%	
	Bacteria	Bacteroidetes	Cytophagia	Cytophagales	Flammeovirgaceae	Amoebophilus					0.001%	
	Bacteria	Proteobacteria	Alphaproteobacteria	Rhizobiales	Phyllobacteriaceae	Aquamicrobium					0.001%	
	Bacteria	Proteobacteria	Alphaproteobacteria	Rhodospirillales	Rhodospirillaceae	Azospirillum					0.001%	
	Bacteria	Bacteroidetes	Cytophagia	Cytophagales	Cytophagaceae	Flexibacter					0.001%	
	Bacteria	Actinobacteria	Actinobacteria	Micrococcales	Micrococcales	Micrococcales					0.001%	
	Bacteria	Proteobacteria	Alphaproteobacteria	Rhizobiales	Hyphomicrobiaceae	Prosthecomicrobium					0.001%	

(b)

Fig. S2.5 Genera with different abundance levels among treatments within legume plots. The color panel under ‘aCaN’, ‘eCaN’, ‘aCeN’ and ‘eCeN’ reflects the relative abundance level at each treatment by LSD test. Red toned cells, (a); Blush toned cells, (ab); White toned cells, (b); Sapphire toned cells, (bc); and Blue toned cells, (c).

	pH	Moisture	Tm (°C)	TC (%)	TN (%)	NO_3^+ (mg kg^{-1})	NH_4^- (mg kg^{-1})	AB (g m^{-2})	RB (g m^{-2})	AB-N (%)	AB-C/N	RB-N (%)	RB-C/N	RIB (g m^{-2})
Acidimicrobiia			-0.46*				-0.48*	0.71***	-0.73***	0.68***	-0.69***	0.63**	-0.63**	-0.84***
Acidobacteria			-0.55**			0.43*	-0.49*	0.66***	-0.77***	0.61**	-0.64**	0.64***	-0.66***	-0.76***
Actinobacteria			0.52**				0.57**		0.47*					0.46*
Alphaproteobacteria	0.44*													
Bacilli			-0.50*		0.43*		-0.49*	0.43*	-0.56**	0.43*	-0.44*			-0.54**
Betaproteobacteria						0.51*								
Chlamydiae						0.52*		0.49*		0.48*	-0.51*	0.46*	-0.45*	
Chloroflexi	0.41*							0.61**	-0.42*	0.54**	-0.52**		-0.43*	-0.43*
Chthonomonadetes														
Cyanobacteria		0.58**	0.45*			-0.69***		-0.82***	0.53**	-0.75***	0.76***	-0.83***	0.83***	0.58**
Cytophagia			-0.41*		0.42*			0.43*	-0.60**	0.51*	-0.56**	0.49*	-0.50*	-0.58**
Deltaproteobacteria														
Erysipelotrichia		0.41*	0.56**			-0.67***		-0.86***	0.69***	-0.72***	0.73***	-0.83***	0.85***	0.69***
Gammaproteobacteria			-0.59**			0.68***		0.73***	-0.67***	0.64***	-0.71***	0.78***	-0.80***	-0.59**
Gemmatimonadetes														
Holophagae														
Ktedonobacteria			0.53**			-0.54**	0.42*	-0.73***	0.72***	-0.68***	0.70***	-0.78***	0.78***	0.74***
Melainabacteria														
Nitrospira			-0.55**				-0.55**	0.51*	-0.65***	0.49*	-0.52*	0.44*	-0.48*	-0.66***
Phycisphaerae		0.45*				-0.56**					0.46*	-0.61**	0.58**	
Planctomycetacia		-0.41*				0.41*		0.44*			-0.43*			
Soil Crenarchaeotic Group			-0.57**				-0.48*		-0.52**		-0.42*		-0.43*	-0.55**
Spartobacteria				0.43*	0.43*	0.59**		0.51*	-0.45*	0.45*	-0.50*	0.46*	-0.48*	
Sphingobacteriia			-0.44*						-0.43*					
TakashiAC-B11														
Thermoleophilia			0.65***				0.49*	-0.71***	0.80***	-0.63**	0.68***	-0.62**	0.66***	0.77***

Fig. S2.6 Spearman's rank correlation coefficient rho of selected classes (with different abundance levels among treatments) with environmental attributes. Coral toned cells represent significant positive correlations; Cyan toned cells represent significant negative correlations. Only classes with different abundance levels among treatments were subjected to this test. *P* values have been adjusted for multiple comparisons by FDR. The first seven columns correspond to correlations of each phylum with soil attributes including pH, moisture, temperature (Tm), total C (TC) and N (TN) content, nitrate, and ammonium. The next seven columns correspond to correlations of each phylum with plant attributes including aboveground biomass (AB), root biomass (RB) (0-20 cm, fine roots), aboveground biomass N (AB-N) and C/N (AB-C/N), root biomass N (RB-N) and C/N (RB-C/N), and root ingrowth biomass (RIB). Soil properties were data collected from the sampling year (2009). All plant properties were calculated as the sum of six harvests measured in both June and August from 2007-2009.

	pH	Moisture	Tm (°C)	TC (%)	TN (%)	NO_3^+ (mg kg^{-1})	NH_4^- (mg kg^{-1})	AB (g m^{-2})	RB (g m^{-2})	AB-N (%)	AB-C/N	RB-N (%)	RB-C/N	RIB (g m^{-2})
Metachlamydia						0.64***		0.48*	-0.49*	0.47*	-0.45*	0.55**	-0.51*	
Nitrososphaera			-0.57**				-0.48*		-0.52**		-0.42*		-0.43*	-0.55**
Protochlamydia						0.64***		0.48*	-0.49*	0.47*	-0.45*	0.55**	-0.51*	
Acidimicrobiales			-0.41*					0.75***	-0.69***	0.79***	-0.77***	0.70***	-0.70***	-0.74***
Acidiphilium							0.50*							0.52**
Acidobacteria Subgroup 17														
Acidobacteria Subgroup 3				-0.44*	-0.54**			-0.42*				-0.50*	0.44*	0.45*
Acidobacteria Subgroup 4			-0.53**			0.45*	-0.47*	0.67***	-0.78***	0.60**	-0.64**	0.65***	-0.66***	-0.76***
Acidobacteria Subgroup 5		0.49*												
Actinoallomurus			0.42*				0.48*							0.43*
Actinomadura							0.53**		0.42*					0.44*
Actinoplanes			0.52**				0.41*							
Adhaeribacter						0.46*		0.58**	-0.55**	0.64***	-0.68***	0.65***	-0.65***	-0.62**
Amycolatopsis			0.49*				0.58**		0.59**					0.66***
Arenimonas			-0.42*				-0.42*		-0.61**					-0.48*
Asteroleplasma		0.41*	0.56**			-0.67***		-0.86***	0.69***	-0.72***	0.73***	-0.83***	0.85***	0.69***
Bauldia			-0.42*			0.50*		0.73***	-0.70***	0.73***	-0.75***	0.70***	-0.70***	-0.65***
Bdellovibrio			-0.58**	0.42*				0.55**	-0.68***	0.63**	-0.63**	0.62**	-0.63**	-0.72***
Beijerinckiaceae														
Betaproteobacteria, other														
Blastococcus			0.49*											
Bradyrhizobiaceae							0.48*	-0.62**	0.59**	-0.51*	0.54**	-0.51*	0.52*	0.63**
Candidatus Protochlamydia														
Catenulispora									0.44*					0.45*
Chitinophagaceae									-0.52**		-0.47*	0.50*	-0.51*	-0.50*
Chlamydiales	-0.41*													
Chloroflexi	0.41*							0.61**	-0.42*	0.54**	-0.52**		-0.43*	-0.43*
Chthoniobacterales				0.43*	0.43*	0.59**		0.51*	-0.45*	0.45*	-0.50*	0.46*	-0.48*	
Chthonomonas														
CL500-29 marine group						-0.60**				-0.44*	0.44*	-0.55**	0.56**	
Cohnella							-0.55**		-0.45*					-0.51*
Corynebacteriales	-0.42*													
Coxiella			-0.46*			0.43*	-0.46*	0.66***	-0.56**	0.54**	-0.59**	0.58**	-0.58**	-0.61**
Cryptosporangium		-0.48*						0.53**	-0.55**	0.55**	-0.61**	0.69***	-0.66***	-0.60**
Curtobacterium				0.43*	0.41*									
Cytophagaceae									-0.44*					-0.42*
Dactylosporangium			0.66***				0.46*	-0.49*	0.71***	-0.52*	0.57**	-0.54**	0.60**	0.68***
Defluviicoccus														
Deltaproteobacteria GR-WP33-30							-0.66***							-0.43*
Devosia		-0.45*	-0.46*	0.50*	0.42*	0.72***		0.75***	-0.63***	0.80***	-0.82***	0.82***	-0.82***	-0.57**
Dokdonella							0.73***		0.51*					0.64***
FamilyI		0.58**	0.45*			-0.69***		-0.82***	0.53**	-0.75***	0.76***	-0.83***	0.83***	0.58**
Frankiales														
Gaiellales														
Gammaproteobacteria NKB5			-0.53**					0.51*	-0.47*	0.49*	-0.57**	0.45*	-0.48*	-0.43*
Gemmata														
Gemmatimonas														
Haliangium						-0.42*		-0.57**	0.54**	-0.46*	0.56**	-0.62**	0.59**	0.61**
Hirschia			-0.47*					0.48*	-0.60**	0.48*	-0.50*	0.41*	-0.45*	-0.54**
Holophagae														
Holophagae Subgroup 10			0.47*											
Holosporaceae		0.47*												
Hyphomicrobium			-0.46*											
Ideonella														
Intrasporangiaceae		-0.48*												
Jatrophihabitans			0.42*											
Kibdelosporangium			0.56**				0.49*	-0.46*	0.71***			-0.50*	0.50*	0.73***
Kribbella		-0.55**				0.70***		0.52**			-0.45*	0.58**	-0.55**	
Ktedonobacteria			0.53**			-0.54**	0.42*	-0.73***	0.72***	-0.68***	0.70***	-0.78***	0.78***	0.74***
Labrys														
Legionella														
Luteibacter						0.64***		0.52**	-0.46*	0.51*	-0.55**	0.72***	-0.66***	-0.45*
Lysobacter			-0.43*					0.59**	-0.61**	0.44*	-0.48*	0.48*	-0.50*	-0.62**
Mesorhizobium			0.44*											
Microbispora			0.68***			-0.45*		-0.74***	0.81***	-0.72***	0.78***	-0.77***	0.80***	0.83***
Micrococcus														
Micromonospora														
Micromonosporaceae			0.62**				0.48*		0.58**		0.41*			0.51*
Modestobacter			0.48*				0.51*		0.44*					
Mycobacterium		-0.56**					0.47*							
Myxococcales			-0.49*					0.47*	-0.51*	0.64***	-0.58**	0.47*	-0.52**	-0.49*

(a)

	pH	Moisture	Tm (°C)	TC (%)	TN (%)	NO_3^+ (mg kg^{-1})	NH_4^- (mg kg^{-1})	AB (g m^{-2})	RB (g m^{-2})	AB-N (%)	AB-C/N	RB-N (%)	RB-C/N	RIB (g m^{-2})
Niabella							0.42*							0.49*
Nitrosomonadaceae														
Nitrospira			-0.55**				-0.55**	0.51*	-0.65***	0.49*	-0.52*	0.44*	-0.48*	-0.66***
Nonomuraea														
Noviherbaspirillum						0.52**								
Obscuribacterales														
Oxalobacteraceae			-0.44*	0.48*	0.46*	0.62**		0.53**	-0.55**	0.57**	-0.60**	0.71***	-0.66***	-0.45*
Paenibacillus			-0.50*		0.42*		-0.49*	0.44*	-0.56**	0.46*	-0.47*	0.42*	-0.43*	-0.54**
Pantoea								0.44*	-0.57**	0.46*	-0.47*	0.48*	-0.48*	-0.53**
Parachlamydiaceae						0.64***		0.48*	-0.49*	0.47*	-0.45*	0.55**	-0.51*	
Patulibacter			0.65***				0.43*	-0.55**	0.67***	-0.48*	0.53**	-0.46*	0.50*	0.60**
Pedomicrobium	0.45*													
Peredibacter			-0.55**					0.50*	-0.70***	0.64***	-0.62**	0.49*	-0.48*	-0.62**
Phycisphaeraceae														
Phycisphaerae WD2101 soil group						-0.60**		-0.43*		-0.43*	0.49*	-0.61**	0.59**	
Phyllobacteriaceae	0.52**													
Pir4 lineage								0.53**	-0.45*		-0.45*			-0.53**
Pla1 lineage														
Planctomyces			-0.63**			0.43*		0.62**	-0.60**	0.60**	-0.63**	0.50*	-0.55**	-0.55**
Planosporangium			0.58**				0.58**	-0.48*	0.72***	-0.45*	0.46*	-0.50*	0.50*	0.72***
Polyangiaceae			0.58**			-0.49*	0.45*	-0.71***	0.64***	-0.63**	0.65***	-0.70***	0.73***	0.70***
Pseudonocardia		-0.48*					0.51*							
Pseudorhodoferax					0.44*							0.44*	-0.41*	-0.46*
Rhabdochlamydia						0.64***		0.48*	-0.49*	0.47*	-0.45*	0.55**	-0.51*	
Rhodomicrobium								-0.41*	0.48*					
Rhodoplanes						-0.46*		-0.76***	0.76***	-0.74***	0.75***	-0.76***	0.73***	0.75***
Rhodospirillales									-0.61**					-0.46*
Saccharopolyspora			0.44*	-0.43*	-0.55**		0.60**	-0.43*	0.62**	-0.51*	0.52**	-0.49*	0.48*	0.70***
Singulisphaera														
Solirubrobacterales			0.62**				0.46*	-0.68***	0.87***	-0.65***	0.68***	-0.72***	0.75***	0.85***
Sorangium			0.58**			-0.49*	0.45*	-0.71***	0.64***	-0.63**	0.65***	-0.70***	0.73***	0.70***
Sphingobacteriales			-0.43*											
Sphingobacteriales env.OPS 17									-0.52**		-0.47*	0.50*	-0.51*	-0.50*
Sphingomonadales		-0.65***				0.53**		0.55**		0.53**	-0.54**	0.61**	-0.61**	
Sporocytophaga								0.44*	-0.57**	0.55**	-0.55**	0.43*	-0.42*	-0.58**
Tahibacter			-0.42*				-0.41*	0.42*	-0.61**			0.45*	-0.46*	-0.49*
TakashiAC-B11														
Thaumarchaeota SCG			-0.57**				-0.48*		-0.52**		-0.42*		-0.43*	-0.55**
Virgisporangium		-0.41*	0.49*											
Woodsholea			0.49*			-0.48*		-0.75***	0.69***	-0.79***	0.79***	-0.78***	0.80***	0.71***

(b)

Fig. S2.7 Spearman's rank correlation coefficient rho of selected genera (with different abundance levels among treatments) with environmental attributes. Coral toned cells represent significant positive correlations; Cyan toned cells represent significant negative correlations. Only genera with different abundance levels among treatments were subjected to this test. *P* values have been adjusted for multiple comparisons by FDR. The first seven columns correspond to correlations of each phylum with soil attributes including pH, moisture, temperature (Tm), total C (TC) and N (TN) content, nitrate, and ammonium. The next seven columns correspond to correlations of each phylum with plant attributes including aboveground biomass (AB), root biomass (RB) (0-20 cm, fine

roots), aboveground biomass N (AB-N) and C/N (AB-C/N), root biomass N (RB-N) and C/N (RB-C/N), and root ingrowth biomass (RIB). Soil properties were data collected from the sampling year (2009). All plant properties were calculated as the sum of six harvests measured in both June and August from 2007-2009.

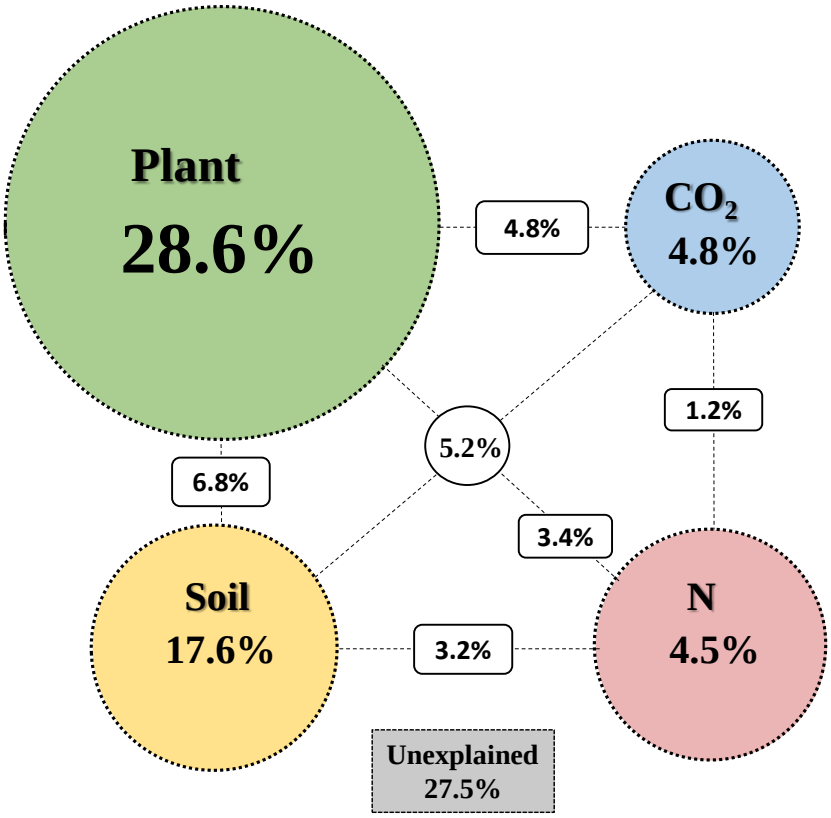

Fig. S2.8 Variation partitioning analysis (VPA) of microbial community structure explained by plant properties, soil geochemical variables, CO_2, and N. Each diagram represents the biological variation partitioned into the relative effects of each factor or a combination of factors. Only contribution of variation larger than 1% were shown. The same sets of plant and soil properties screened for Mantel tests were used. The concentrations of CO_2 are 368 p.p.m. for ambient and 560 p.p.m. for elevated plots; the N addition are 0 $g \cdot m^{-1} \cdot yr^{-1}$ for ambient and 4 $g \cdot m^{-1} \cdot yr^{-1}$ for elevated plots.

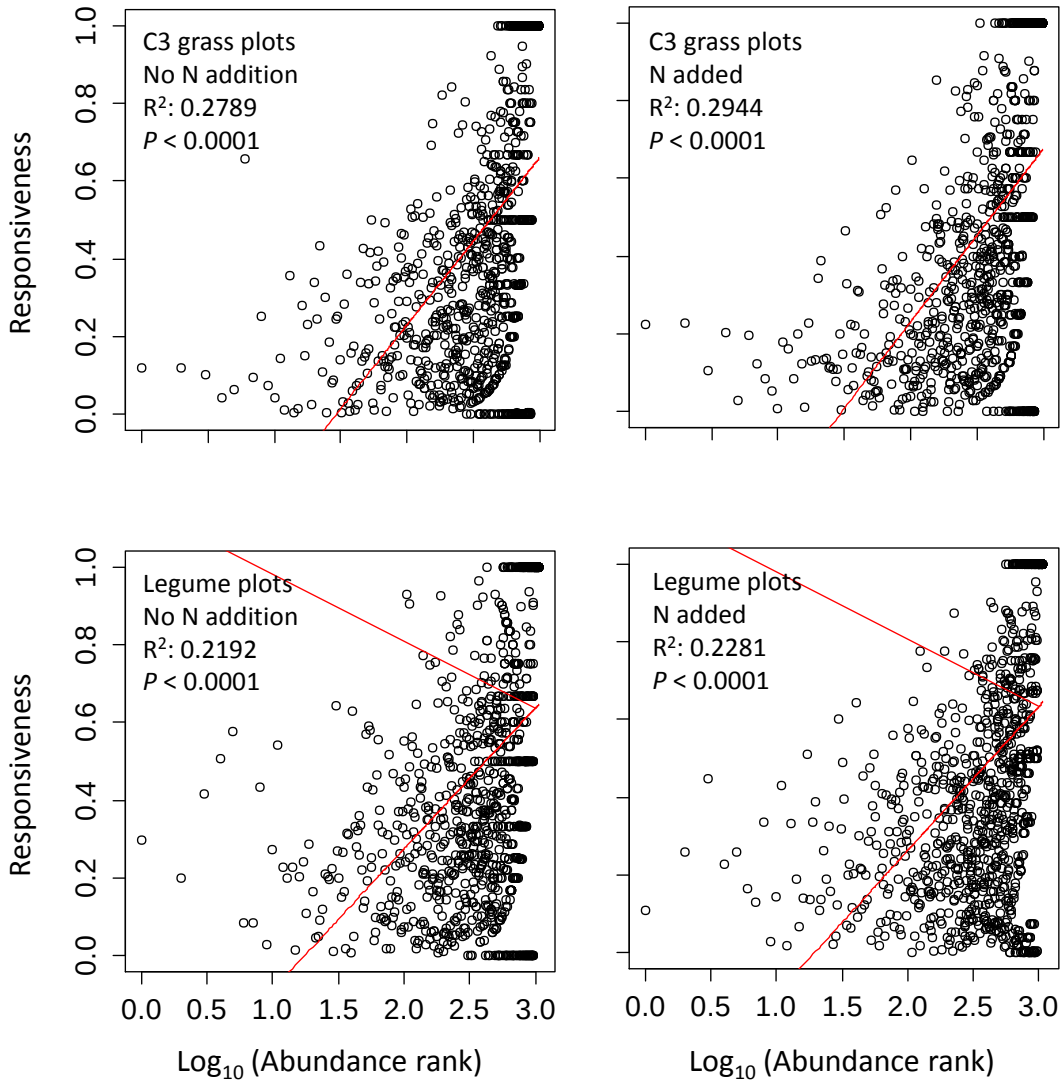

Fig. S2.9 Relative difference of each genus between treatment and control as a function of genus abundance rank in control. The relative differences are calculated as $|R_{treatment}-R_{control}|/Max\{R_{treatment}, R_{control}\}$, where $R_{treatment}$ is the relative abundance of certain genus in treatment plots, $R_{control}$ is the relative abundance of the same genus in control plots receiving no elevated CO_2 and no N addition. Each circle in the plot represents a detected genus. R square values and P values are based on linear regression analysis.

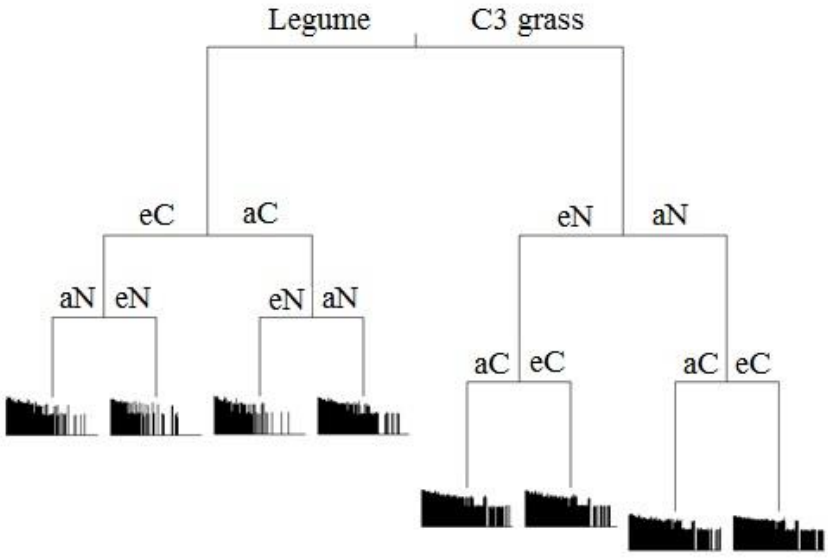

Fig. S3.1 Multivariate regression tree (MRT) analysis to illustrate the relative contributions of plant functional group (C3 grass and legume), eCO_2 and eN in shaping microbial functional composition and structure derived from GeoChip 3.0.

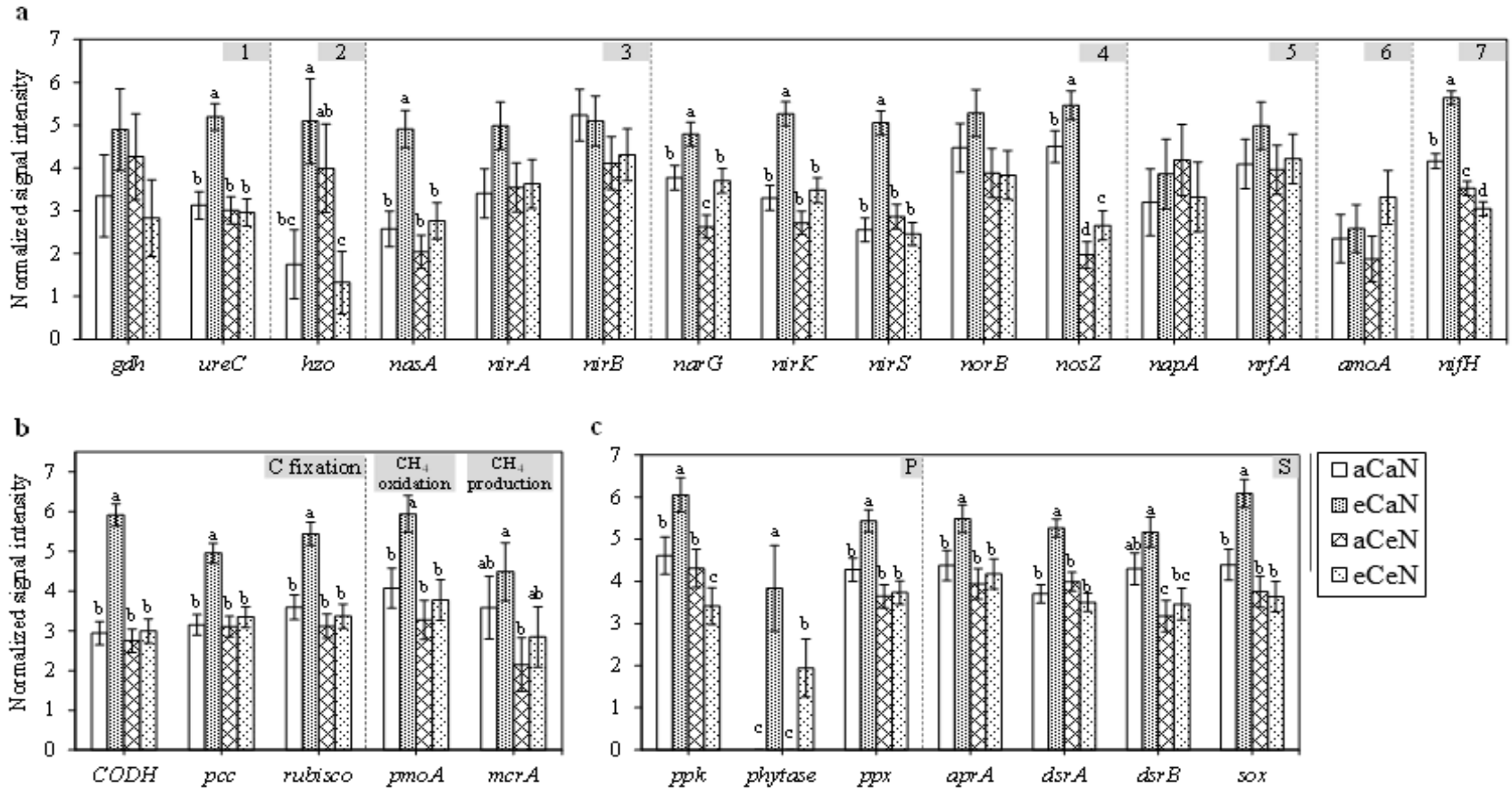

Fig. S3.2 Elevated CO_2 and eN effects on genes in C3 grass plots involved in N cycle (a), C fixation and CH_4 processes (b), and P/S cycles (c). The processes involved in N cycle include ammonification (1), Anammox (2), assimilatory N reduction (3), denitrification (4), dissimilatory N reduction (5), nitrification (6), and N fixation (7). Bars labeled with different letters are significantly different ($P < 0.05$) according to ANOVA, followed by Fisher's least significant difference (LSD) test with Holm-Bonferroni adjustment.

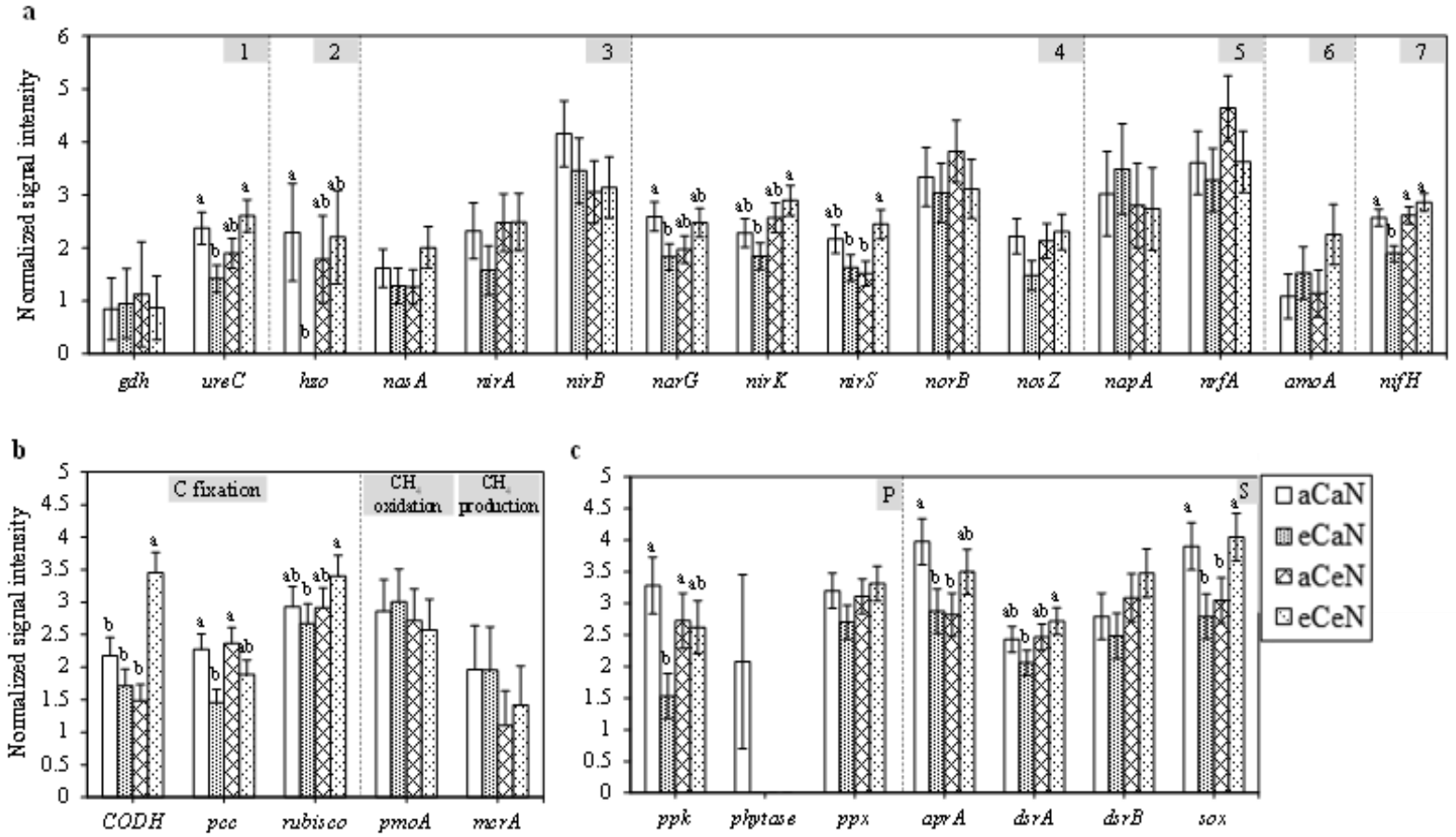

Fig. S3.3 Elevated CO_2 and eN effects on genes in legume plots involved in N cycle (a), C fixation and CH_4 processes (b), and P/S cycles (c). The processes involved in N cycle include ammonification (1), Anammox (2), assimilatory N reduction (3), denitrification (4), dissimilatory N reduction (5), nitrification (6), and N fixation (7). Bars labeled with different letters are significantly different ($P < 0.05$) according to ANOVA, followed by Fisher's least significant difference (LSD) test with Holm-Bonferroni adjustment.

(a)

C degradation genes	Detected gene No.	SCF[a]	HR[b]
All	**692**	**	**
Starch	131	*	
Hemicellulose	85		
Cellulose	51	**	**
Pectinase	9		**
Chitin	68		**
Aromatics	282	**	**
Lignin	66	**	*

(b)

C fixation genes	Detected gene No.	^{13}C sequestration
All	**234**	**
CODH	68	**
pcc	95	*
Rubisco	71	*

(c)

N fixation gene	Detected gene No.	^{15}N fixation
nifH	**235**	*

(d)

Processes	Genes	Detected gene No.	Mantel test
Ammonification rate	**All**	**69**	**
	ureC	62	***
	gdh	**7**	
Nitrification rate	**All**	**17**	**
	bacterial *amoA*	6	**
	archaeal *amoA*	10	
	hao	1	

[a] Soil C flux.
[b] Heterotrophic respiration.

Fig. S3.4 Significance of correlations between individual or all genes involved in C degradation and SCF or HR (a); genes involved in C fixation and ^{13}C sequestration strength (b); *nifH* gene involved in N fixation and ^{15}N fixation across samples at aN plots (c); genes involved in ammonification or nitrification and soil N processes (d). Significance is represented by ** when $p<0.05$ and * when $p<0.10$.

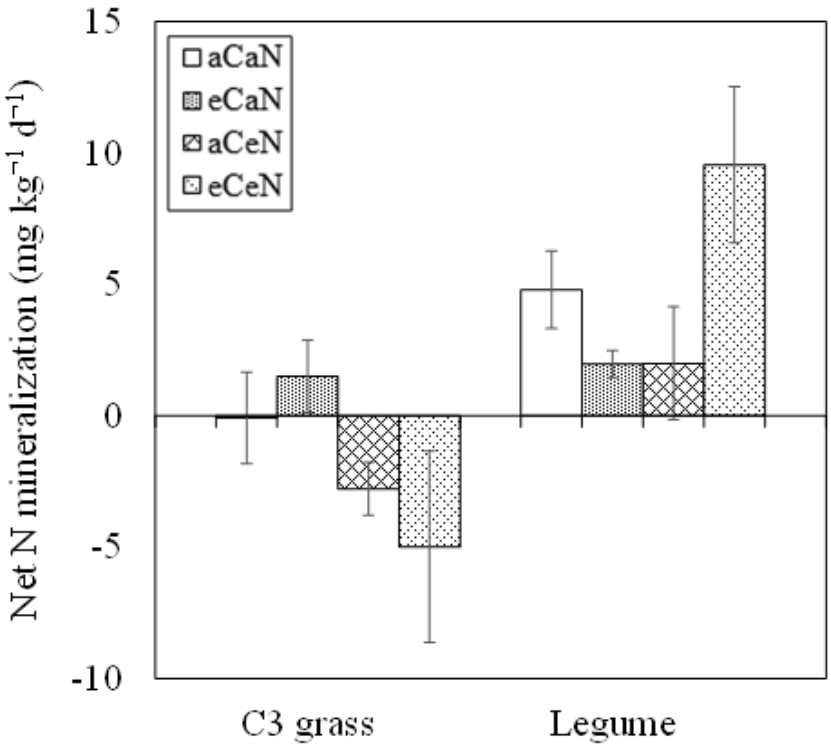

Fig. S3.5 Quantitative ^{13}C and ^{15}N enrichment in soils from C3 grass and legume plots at CO_2 and N treatments.

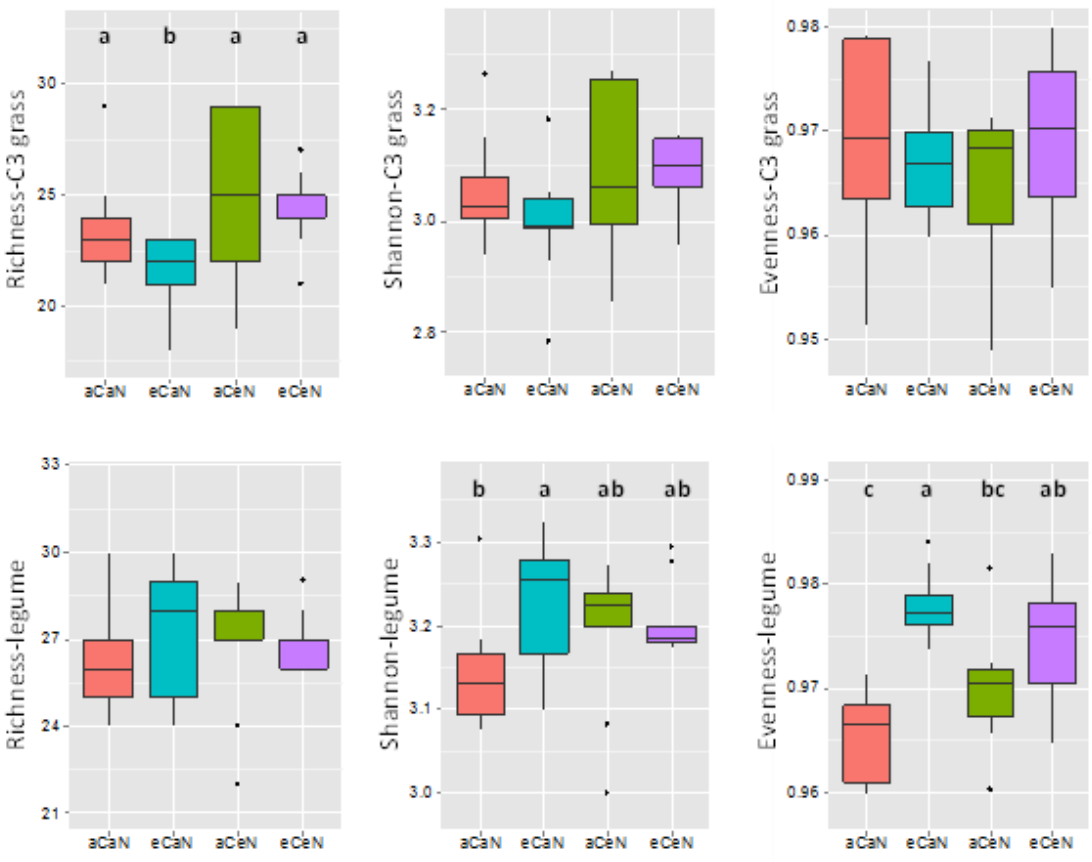

Fig. S4.1 Effects of eCO_2 and eN on microbial metabolic diversity represented by Richness, Shannon, and Evenness. Boxes labeled with different letters are significantly different ($P < 0.05$) according to ANOVA, followed by Fisher's least significant difference (LSD) test with Holm-Bonferroni adjustment. Abbreviations: aCaN: ambient CO_2 and no fertilization; eCaN: elevated CO_2 and no fertilization; aCeN: ambient CO_2 and fertilized; eCeN: elevated CO_2 and fertilized.

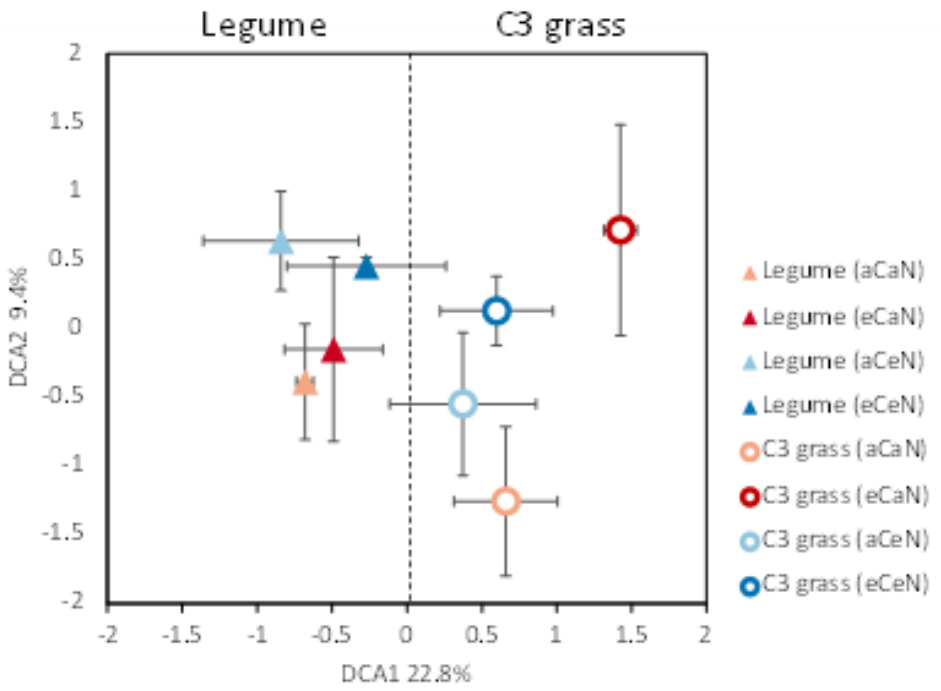

Fig. S4.2 DCA analysis of microbial communities based on metabolic diversity obtained through Biolog EcoPlate after 156h incubation. Abbreviations: aCaN: ambient CO_2 and no fertilization; eCaN: elevated CO_2 and no fertilization; aCeN: ambient CO_2 and fertilized; eCeN: elevated CO_2 and fertilized.

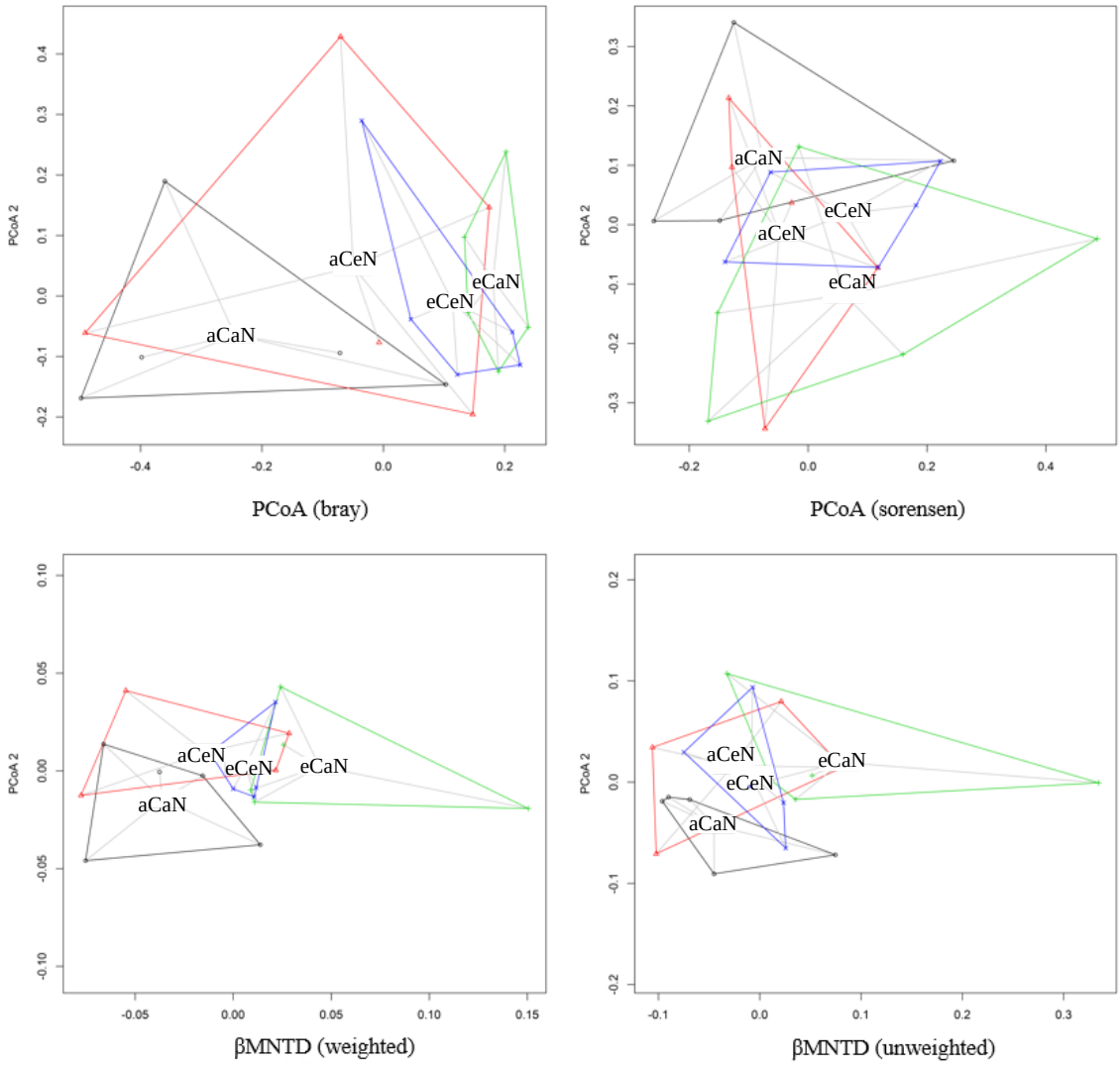

Fig. S5.1 UniFrac PCoA and βMNTD analyses of the archaeal-*amoA* community. Gray: aCaN; Red: aCeN; Blue: eCeN; Green: eCaN.

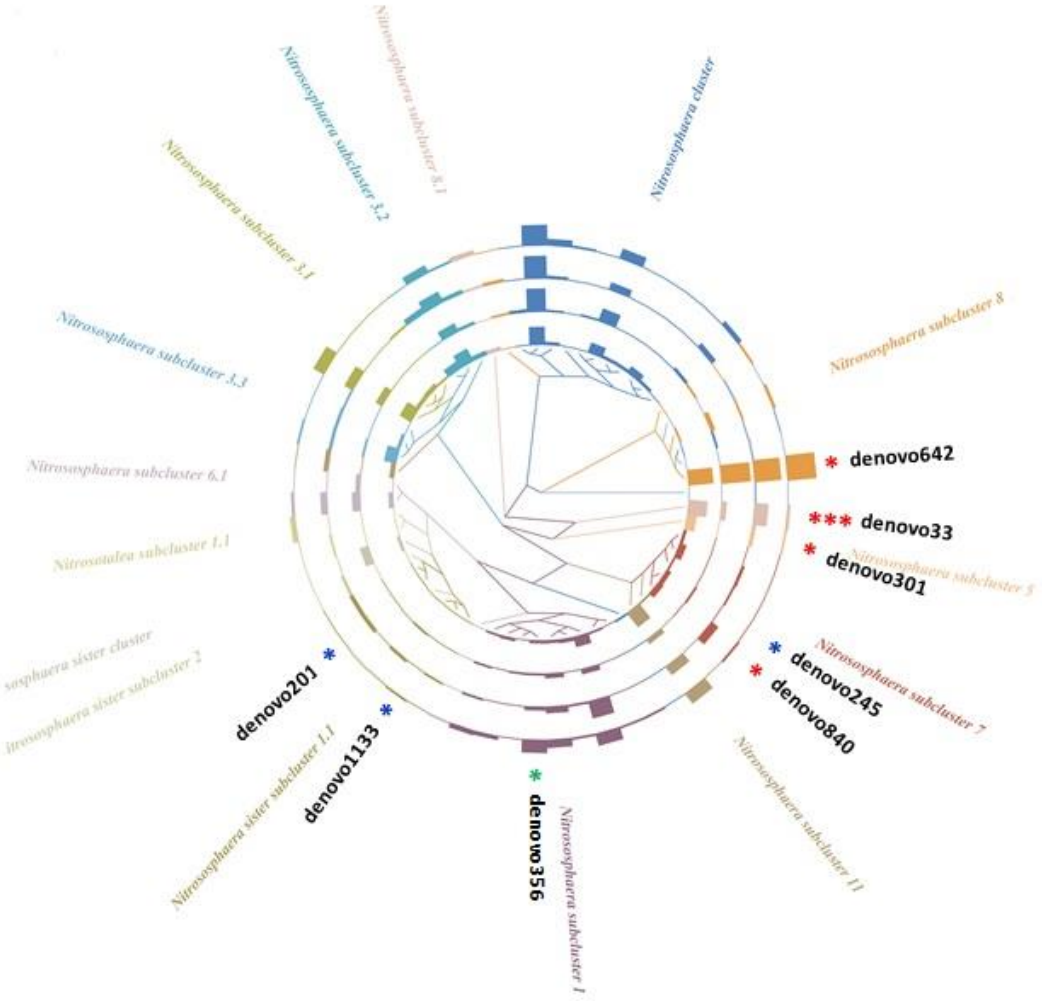

Fig. S5.2 Detection frequency and relative abundances of archaeal-*amoA* genes at OTU level in the four CO_2 and N conditions. Phylogenetic tree was constructed based on neighbor-joining criterion. Rings from inner to outer represents aCaN, eCaN, aCeN, and eCeN conditions, respectively. * in red, blue and green represent significant CO_2, N and their interactive effects, respectively (* $p < 0.05$, ** $p < 0.01$, ***$p < 0.001$, ANOVA test).